Investigation of Changes in Hydrological Processes using a Regional Climate Model.

by

AKM Hassanuzzaman Bhuiyan

A thesis submitted to the Faculty of Graduate studies of
the University of Manitoba
in partial fulfillment of the requirements of the degree of

DOCTOR OF PHILOSOPHY

Department of Civil Engineering
University of Manitoba
Winnipeg, Manitoba

Abstract

This thesis evaluates regional hydrology using output from the Canadian Regional Climate Model (CRCM 4.1) and examines changes in the hydrological processes over the Churchill River Basin (CRB) by employing the Variable Infiltration Capacity (VIC) hydrology model.

The CRCM evaluation has been performed by combining the atmospheric and the terrestrial water budget components of the hydrological cycle. The North American Regional Reanalysis (NARR) data are used where direct observations are not available. The outcome of the evaluation reveals the potential of the CRCM for use in long-term hydrological studies. The CRCM atmospheric moisture fluxes and storage tendencies show reasonable agreement with the NARR. The long-term moisture flux over the CRB was found to be generally divergent during summer.

A systematic bias is observed in the CRCM precipitation and temperature. A quantile-based mapping of the cumulative distribution function is applied for precipitation adjustments. The temperature correction only involves shifting and scaling to adjust mean and variance. The results indicate that the techniques employed for correction are useful for hydrological studies. Bias-correction is also applied to the CRCM future climate. The CRCM bias-corrected data is then used for hydrological modeling of the CRB. The VIC-simulated streamflow exhibits acceptable agreement with observations. The VIC model's internal variables such as snow and soil moisture indicate that the model is capable of simulating internal process variables adequately. The VIC-simulated snow and soil moisture shows the potential of use as an alternative dataset for hydrological studies.

Streamflow along with precipitation and temperature are analyzed for trends. No statistically significant trend is observed in the daily precipitation series. Results suggest that an increase in temperature may reduce accumulation of snow during fall and winter. The flow regime may be in transition from a snowmelt dominated regime to a rainfall dominated regime. Results from future climate simulations of the A2 emission scenario indicate a projected increase of streamflow, while the snow depth and duration exhibit a decrease. Soil moisture response to future climate warming shows an overall increase with a greater likelihood of occurrences of higher soil moisture.

Acknowledgments

All praises goes to the Almighty Allah, the most gracious and merciful, who has made this path smooth in order to come to a successful end.

I would like to take this opportunity to express sincere thanks and gratitude to my advisor Dr. Peter Rasmussen, Professor, Department of Civil Engineering at University of Manitoba for his constant guidance, encouragement, and technical input throughout my Ph.D research.

I would like to express my heartfelt thanks to my co-advisor Dr. John Hanesiak, Associate Professor, Department of Environment and Geography/CEOS for being inspirational and supportive throughout the study.

I would also like to thank the members of the committee: Dr. Ronald Stewart, Head of the Department, Department of Environment and Geography, University of Manitoba and Dr. Tricia Stadnyk, Assistant Professor, Department of Civil Engineering, University of Manitoba for taking time to read my dissertation and providing important feedback toward its completion.

I am indebted to all my fellow students from the hydrological processes laboratory for their inspiration, kind support and sharing ideas.

Finally, no acknowledgment is complete without mentioning my wife (Dr. Nazmun N. Bhuiyan) for her inspiration, support and for her many hours alone with the children while I worked on this research. An appendix of acknowledgments is provided for funding and data support towards the study.

Dedicated to my mother SAYEDA MEHERUNNESSA

and

in memory of my father ABDUL AWAL BHUIYAN.

Contents

List of Figures

List of Tables

Chapter 1

Introduction

1.1 Introduction

The earth's climatic system is undergoing considerable change (*IPCC*, 2007a), leading to an acceleration of the hydrological cycle. *Sauchyn and Kulshreshtha* (2008) state that projections for the future as well as recent trends indicate increasing soil-surface-water deficits, lower summer streamflows, and falling lake levels in Canada. These changes will influence every aspect of human life and well-being.

Streamflow plays an important role in economic growth and many aspects of social development (*Grey and Sadoff*, 2007). A change in streamflow will have impacts on irrigation and the development of agriculture and agriculture-based industries. Also, changes in flow may necessitate land use change, changes in agriculture practice, and altering of the cropping patterns of a region. The amount of available water in streams and lakes is important for aquatic ecosystems. Streams have navigational as well as recreational values. Extreme low flow during summer months can make such uses difficult or impossible. Also, continuous low flow can cause destruction in the aquatic ecosystem. On the other hand, floods can cause considerable structural damage and loss of human life.

The demand for water is increasing with the growth of the world's population. The

climate warming puts additional pressure on the water supply system. It is important to know the effect of changes due to warming on the water regime in a region (*Lemmen et al.*, 2008). The province of Manitoba has a large hydro-electric generation system that is entirely dependent upon a supply of fresh water. Estimates of the future supply of water is of significant interest to Manitoba Hydro. Although the impact of water supply would vary on a regional basis, all areas of Canada and virtually every economic sector would be affected. Further research into the potential impacts of climate change and the processes of adaptation would contribute to reduce the vulnerability (*Warren*, 2004).

General Circulation Models (GCMs), also known as global climate models, can simulate and reproduce the observed large-scale changes in climate over the past, and are used to simulate future climate conditions (*McGuffie and Henderson-Sellers*, 2001). GCMs create predictions on a relatively coarse scale unsuitable for regional climate change impact studies in which hydrological assessment is a prime concern (*Hostetler*, 1994). *Wood et al.* (2004) and *Maurer* (2007) suggested downscaling of climate data to a scale of 1/8° for hydrological modeling.

Use of a Regional Climate Model (RCM) is a well known approach for downscaling and incorporating regional details into GCMs (*Feser et al.*, 2011). Recent RCMs have introduced a multiple nesting process and can be coupled with land surface models. RCM scenarios can be used to investigate hydrological changes in river basins (*Teutschbein and Seibert*, 2010). In such studies, inputs from RCMs are used to drive a hydrological model in order to obtain variables for change investigation (*Xu et al.*, 2005). A distributed hydrology model is required in order to make the best use of gridded RCM data as an input. Distributed models require an extensive array of observed datasets for the purpose of validating their simulated output. Hence, the parameterization of hydrological model is constrained by the availability of observed data. Due to the limitations of dependable observed data and their sparsity, the modelling of northern river basins can be challenging.

A coupled RCM with a sophisticated land surface scheme exchanges water and energy

between the land surface and the atmosphere, and thus provides presumably realistic surface variables as well as authentic moisture return to the atmosphere (*Laprise*, 2008). The reliability of RCM simulated data must ideally be demonstrated by showing that they are statistically compatible with other independent data sources. Considering the advantages of coupled RCMs, the major science questions to be addressed by the current study are as follows: (a) How will local climate systems be resolved in a RCM when the boundary forcings are provided by a GCM? (b) How and to what extent can one use the RCM dataset in regional hydrological studies?

In response to these questions, datasets from the Canadian Regional Climate Model (CRCM) will be explored for change studies using different climate scenarios. The goal is to demonstrate that these CRCM scenario datasets are dependable pictures of hydrological change. The atmospheric moisture integrated over an area such as a river basin is a useful piece of hydrological information that can be used for hydrological change assessment on a long-term basis. The purpose of this research is to test the hypothesis that output variables derived solely from the CRCM with improved moisture partitioning through the land surface scheme can provide an estimate of long-term hydrological changes in a river basin. In order to test this hypothesis, the Churchill River basin (CRB) and the CRCM coupled with the Canadian LAnd Surface Scheme (CLASS) have been selected.

1.2 Research objectives

The followings are the key objective of this study:

- To improve the understanding of how and to what extent climate change will affect hydrological systems in the CRB, using input from a CRCM
- To examine changes in the hydrological processes by employing a distributed hydrological model with input from the CRCM. This will facilitate identification of the dominant hydrological process variables and their feedback to the system.

The thesis will employ a comprehensive approach to validating CRCM through its atmospheric moisture, along with surface variables over the CRB, in order to determine whether the quality of the output from the selected CRCM is adequate for the study of long-term hydrological change. A combined atmospheric and terrestrial water budget approach is used to determine changes in the hydrological cycle of the CRCM and to provide justification for the use of the CRCM in hydrological studies.

This study integrates a state-of-the-art distributed hydrology model using the CRCM gridded meteorological variables as input. These meteorological variables propagate through the modeled hydrological system and produce the hydrological variables of interest. The CRCM input to the hydrological model affects output variables such as snow, soil moisture, and stream discharge that in turn depend upon the characteristics of the system. The study will examine these dominant hydrological process variables and their feedback within the changed climate.

Prior to using the CRCM output in hydrological change studies, the simulated values for current (control) climate must be comparable to observed values. Some studies have reported that the CRCM variables are subject to systematic errors (*van Pelt et al.*, 2009; *van Roosmalen et al.*, 2010). Therefore, variables obtained from the CRCM should be corrected for bias. In order to achieve the objectives of this study, the following tasks will be performed:

1. Evaluation of regional hydrology using the CRCM, by means of a comparison with observation and re-analysis data.

2. Bias-correction of the CRCM precipitation and temperature, if necessary.

3. Assessment of changes in hydrological processes for the CRB derived from the hydrological model, using multiple CRCM scenarios as input.

1.3 Outline of the thesis

The thesis consists of eight main chapters. Chapter 2 reviews the literature regarding climate and climatic change, climate modelling, as well as the reasons for selecting a regional climate model for this study. A review of hydrological models is also discussed in Chapter 2. Chapter 3 presents the description of the study area. Chapter 4 discusses the CRCM dataset used in this research. Chapter 5 presents the evaluation of regional hydrology as simulated by the CRCM. The NARR atmospheric dataset has been used for validation. Chapter 6 provides a discussion of CRCM bias-corrections that are applied in order to obtain a suitable dataset for hydrological modelling. Chapter 7 presents the hydrological modelling of the Churchill River Basin using the VIC model and includes a discussion of the region of study. In Chapter 7, an evaluation of the dominant hydrological processes, as well as an assessment of hydrological changes due to climate change are provided. Chapter 8 summarizes the overall findings of this study, discusses the shortcomings, and provides suggestions for future research.

Chapter 2

Literature Review

2.1 Climate Change

The earth experiences continuous climatic changes initiated by external factors which impinge on the climate system. These climate forces include human and natural factors of influence (*Moss et al.*, 2010). Due to the enormous increase in the global population and the advancement in technologies based upon carbon-based fuels, significant changes in global climate are occuring. Climate change is directly linked to the increase in greenhouse gas concentration. For example, the recent *IPCC* (2007b) report states that most of the observed increases in global average temperatures since the mid-20^{th} century are due to the observed increases in anthropogenic green house gas (GHG) concentrations. The impact on the climate system by human activities greatly exceeds the impact of natural events (*Solomon et al.*, 2007).

The climate system consists of the following major components: (i) the atmosphere; (ii) the hydrosphere; (iii) the terrestrial and marine biospheres; (iv) the cryosphere and (v) the land surface. When dealing with climate change over longer periods, *Houghton and Morel* (1984) suggest that consideration of the atmosphere alone is not sufficient. All components of the climate system must be considered. The collective interaction among

these various components determines the climate. Climate interactions are often referred to as feedbacks. Thus, the climate system can be defined as a set of *components* and their *feedbacks* influencing one another, which in turn influence the system as a whole. Knowledge of the components of the climate system, including their feedback and change mechanisms, is essential.

2.2 Climate Models: Global and Regional

In recent decades, increases in computing power have enabled the development of climate system models. These sophisticated models facilitate our understanding of complex climate processes and enable predictions of future climate change (*McGuffie and Henderson-Sellers*, 2001). Besides these sophisticated models, simple models are used to explore individual aspects of the climate system. With this expanding knowledge of the climate system, the associated modelling needs have also increased which has led to the development of more comprehensive models. The most comprehensive models available are atmosphere-ocean general circulation models (AOGCMs) which provide the most realistic representations of nature.

The General Circulation Models (GCMs) have been developed based on interactions between climate components and their feedbacks. The more recent GCMs capture greater process detail including improved representations of the land surface process and are linked to the ocean models (*McGuffie and Henderson-Sellers*, 2005, Chapter 5). By coupling the models of the atmosphere, the ocean and the land surface, the interplay among the components of the climate system can be studied in order to make predictions of future change. In addition, the transient climate changes produced by anthropogenic forcing, the behavior of the climate system as it adapts to annual increases in greenhouse gas concentrations, can also be simulated (*Shepherd and McGinn*, 2003). Currently, the highest resolution GCMs have spatial resolutions in the order of 150 to 300 km. Outputs from these

models are generally only available as decadal length series of monthly means or totals. A demand exists for higher resolution information for climate impact and adaptation studies.

The GCM outputs are insufficient in terms of spatial and temporal resolution for regional hydrological impact studies (*Hostetler*, 1994). The representation of orography, coast-line, lakes, and land surface characteristics are much simplified in GCMs. The lack of some of these characteristics in GCMs has long been acknowledged by scientists (*Laprise*, 2008). Different studies (e.g., *Dickinson et al.* (1989); *Russo and Zack* (1997); *Giorgi and Mearns* (1999); *Teutschbein and Seibert* (2010)) have suggested the use of regional climate models (RCMs) driven by GCMs, with the objective of bridging the gap between the different spatial and temporal resolutions caused by simplification of schemes in the global models. Recent RCMs have introduced multiple nesting and can be coupled with land surface models. The effects of domain size, resolution, boundary forcing and internal model variability in RCM are now better understood (*Varis et al.*, 2004; *Braun et al.*, 2012).

Recent RCMs can provide high resolution output in the order of 10 km. These models are driven at their lateral boundaries by time-dependent, large-scale atmospheric data. As these models are able to resolve fine-scale physiographic details, they can also generate meteorologically coherent small-scale features (*Frigon et al.*, 2002; *Eum et al.*, 2012). The objective behind the high resolution nested RCMs, in the context of climate change projections, is to add finer scale detail retaining the large scale circulations of the GCM. In a RCM, the fine scale surface processes linked to hydrology, including topography, are better resolved. The added detail provided by using high resolution RCMs appear quite realistic when driven at their boundaries by coarse resolution GCM (*Laprise*, 2008).

2.2.1 Climate Change Impacts on Hydrology

Many studies have been conducted to examine the effect of climate change on components of the hydrological cycle. These studies can be classified differently depending on the approach. The most common approach has been to combine basin-scale hydrology models

with climate change scenarios derived directly from GCMs.

Wolock and McCabe (1999) examined changes in mean annual runoff in response to potential climate change in the continental United States. These researchers identified the main uncertainty as related to the GCMs' ability to estimate change in precipitation. The *Wolock and McCabe* study showed that determining surface hydrology at the continental scale using direct output of GCM can be misleading.

Recent developments of hydrological and land-surface parameterizations coupled with GCMs have improved the current situation. *Arora* (2001) performed simulation of 23 continental-scale river basins from the third generation Canadian GCM, where components of the global hydrological cycle and globally averaged precipitation and overland runoff were accurately estimated. On the other hand, the study showed discrepancies in the simulations of regional precipitation and consequently the runoff. *Arora*'s study explained these discrepancies as being due to poor partitioning of precipitation into evapo-transpiration and runoff in the land surface scheme. Further development of hydrological processes in land surface schemes will lead to improved estimations of continental or sub-continental level basin hydrology.

Hostetler and Giorgi (1993) investigated the feasibility of coupling RCMs with a landscape-scale hydrological model. Streamflow simulations demonstrated agreement in the seasonal cycle of streamflow but underestimated winter flow due to discrepancies in simulating winter time precipitation with the RCM used in the simulation. The results of the study indicated that coupling an RCM with a hydrology model would be a useful approach for evaluating the effects of climate change on hydrological systems.

Graham et al. (2007b) used 11 different RCMs for assessing hydrological change. Their study concluded that hydrological results from different RCMs vary considerably from model to model, although representations of hydrology are included in all RCMs. These researchers further explained the results as due to poor partitioning of precipitation into evapo-transpiration and runoff, similar to *Arora* (2001). *Graham et al.* (2007b) concluded

that RCM runoff can be used to analyze scenario trends, but attention must be given to the precipitation biases that most RCM show. Similarly, *Fowler et al.* (2007) used RCM data in hydrological modelling for a catchment in north-west England where they made a correction to the RCM data to overcome seasonality bias.

Frigon et al. (2002) evaluated surface hydrology as simulated by the Canadian regional climate model (CRCM). Two years of simulation presented in the study served as a first experiment to evaluate CRCM surface hydrology when the CRCM was coupled with a simple land surface scheme. *Frigon et al.* noted a seasonal bias which they attributed to the oversimplification imposed by the single-layer surface scheme. Nevertheless these researchers' conclusion from the first experiment suggest the possibility of using the CRCM to feed a hydrology model.

The CRCM is continuously being improved, and recent developments include the coupling of a sophisticated land surface scheme with the model. The CRCM version 4 and more recent versions are coupled with the Canadian Land Surface Scheme (CLASS) version 2.7 (*Verseghy*, 1991; *Verseghy et al.*, 1993; *Verseghy*, 2000). OURANOS has performed several successful experiments using the CRCM coupled with an improved version of CLASS (*Music and Caya*, 2009). The present study will use a recent CRCM (version 4.1), and will also examine the improvements in surface hydrology in CRCM 4.1 simulations due to the inclusion of multi layer CLASS.

2.3 Hydrological Models

A hydrological model deals with the estimation of the partitioning of water among the various pathways of the hydrological cycle (*Dooge*, 1992). The entire modelling process can be divided into several sub-processes that interact with each other in a confined geographical area called a watershed. Each of these sub-processes is represented by an analytical formulation based on an empirical relationship or on a function derived from a physical relationship.

Depending on the formulation of the processes, a model can be classified in different ways.

A wide variety of hydrological models have been developed and used in the past century and applied to study water resources (*Singh*, 1988, Chapter 3). These models can be grouped or classified in many different ways depending on (i) the purpose of modelling - i.e., real-time application, long-term prediction, process understanding; (ii) the basis of the model structure - i.e., models based on fundamental laws of physics, conceptual models calibrated on field data, black box analysis of input output translation or empirical analysis; (iii) spatial discritization - i.e., lumped parameter, distributed parameter; (iv) temporal scale - i.e., hourly, daily, monthly, annual, and (v) spatial scale - i.e., point, field, basin, region, global (*Leavesley*, 1994). Although hydrological models can be classified in numerous ways based on the above criteria, the models in this literature review will be grouped according to model structure and spatial discretization criteria.

2.3.1 Empirical and Physically based Models

Hydrological models can be grouped into empirical models and physically-based models according to their theoretical background. An empirical model is based on an empirical relationship that fits the observed data set. Such models do not explicitly take into account all governing physical laws of the processes involved in a basin's hydrology, but consider only the functional relationship between the input and output of a basin (*Leavesley*, 1994). These relationships are only applicable to the watershed for which they are developed. These empirical algorithms are limited as they are unable to take into account changes in landuse and channel properties through time and space (*Frakes and Yu*, 1999) . On the other hand, physically-based models are based on an understanding of the physical processes that govern the basin response. These fundamental physical principles are expressed by mathematical formulae (*Abbott et al.*, 1986).

2.3.2 Lumped and Distributed Models

Lumped model parameters do not vary spatially over the basin. The representation of hydrological processes in a lumped model is to some extent simplified. Sub-basin responses are grouped or lumped together and the entire basin response is measured only at the outlet. As the physical features of the hydrological processes are lumped together, this type of model includes a certain level of empiricism. Lumped models are user-friendly because they are simple in nature, the input requirement is less, and they are easy to use, easy to set-up and to calibrate. These models work well in the case where hydrological predictions are required only at the outlet. For their calibration, they need sufficiently long climatological and hydrological records which are not always available (*Beven*, 1989). This requirement is considered a limitation of this type of model.

Distributed model parameters vary spatially over the basin. In this type of model, the spatial variability of a basin is considered to facilitate process simulation in a distributed manner using a grid-based approach or a topographically distributed approach. Process equations are required for each grid cell or topographic unit (*Abbott et al.*, 1986; *Beven*, 1989). Patterns of spatial distribution and the ability to simulate hydrological responses based on the spatial patterns make this approach more acceptable for coupling with a variety of physically distributed models. Distributed models require a large amount of input data for parameterization of processes in each grid unit, a requirement often considered a limitation of this approach. Because governing physical equations are modeled in a distributed manner, this approach can perform simulations with a high degree of accuracy, provided initialization and data input are managed correctly (*Nandakumar and Mein*, 1997). Models which fall in between distributed and lumped designations are called semi-distributed and are essentially simplifications of a distributed model.

2.3.3 Selection of a Hydrological Model

Hydrological models have been developed to address a range of problems and are used for many different purposes. In order to select an appropriate model for this study, several issues were considered: (i) the nature of the problem to be solved; (ii) the availability of input data; (iii) the output requirement and (iv) the availability of software and appropriate hardware. *Singh* (1988, Chapter 3) provides guidance regarding how to select an appropriate hydrological model for a study.

The objective of the present study is to utilize a hydrological model as a tool for assessing climate change impact on hydrology. As the study aims to investigate the long term impact of climate change on hydrology, short term event driven models have been excluded. Empirical models can be excluded as well, because the model will run under different climate scenarios, and the ability of empirical models to accommodate future change (e.g., changes in landuse and channel properties over time) is in question (*Frakes and Yu*, 1999). Therefore, the model should be physically-based.

As discussed in Section 2.2.1, a climate change scenario derived from a regional climate model will be used as input to the hydrology model in order to assess changes in hydrology. The hydrology model must be capable of using gridded data from a regional climate model as input. A distributed model would be the correct choice in order to used spatially-distributed gridded data (*Bell et al.*, 2007). The utility of physically-based distributed hydrology models to assess the effect of climate change has been recognized by researchers (*Beven*, 1989; *Nandakumar and Mein*, 1997). Therefore, model selection can be narrowed down to the family of distributed physically-based hydrological models. Also, in the selection of a model, attention must be given to models with less input data requirements, as data availability is a crucial issue for high-latitude northern Canada basins. Considering the factors discussed in this section, the Variable Infiltration Capacity (VIC) (*Liang et al.*, 1994, 1996), a distributed hydrological model, has been selected for this study. The VIC model takes into account the dynamics of surface and ground water interactions and calculates the watertable (*Liang*

et al., 2003). The VIC model can be applied to high-latitude basins where snow and frozen soil processes play an important role (*Cherkauer and Lettenmaier*, 1999; *Cherkauer et al.*, 2003).

2.4 Model Uncertainty

Model uncertainty is an important issue in climate change studies. Models represent approximations to real-world systems but may not include all factors involved in a system as not all internal processes are fully understood or can be described by simple mathematical models. The models used for understanding the complex climate system are likely to produce a range of uncertainties in their predictions (*Maslin and Austin*, 2012).

In this research, regional climate model data have been used for future climate projections as well as for the historical climate. Hydrological simulations are performed using input from a regional climate model. Regional climate model data are derived from coarse resolution GCMs by downscaling. A hierarchy of uncertainties are therefore introduced. The first level of uncertainty comes from GCMs and their choice of emission scenarios. The second level of uncertainty arises from the downscaling process. Another level of uncertainty is associated with the selection and implementation of hydrological model. *Wilby and Harris* (2006) and *Teutschbein and Seibert* (2010) suggested a framework for hydrological impact studies where the sources of uncertainties are ranked and summarised as follows: choice of GCMs and emission scenario $>$ downscaling method (i.e. RCMs) $>$ choice of hydrological model $>$ parameter estimation of a hydrological model. Assessing and combining the uncertainties from the individual sources is a major undertaking. Also the relative importance of various sources uncertainty is not easy to assess.

The majority of hydrological impact studies are looking at uncertainties associated with hydrological modelling and its parametrisation (*Muleta and Nicklow*, 2005; *Jung et al.*, 2012; *Kienzle et al.*, 2012). The sources of uncertainty in hydrological modelling may

come from model structure, from the calibration procedure, and from errors in the data used for calibration. The parameter uncertainty may be associated with the physical basin characteristics and its dominant processes (*Brigode et al.*, 2013).

For UK catchments, *Arnell* (2011) showed that the uncertainty from different climate models is considerably greater than the range of uncertainty from hydrological model parametrisation. In a study of hydrological impact assessment over Canadian watersheds, *Chen et al.* (2011) also showed that the choice of GCMs and emission scenarios is the major contributor to uncertainty. Other sources of uncertainties, such as hydrological model structure and parameter estimation, appear to be less important in hydrological impact studies.

Given the large number of GCMs, a family of emission scenario, and different down-scaling techniques, it is a major effort to study all possible combinations of sources of uncertainty in one study. In addition, the choice of hydrological model and estimation of model parameters must be considered in hydrological studies. Despite all these difficulties, it has been recognized that sources of uncertainties should be taken into account in hydrological impact studies (*Teutschbein and Seibert*, 2010; *Chen et al.*, 2011).

The goal of this study is to provide a comprehensive evaluation of a CRCM through a combined atmospheric-terrestrial water balance study along with hydrological modelling using VIC. The study was somewhat constrained by the availability of CRCM atmospheric datasets. We could only get a recent CRCM (4.1) simulation driven by CGCM3 (4^{th} ensemble member) member with the required atmospheric fields. The driving data of CGCM3 are based on the SRES A2 scenario. The choice of a model as well as a single scenario is a limitation of this research.

Chapter 3

Study Area

This chapter will provide a description of the selected study area, its physiography as well as other relevant information necessary for hydrological research. The chapter also provides information on hydrometric and climatological data used in the study.

3.1 Churchill River Basin

Figure 3.1 shows the major drainage basins contributing to Manitoba. The Churchill River is a major river in Saskatchewan and Manitoba. Geographically, the basin ranges from 53°N to 60°N latitude and from 113°W to 95°W longitude. Its source, located in central-east Alberta, drains through the lowlands of Saskatchewan and Manitoba. Although the Upper Churchill River drainage is separate from the Nelson River basin, the Churchill River contributes a large portion (approximately 85%) of the flow through a diversion into the Nelson River at Southern Indian Lake (*Hertlein*, 1999). The Nelson River drains Lake Winnipeg into Hudson Bay. Lake Winnipeg receives water from several large river systems: the Saskatchewan River system, the Red River system, and the Winnipeg River system.

The net flow of the Nelson River, including diversions of the Churchill River, provides approximately 80% of the hydropower production of Manitoba Hydro. Apart from its significance for hydro-power generation, the Churchill River basin has been selected in this

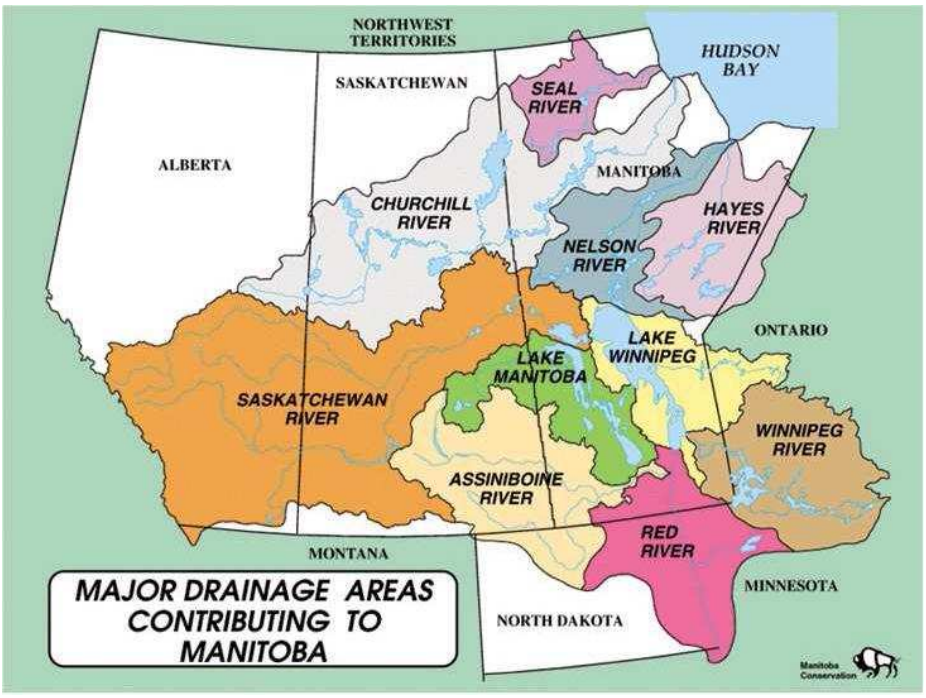

Figure 3.1: Major drainage basins contributing to Manitoba (Reproduced with permission from Manitoba Water Stewardship).

study because of its high-latitude location where climate change impacts are expected to be particularly strong.

Geography and Climate

The Churchill River basin has an area of approximately 283,350 km^2 and drains into Hudson Bay via its natural outlet and via the Nelson River. It lies to the north of the Nelson and Saskatchewan River basins, with its headwaters in east-central Alberta adjoining the Athabasca River drainage basin on the north and west. A map of the Churchill River basin is shown in Figure 3.2. The map also presents the delineated part of the basin used for this study. A detailed discussion of the delineated basin above Otter Rapids (station # 06CD002) is provided in Section 3.1.3.

Many lakes of various sizes can be found in the Churchill River basin. The river system is made up by a series of lakes interconnected by natural channels with a gradual, mild slope. Essentially, one lake drains into the next. Some of the major lakes in this system

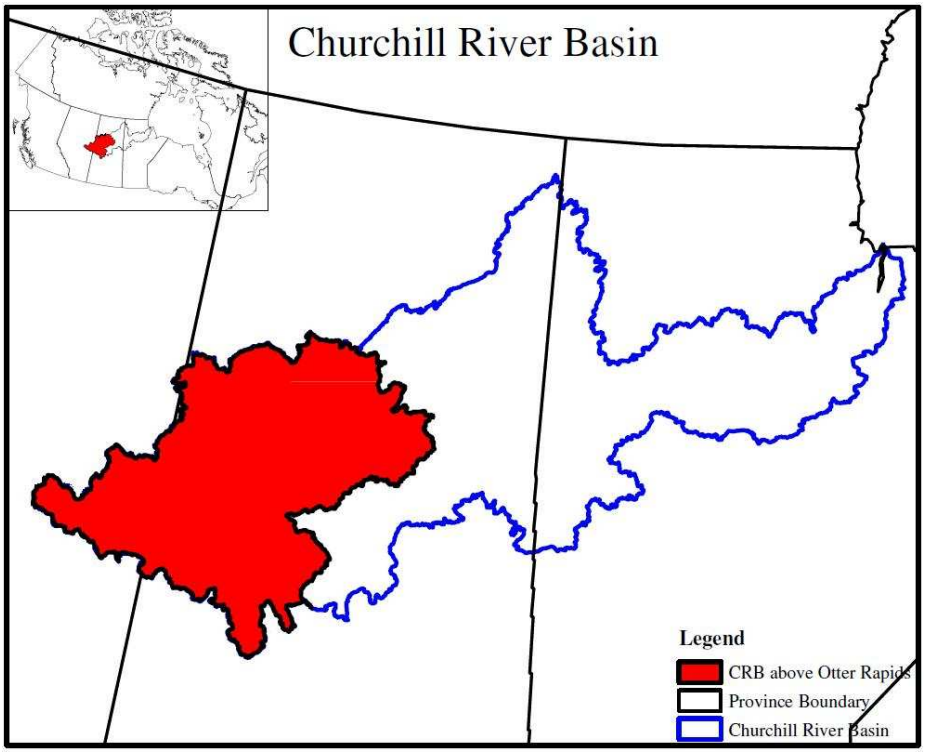

Figure 3.2: The Churchill River basin and the delineated basin above Otter Rapids (Station # 06CD002).

are Churchill Lake, Pinehouse Lake, Otter Lake, Lac La Ronge and Reindeer Lake. The presence of interconnected lakes in the drainage systems strongly modulates the flow of the Churchill River.

During summer months, the evaporation of the basin area is relatively high due to open water evaporation from lakes and wetlands. The basin outflow is attenuated due to the significant lake storage. The attenuation applies to peak flow as well as low flows. The majority of flow originates as snowmelt in May, reaches a maximum in July, and gradually recedes to a relatively constant flow, maintained in part by the existence of lakes.

The average annual accumulated precipitation of the Churchill River basin is approximately 440 mm. The mean annual average temperature of the basin is below 0°C. The average precipitation and temperature data are calculated from the thirty-year data series of selected weather stations. A list of stations as well as a map of station locations are given in Section 3.1.1. The basin area is dominated by long cold winter and short mild summer. Therefore, most of the basin area is underlaid with continuous or discontinuous permafrost.

Its headwaters are in the interior plains of east-central Alberta and in the Boreal Plains and Boreal Shield of west-central Saskatchewan.

There are two major dams in the Churchill River as part of the diversion project. The diversion project began operation in 1977, allowing Manitoba Hydro to divert water into the Nelson River system at South Indian Lake. This study will mainly focus on the basin area upstream of the diversion project in order to avoid the highly regulated portion of the basin.

3.1.1 Climatological Data

The climatological data used in this research were obtained from Environment Canada's data archives. These data can be accessed on-line through Environment Canada's web portal[1]. Daily precipitation and temperature data series, two essential inputs of a hydrological model, were retrieved from the data archives. Thirty weather stations were used to derive observed gridded data series for hydrological simulations. These stations were selected based on their geographic location as well as the length of the daily data series. The distribution of these stations is shown in Figure 3.3. Stations in the Alberta portion of the basin are well distributed. Over Manitoba, the station distribution is sparse and most stations are located in the southern part of the basin. These stations all have thirty years of continuous record for the study period (1976-2005). A list of selected weather stations is provided in Table 3.1 showing their geographic location and record length.

3.1.2 Hydrometric Data

The Water Survey of Canada (WSC)[2] provided the streamflow data. The selection of flow data was a function of the availability and the quality of the data. Many northern gauging stations are seasonal, measuring only periodic flow in order to satisfy a specific requirement. Flow series should be long enough for validation and calibration of a hydrological model. A

[1] http://climate.weatheroffice.ec.gc.ca, accessed June 19, 2012.
[2] http://www.wsc.ec.gc.ca/applications/H2O/index-eng.cfm. Accessed June 19, 2012.

Table 3.1: Environment Canada's weather stations used in the study.

Station ID	Station name	Latitude (N)	Longitude (W)	Elev. (m)	Record length (YYYY-MM-DD)
3010234	Andrew	54.02°	-112.23°	610.0	19730601 20080627
3015672	ST Lina	54.30°	-111.45°	632.5	19700501 20080402
3061800	Conklin LO	55.62°	-111.18°	670.6	19540501 20080627
3061930	Cowper LO	55.83°	-110.38°	563.3	19570501 20080627
3062889	Gordon Lake LO	56.62°	-110.50°	515.0	19640401 20080627
3063120	Heart Lake LO	55.00°	-111.33°	887.0	19470701 20080627
3063685	Lac La Biche (AUT)	54.77°	-112.02°	567.0	19581001 20030929
3065305	Primrose LO	54.75°	-110.05°	678.2	19670601 20080627
3065710	Sand River LO	54.65°	-110.98°	731.5	19570401 20080627
3067590	Winfered LO	55.33°	-110.20°	743.7	19570401 20080627
3081680	Cold Lake A	54.42°	-110.28°	541.0	19521101 20080627
4041000	Butte St Pierre	53.45°	-109.20°	571.5	19550501 20080627
4043246	Hillmond	53.43°	-109.72°	587.0	19700601 20080627
4060620	Big River	53.83°	-107.03°	502.9	19561001 20031030
4063560	Island Falls	55.53°	-102.35°	299.3	19290901 20051003
4063755	Key Lake	57.25°	-105.62°	509.0	19761001 20080627
4064150	La Ronge A	55.15°	-105.27°	378.6	19590601 20040714
4064600	Loon Lake CDA	54.05°	-109.10°	542.8	19510101 20080627
4065058	Medow Lake A	54.13°	-108.52°	480.4	19770801 20080605
4065710	Otter Rapids	55.65°	-104.73°	358.0	19641001 20080627
4068840	Whitesand Dam	56.23°	-103.15°	344.0	19380101 20061213
5050920	Flin Flon	54.77°	-101.88°	320.0	19270101 20080627
5050960	Flin Flon A	54.68°	-101.68°	303.9	19681201 20080627
5060520	Brochet A	57.88°	-101.68°	346.3	19480801 20080627
5061646	Lynn Lake A	56.86°	-101.08°	356.6	19680801 20050606
3013770	Lavoy	53.53°	-111.87°	670.0	19580801 20080627
4048520	Waseka	53.13°	-109.40°	638.0	19070701 20080627
4056240	Prince Albert A	53.22°	-105.67°	428.2	19421201 20021211
4075518	Nipawin A	53.33°	-104.00°	371.9	19730801 20050901
5062922	Thompson A	55.80°	-97.86°	223.1	19670401 20080627
3066160	Stoney Mount. LO	56.38°	-111.23°	762.0	19540501 20080627
3065560	Round Hill LO	55.30°	-111.98°	749.8	19510701 20080627

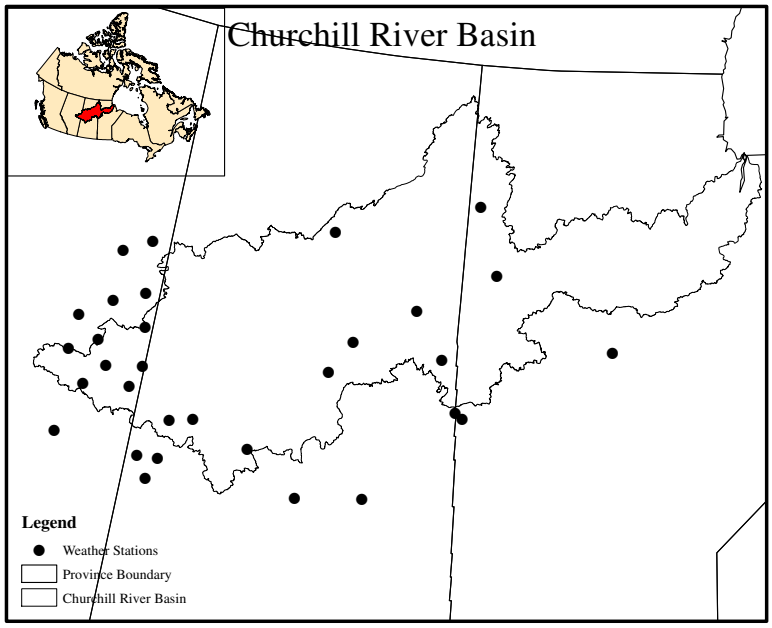

Figure 3.3: Location of weather stations within and around the Churchill River Basin.

list of twelve hydrometric stations located in the Churchill River basin is provided in Table 3.2. A map showing the geographic locations of the WSC gauge stations is provided in Figure 3.4. The gauge stations are fairly well spread across the basin. The downstream part of the Churchill River basin below Otter Rapids (station # 06CD002) is highly regulated. The flow station at Otter Rapids is unregulated and has more than forty years of data which is reasonable for hydrological modelling.

3.1.3 The Basin above Otter Rapids

Figure 3.5 shows the delineated basin above the Otter Rapids hydrometric station (# 06CD002). The digital elevation model (DEM) used in this study is from the USGS HYDRO1K. The location of three southern study areas (SSA) from BOREAS is also shown on the map as these data are used for model evaluation (see Chapter 7).

Figure 3.6 shows the land cover classification map of the basin. The land cover classes were derived from the University of Maryland's 1km global land cover dataset. The land

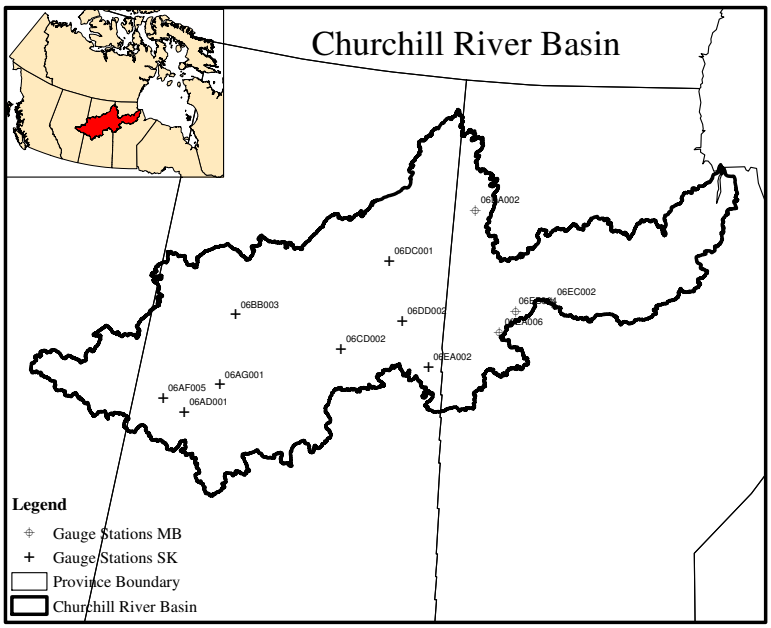

Figure 3.4: The Water Survey of Canada (WSC) hydrometric gauge stations in the Churchill River basin. The WSC station numbers are shown in the map.

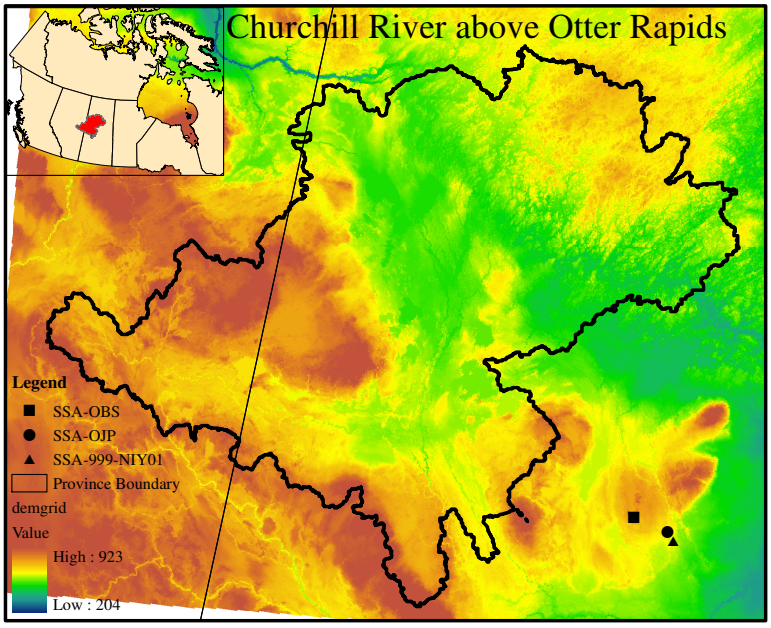

Figure 3.5: The Churchill River above Otter Rapids (station # 06CD002). The location of three BOREAS southern study areas (SSA) are also shown in the map.

Table 3.2: Location of hydrometric gauging stations within the Churchill River Basin.

Station ID	Station Name (Province[a])	Lat. (N)	Long. (W)	Record length (yr)	Flow type
06AD001	Beaver river near Dorintosh (SK)	54.3°	108.6°	24(1972-1995)	Natural
06AF005	Waterhen river near Goodsoil (SK)	54.4°	109.2°	31(1969-1995)	Natural
06AG001	Beaver river below waterhen river (SK)	54.8°	107.8°	25(1971-1995)	Natural
06BB003	Churchill river near Patuanak (SK)	55.9°	107.7°	23(1972-1994)	Natural
06CD002	Churchill River above Otter Rapids (SK)	55.6°	104.7°	43(1963-2005)	Natural
06DC001	Wathaman river below wathaman lake (SK)	57.1°	103.7°	35(1971-2005)	Natural
06DA002	Cochrane river near brochet (MB)	58.0°	101.4°	29(1975-2005)	Natural
06DD002	Reindeer river above Devil Rapids (SK)	56.2°	103.1°	21(1985-2005)	Regulated
06EA002	Churchill river at Sandy Bay (SK)	55.5°	102.3°	78(1928-2005)	Regulated
06EA006	Churchill river above Granville falls (MB)	56.1°	100.4°	60(1951-2005)	Regulated
06EB004	Churchill river above Leaf Rapids (MB)	56.5°	100.0°	33(1973-2005)	Regulated
06EC002	South bay diversion channel at South bay (MB)	56.6°	99.0°	13(1993-2005)	Regulated

[a]SK = Saskatchewan, and MB = Manitoba

cover of the basin is diverse. The headwaters of the basin are in the interior plains of east-central Alberta, and in the Boreal Plains and Boreal Shield of west-central Saskatchewan. The South-western portion of the basin is dominated by cropland and mixed cover. The grassland and deciduous trees are found at the headwaters of the basin and are typical in the Boreal plains. The wetlands and coniferous (evergreen needle-leaf) forest dominate the basin over the Boreal shield from the middle section to the north-eastern outlet of the delineated basin.

The flow of water (overland and subsurface) generally depends on the land cover class and retention time varies based on the physical characteristics of the vegetation. The soil type also plays an important role in the movement of water. Soil permeability varies based on landform (bedrock), organic matter accumulation, and vegetation cover. The Boreal shield is composed of bedrock with shallow top soil deposits and the Boreal plains, formed by glacial deposits, consists of a fairly deep layer of soil. Permeability is generally higher in the Boreal plain than in the Boreal shield. Low permeability soils increase the potential for lateral flow by limiting vertical flow.

Apart from hydrological modelling, this research also aims to perform an evaluation of regional hydrology using the combined atmospheric-terrestrial water balance approach presented in Chapter 5. The accuracy of atmospheric water-balance computations depends on the size of the selected basin. The critical size for atmospheric water-balance computations is in the order of 10^5 km^2 (*Abdulla et al.*, 1996; *Berbery and Rasmusson*, 1999; *Hirschi et al.*, 2006). The basin above the Otter Rapids is approximately 112,000 km^2 which meets the critical size requirement. Therefore, the Churchill River basin above Otter Rapids is selected for this study.

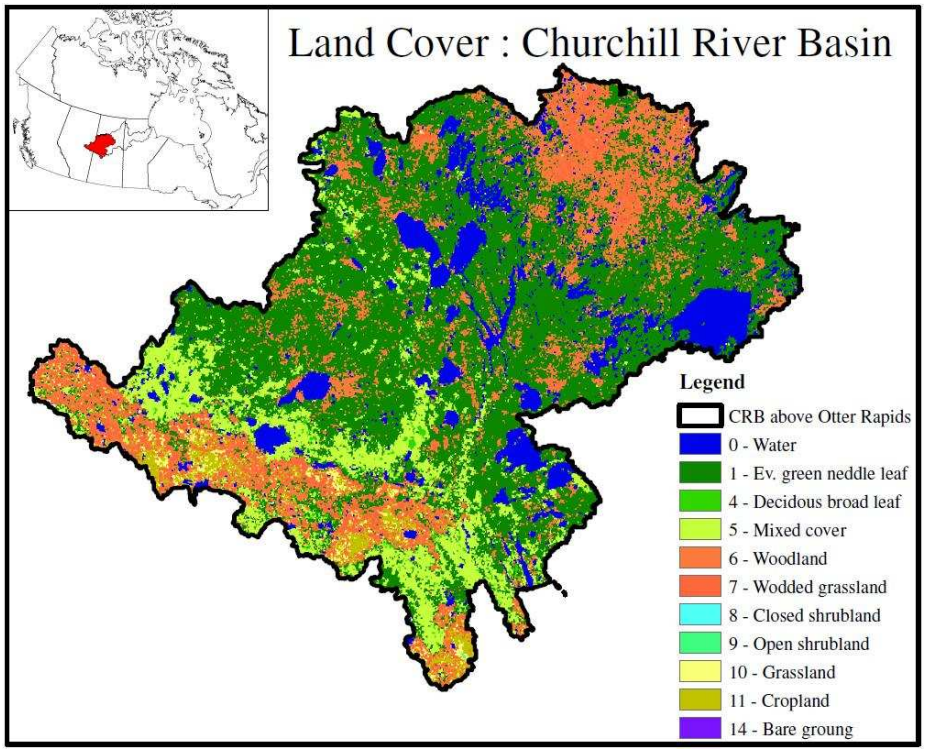

Figure 3.6: Land cover classification of the Churchill River basin above Otter Rapids (station # 06CD002).

Chapter 4

The Canadian Regional Climate Model

4.1 Description of the CRCM

The CRCM is a limited-area regional climate model developed at Université du Québec à Montréal (UQAM). The CRCM simulations are performed using GCM output or atmospheric reanalysis as driving data through its lateral boundary. The initial conditions are also taken from a GCM or reanalysis. At the boundary of the domain the CRCM blends the input fields received from the GCMs through one-way nesting. Beyond the blending zone, the variables of the CRCM evolve freely and are not affected by the inputs from the GCM. The CRCM produces finer resolution variables that are suitable for regional studies. Many aspects relevant to hydrology are better represented in the CRCM than in the driving GCM. The vertical grid of the model follows the terrain with 29 vertical levels. The model's horizontal grid resolution is 45 km at polar-stereographic projection. The CRCM covers North America with 201×193 grid points. The North-American domain of the CRCM is shown in Figure 4.1. A detailed description of the model can be found in *Caya and Laprise* (1999) and *Plummer et al.* (2006).

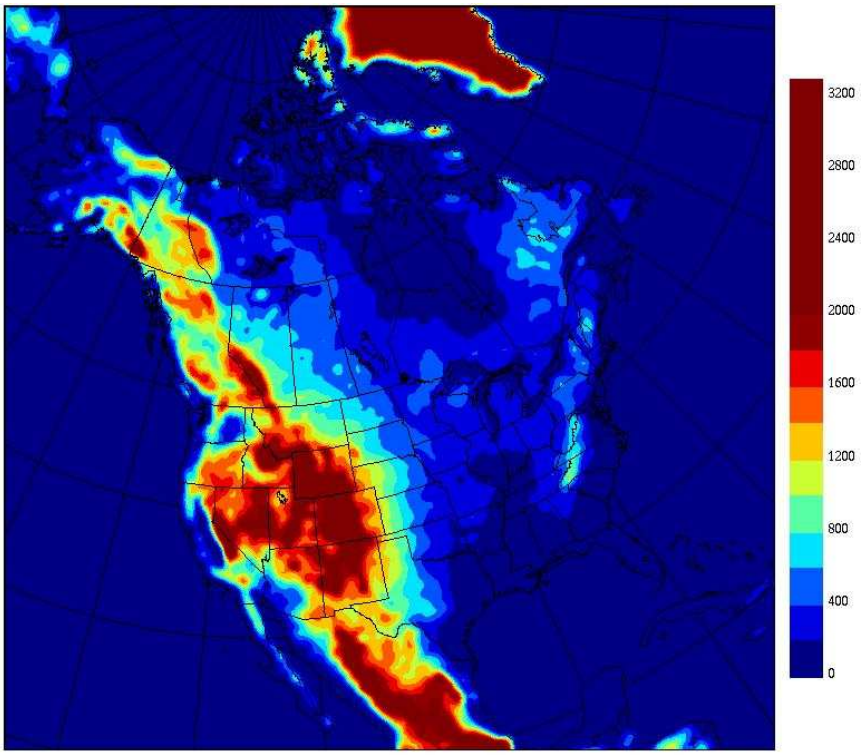

Figure 4.1: The North-American domain of the CRCM. This figure is reproduced from the Data Access Integration (DAI) site.

4.1.1 CRCM versions

The earlier CRCM (version 3.6) utilized the physical parametrization package of the second generation CGCM2. The CRCM 3.7 used a modified set of physical parametrization of CGCM2 compared to version 3.6, where bucket representation of soil was updated to address summer time surface fluxes (*Plummer et al.*, 2006).

The CRCM version 4 (and newer) offers a major improvement over earlier versions (*Braun et al.*, 2012). Earlier versions of the CRCM used a simple force-restore land surface scheme. The CRCM version 4 is coupled with the Canadian LAnd Surface Scheme (CLASS) (*Verseghy*, 2000; *Verseghy et al.*, 1993; *Verseghy*, 1991). The physical parametrization of CRCM version 4 is based on the CGCM3 package. The latest CRCM, version 4.2, provides a more realistic representation of water and energy exchange between the land surface and atmosphere by using the CLASS. The CLASS includes three soil layers and treats the vegetation canopy based on four vegetation types (coniferous, deciduous, crops, and grass).

An overview of the CLASS scheme used in the CRCM is presented in *Music et al.* (2009).

4.1.2 CRCM scenarios

The emission scenarios prescribed in the Special Report on Emissions Scenarios (SRES) are possible future states of the world. These scenarios were determined by assumed climate driving forces such as demographic development, socio-economic development, and technological change. Climate driving forces are grouped to form the four main families (A1,A2,B1,B2) of scenarios, and a total of 40 different scenarios across the four families have been constructed.

The CRCM uses CGCM driving data at the boundary. The scenario of a CRCM is inherited by the CGCM driving data. The CGCMs have been used to produce climate change projections using different scenarios. The CRCM 3.7 simulations used in this study are performed using the CGCM2 with the A2 scenario as forcing. The CRCM 4 (and newer) simulations used in this study were driven by CGCM3 following the A2 scenario.

The A2 scenario is at the higher end (albeit not the highest) of the SRES scenario family. Presently the available CRCM simulations are based on the A2 scenario only. The North American Regional Climate Change Program (NARCCAP) adopted the A2 emission scenario from an impact and adaptation perspective. The NARCCAP provided justification for selecting the higher end emission scenario because if the impacts from a higher emission scenario can be adapted to, then the impacts from a lower emission scenario can also be adapted to. A low emission scenario provides less information from an impact and adaptation point of view. Considering the above rationale, the selection of the A2 scenario in this research is justified.

4.1.3 Selected CRCM Simulations

The CRCM climate simulations employed in this study used observed greenhouse gas and aerosol (GHG+A) for the present climate and the A2 scenario GHG+A for the future climate.

Table 4.1: List of the CRCM experiments used in this study.

Experiment[a]	Model Version	Driving Atmos. Ocean Data	GHG+A Evolution	Start Time	End Time
abf	3.7.1	NCEP and AMIP II	-	1960-12	1990-12
ade	4.1.1	NCEP and AMIP V	-	1960-12	2005-05
adj	4.2.0	CGCM3 4^{th} member (6h)	Obs +SRES A2	1960-12	2050-12
adk	4.2.0	CGCM3 4^{th} member (6h)	SRES A2	2040-12	2070-12

[a]The climate simulations of 'adj' and 'adk' are the most recent (as of December 3, 2012) dataset available to date through the Ouranous consortium.

The CRCM simulations were driven by the 4^{th} ensemble member of the CGCM3. The earlier version of CRCM (3.7) simulations used in this study are driven by the global re-analysis dataset from the National Centers for Environmental Prediction (NCEP) as boundary forcing and ocean data (i.e., sea surface temperature and sea-ice) provided by the Atmospheric Model Intercomparison Project (AMIP) II/V. A list of the CRCM simulations used in this research are provided in Table 4.1.

Averages of 30-year time slices provide more effective representation of the climate scenarios than a shorter period (*IPCC*, 2007b). Differences between emission scenarios become more important with time into the future, for example the 2050's versus the 2030's (*Merritt et al.*, 2006). From the perspective of developing management practices, the time slice from the near future (2030's) may be of most practical interest. Therefore, in this research, two future time slices of CRCM simulations were taken into consideration: the near future time slice of the 2030s (2020-2049), and the distant future time slice of the 2050s (2041-2070). A thirty-year climate between 1976 to 2005 is considered as baseline climate.

Chapter 5

Evaluation of Regional Hydrology using a Canadian Regional Climate Model

5.1 Introduction

Understanding the hydrology of a region is essential for the development and utilization of water resources. Knowing various hydrological cycle processes and associated feedbacks contributes to our understanding of long term change in the climate system. Climate models are powerful tools to simulate complex interactions of climatic systems, especially with the improved representation of land surface components of the hydrological cycle (*McGuffie and Henderson-Sellers*, 2001). Regional climate models are capable of multiple nesting using global climate model data at the boundaries (*Rummukainen et al.*, 2001). These regional climate models can resolve fine-scale surface features of topography and land surface. Regional climate models can be useful in climate change impact studies in which regional hydrological assessment is a key concern.

The atmospheric-based water balance is often used to evaluate watershed storage change, land-atmosphere interactions, groundwater recharges, and drought events. The moisture change in a large region is determined by calculating the moisture flux across the boundaries

of a region. The inflow and outflow of moisture over a region is calculated by estimating whether water is being added to or removed from the atmosphere by means of evaporation and precipitation. Several studies investigated this technique in order to derive evaporation minus precipitation from a closed atmospheric region such as a river basin (*Walsh et al.*, 1994; *Strong et al.*, 2002). In the terrestrial-based water balance, the water is being added to and removed from a bounded region, typically a river basin, by means of precipitation and evaporation. The precipitation minus evaporation is equivalent to the surface and subsurface storage change plus the outflow from the bounded region. The process of precipitation minus evaporation acts as a linkage between the atmospheric and terrestrial water balances.

By estimating the precipitation minus evaporation from the atmospheric-based water balance technique and then coupling this estimate with the measured streamflow at the outlet of the basin, one can estimate the basin total water storage. Similarly, the basin total water storage can be estimated from the traditional hydrological models using precipitation as an input to the model; and runoff, either estimated from the model or measured at the outlet of the basin, as output. Evaporation is calculated by the model. For data sparse areas where calibration and validation of a hydrological model is difficult, the combined atmospheric-terrestrial water budget technique would provide an estimate of the storage change of a basin. Two independent techniques for estimating the basin total storage would provide a basis for comparison as well as help to better understand the mechanisms associated with the hydrological cycle and the water balance of a basin. In the present research, the Canadian Regional Climate Model (CRCM) coupled with the Canadian Land Surface Scheme (CLASS) is used to evaluate the combined atmospheric-terrestrial water budget technique. The comparison of the basin total water storage estimated from these two independent techniques would help to better understand the mechanisms associated with the hydrological cycle and the water balance of a basin. The following sections in this chapter will present a detailed review of the coupled water budget technique over the Churchill River Basin. In the later chapter, the second approach using a hydrology model will be presented.

The CRCM is validated using its water budget components through observations over the Churchill River Basin (CRB). The observation data includes climatological data from weather stations, gauge station data, gridded CANGRID data, and the North American Regional Re-analysis (NARR) data. A short description of CANGRID and NARR data is presented in the following section of this chapter.

5.2 Literature Review

Atmospheric and terrestrial water balance estimates with acceptable accuracy are fundamental for understanding the hydrological cycle. The Global Energy and Water Cycle Experiment (GEWEX) is an international effort focusing on understanding energy and water cycle within the climate system, initiated by the World Climate Research Programme (WCRP). The focus of Canada's contribution to GEWEX is the Mackenzie River basin (MAGS)(*Stewart et al.*, 1998). The objectives of MAGS was to understand and model the high latitude water and energy cycles as well as to improve the ability to assess the changes to Canada's water resources (*Stewart*, 2002). MAGS provided a comprehensive description of water and energy budgets by summarizing the estimates of several models as well as data from global and regional re-analysis. The MAGS concluded that despite some agreement between the modelled and observed water budget components, many quantitative uncertainties remains. Many authors have undertaken energy and water budget studies dealing with these uncertainties (*Berbery and Rasmusson*, 1999; *Roads and Betts*, 2000; *Ek et al.*, 2003; *Szeto et al.*, 2007). These studies contribute to our present understanding of the improvements that are necessary in the models as well as in reanalysis products to describe the hydrological cycle process.

With the recent development of remote sensing techniques, researchers are using radar or satellite remote sensing data to estimate water budget components for large spatial scale studies. These recent developments substitute traditional methods of estimating the water

budget using observed data at the ground surface; however, there are still shortcomings of these estimates. On the other hand, water balance estimation for large basins using atmospheric data only is becoming easier to apply than before due to the availability of high resolution atmospheric data (*Oki et al.*, 1995).

Elguindi et al. (2011) evaluate the ability of a GCM to estimate hydrological budget components (precipitation minus evaporation and runoff) over the Mediterranean, Black and Caspian sea basins. Their results suggest that high resolution global models, or downscaling models such as regional climate models (RCMs) are necessary in order to assess the climate change impact in the hydrological components of these basins.

Bresson and Laprise (2011) investigated a scale-decomposed atmospheric water budget over North America as simulated by CRCM for current and future climates. The contribution of water budget on each scale, as well as its change in a warmer climate was investigated. In both the current atmospheric water budget climatology or its projected evolution, small scales appeared to contribute significantly. These studies (*Brochu and Laprise*, 2007; *Music and Caya*, 2009; *Bresson and Laprise*, 2011) demonstrate that great progress has been made in the area of nested high-resolution regional climate models (RCMs). The final quality of the results from the nested RCMs depends in part on the large-scale forcing as well as the parametrization of sub-grid scale processes.

Strong et al. (2002) performed a comparison of land surface water budget with the atmospheric based water budget over the Mackenzie basin. This study used WATFLOOD to estimate changes in surface storage. The result demonstrated a monthly water budget deemed to be within acceptable accuracy. These results show significant advancement compared to previous studies. The limitations identified in *Strong et al.* (2002) were attributed to poor spatial and temporal resolution of atmospheric data. Further studies are required using higher spatial resolution data along with an inter-comparison with independently measured or estimated data from a hydrological model.

5.3 Methodology

The Canadian Regional Climate Model (CRCM) is a logical choice for regional hydrological analysis of Canadian watersheds. However, one should first evaluate the output for the purpose for which the model is being used. The test should demonstrate that the CRCM simulations are consistent with the theory and physical understanding of the processes involved.

Recent CRCM versions are coupled with a sophisticated land surface scheme. The improved land surface parametrization provides realistic representations of water and energy exchange between the land surface and the atmosphere. The skill of the CRCM depends also on the driving data that generally comes from a global model. Therefore, the CRCM simulations will vary as a function of the model version and the forcing data (*Music and Caya*, 2009).

In the present thesis, a simple test on precipitation, and temperature from two CRCM model versions have been carried out to investigate whether the use of a sophisticated multi-layer land surface scheme improves the CRCM simulation.

A comprehensive CRCM evaluation of the chosen model has been performed on selected variables. A combined atmospheric and terrestrial water budget technique is used to estimate the components of hydrological cycle. Detailed validation methodologies are presented later in this section. The validation of the hydrological cycle components takes into account the available observations. In this thesis, in situations where direct observations are not available, data from the North American Regional Reanalysis have been used as quasi-observed. Surface flux measurements are useful for model evaluations but they are difficult to obtain from dependable sources. Attempts have been made to test these variables using quasi-observed data as well as satellite remote sensing data.

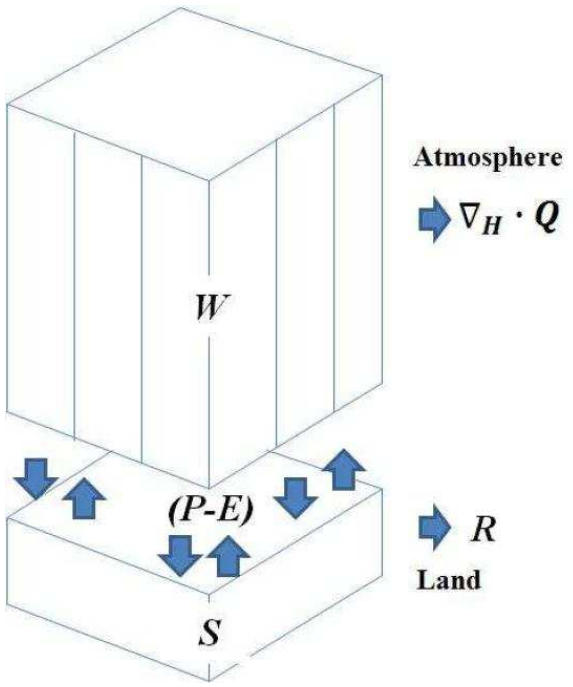

Figure 5.1: Schematic representation of the combined atmospheric and terrestrial water balance.

5.3.1 Water Budget Equations

This section presents a brief overview of the atmospheric, terrestrial, and combined water budget equations along with some explanation of their assumptions and applications in this research. For a given river basin, the terrestrial water budget equation can be written as

$$\left\{\frac{\overline{\partial S}}{\partial t}\right\} = -\{\overline{R}\} + \{\overline{P} - \overline{E}\} \tag{5.1}$$

where S (kg m^{-2}) represents the terrestrial water storage of the given basin, R (kg m^{-2}s^{-1}) represents the streamflow (assumed to include both surface and the groundwater runoff of the basin), P (kg m^{-2}s^{-1}) represents the basin precipitation, and E (kg m^{-2}s^{-1}) represents the basin evapotranspiration. The overbar denotes a temporal average (i.e., monthly means) and $\{\}$ denotes a spatial average over the basin.

Neglecting the contribution of the liquid and solid water storage in clouds, the atmo-

spheric water budget equation of the same area can be expressed as

$$\left\{\overline{\frac{\partial W}{\partial t}}\right\} = -\left\{\overline{\nabla_H \cdot \mathbf{Q}}\right\} - \left\{\overline{P} - \overline{E}\right\} \tag{5.2}$$

where W (kg m^{-2}) represents the precipitable water in the atmosphere, which means the amount of water in vapour form that would precipitate if it condensed over the region; the operator $(\nabla_H \cdot)$ represents the horizontal divergence, and $\mathbf{Q}$ is the vertically integrated horizontal vapour flux.

$$Q = \frac{1}{g}\int_{p_s}^{p_t} q\mathbf{V}dp \tag{5.3}$$

where p_s is the surface pressure, p_t is the pressure at the top of the atmosphere considered, q is the specific humidity, $\mathbf{V}$ is the horizontal velocity vector, and g is the gravitational acceleration constant. The horizontal velocity vector can be expressed as

$$\mathbf{V} = u\vec{i} + v\vec{j} \tag{5.4}$$

where u and v are the eastward and northward wind components, respectively.

The term $\left\{\overline{P} - \overline{E}\right\}$ is common for Equations (5.1) and (5.2), which establish the connection between the terrestrial and atmospheric branches of the hydrology cycle. A schematic representation of the connection between the terrestrial and atmospheric water balance is shown in Figure 5.1. Eliminating the term $\left\{\overline{P} - \overline{E}\right\}$ between these two equations, a combined equation can obtained as

$$-\left\{\overline{\frac{\partial W}{\partial t}}\right\} - \left\{\overline{\nabla_H \cdot \mathbf{Q}}\right\} = \left\{\overline{\frac{\partial S}{\partial t}}\right\} + \left\{\overline{R}\right\} \tag{5.5}$$

A comprehensive review of these classic equations of water budget is presented in *Peixoto and Oort* (1992, Chapter 12). The terrestrial storage change $\{\overline{\partial S/\partial t}\}$ can be expressed as the sum of three terms: the atmospheric storage change $\{\overline{\partial W/\partial t}\}$, the horizontal moisture

divergence $\{\overline{\nabla_H \cdot \mathbf{Q}}\}$, and stream flow $\{\overline{R}\}$. The term $\{\overline{\partial W/\partial t}\}$ can be neglected for long-term average (i.e., multi-year average) but can not be neglected for monthly averages as this term can be large for spring and fall (*Rasmusson*, 1968).

The accuracy of atmospheric water-balance computations using water vapour flux convergence depends on the size of the selected basin. The critical size for atmospheric water-balance computations using high-resolution data (e.g., a grid resolution of 45 km for CRCM) is in the order of 10^5 km^2 (*Abdulla et al.*, 1996; *Berbery and Rasmusson*, 1999; *Hirschi et al.*, 2006). The Churchill River Basin above the Otter Rapids is approximately 112,000 km^2 which meets the critical size requirement.

5.3.2 Validation approach

An integrated analysis approach is used to validate the CRCM hydrological cycle. The combined terrestrial and atmospheric water balance equations have been used to estimate components of the hydrological cycle that are not directly observed. The validation approach involves long term time averages (annual means and annual cycle) of the equation components, spatially averaged over the upper Churchill River Basin above Otter Rapids.

The terrestrial water budget in Equation (5.1) can be simplified by taking the time and spatial average for a multi-year period and over the entire basin. This results in

$$\{\overline{R}\} = \{\overline{P}\} - \{\overline{E}\} \tag{5.6}$$

where $\{\overline{\partial S/\partial t}\}$ is neglected as this term tends to zero when averaged over multi-year periods. Similarly, the atmospheric water budget in Equation (5.2) can be simplified as

$$\{\overline{\nabla_H \cdot \mathbf{Q}}\} = -\{\overline{P}\} - \{\overline{E}\} \tag{5.7}$$

where $\{\overline{\partial W/\partial t}\}$ is neglected as this term tends to zero when averaged over a large basin for a multi-year period of time. In order to validate Equations 5.6 and 5.7, observed data

are required. Observed precipitation data for the basin $\{\overline{P}\}_{obs}$ can be obtained from the Canadian gridded homogenized dataset (CANGRID). Mean annual runoff $\{\overline{R}\}_{obs}$ data for the CRB can be obtained from HYDAT.

Evaporation data are difficult to obtain at the regional scale. In order to validate the model evaporation in this study, $\{\overline{E}\}_{quasi-obs}$ is calculated by rearranging Equation 5.6 as follows

$$\{\overline{E}\}_{quasi-obs} = \{\overline{P}\}_{obs} - \{\overline{R}\}_{obs} \tag{5.8}$$

Also, the time and space averaged evaporation $\{\overline{E}\}_{NARR}$ can be derived from the North American Regional Reanalysis (NARR) dataset. The NARR is a reanalysis dataset assimilated with observations. The atmospheric moisture convergence $\{\overline{\nabla_H \cdot \mathbf{Q}}\}_{CRCM}$ derived from the CRCM over the basin can be compared with the moisture convergence $\{\overline{\nabla_H \cdot \mathbf{Q}}\}_{NARR}$ calculated from the NARR.

The terrestrial and atmospheric storage terms $\{\overline{\partial S/\partial t}\}$ and $\{\overline{\partial W/\partial t}\}$ neglected for multi-year means cannot be neglected for annual cycle validation. Quasi-observed evaporation can be calculated using the atmospheric water balance Equation (5.2) as shown below

$$\{\overline{E}\}_{quasi-obs} = \left\{\overline{\frac{\partial W}{\partial t}}\right\}_{NARR} + \{\overline{\nabla_H \cdot \mathbf{Q}}\}_{NARR} + \{\overline{P}\}_{obs} \tag{5.9}$$

Similarly, quasi-observed terrestrial storage change can be calculated from the combined Equation 5.5 as follows

$$\left\{\overline{\frac{\partial S}{\partial t}}\right\}_{quasi-obs} = -\left\{\overline{\frac{\partial W}{\partial t}}\right\}_{NARR} - \{\overline{\nabla_H \cdot \mathbf{Q}}\}_{NARR} - \{\overline{R}\}_{obs} \tag{5.10}$$

5.3.3 Validation datasets

For climate model evaluation, a gridded dataset is preferred, as gridding helps homogenization for irregular station distribution (*New et al.*, 2000). The homogenized precipitation and

temperature data from the Canadian gridded datasets (CANGRID) are used as observed data. The North American Regional Reanalysis (NARR) dataset is also used in this study. The reanalysis data is a good source of information since they are derived from observed assimilated data. A brief description of CANGRID and NARR data is provided below.

CANGRID data

The Canadian gridded data sets (CANGRID) offers monthly temperature and precipitation data from the Climate Research Branch of Environment Canada. The dataset covers Canada with a horizontal grid resolution of 50 km at the polar stereographic projection. The dataset passed through different quality control processes. The temperature time series are adjusted and homogenized using neighbouring stations (*Vincent and Gullett*, 1999). The precipitation data series are corrected in order to remove systematic biases induced by observation system change as well as for station re-location. Also, the precipitation series are adjusted for gauge catch for wind induced errors, wetting loss, and evaporation (*Metcalfe et al.*, 1997). Therefore, corrected precipitation series are representing true precipitation amount (*Mekis and Hogg*, 1999; *Vincent and Mekis*, 2006). The gridded representation of CANGRID may be different from other gridded dataset due to the interpolation technique employed for gridding. The precipitation amount may also vary from other dataset as the difference in computation of the precipitation during rehabilitation process.

North American Regional Reanalysis (NARR)

The NARR is a high-resolution climate dataset for North America. The dataset covers North America with a 32 km spatial resolution in 45 vertical layers. The NARR is an assimilation of meteorological observations into the atmospheric analysis. The NARR is a follow-up of the NCEP global re-analysis which appears to be a major improvement upon the earlier global reanalysis in terms of resolution and accuracy (*Ruiz-Barradas and Nigam*, 2006; *Mesinger et al.*, 2006).

The NARR data have been evaluated and applied by a few studies. *Choi et al.* (2009) used NARR data for hydrological modelling of selected watersheds in northern Manitoba. The study suggests that the Semi-distributed Land Use based Runoff Process hydrological model (SLURP) can be adequately calibrated with NARR data and used for modelling hydrological processes in data sparse areas. *Woo and Thorne* (2006) applied NARR data for modelling western Canada basins using SLURP and showed that the model produced reasonable output. A similar conclusion has been drawn by *Keshta and Elshorbagy* (2010) for a northern Alberta watershed. Considering these research recommendations, the NARR data have been used in validating CRCM atmospheric water budget and have also been used in a later chapter to validate the hydrological model output from VIC.

5.4 Results

Compared to previous model versions, the CRCM 4.0 or later provides a more realistic representation of water budget components by including the CLASS (*Music and Caya*, 2007). In order to evaluate the performance of the CRCM with or without CLASS, a simple test has been carried out on two selected CRCM versions. Two CRCM simulations, 'abf' using version 3.7.1. and 'ade' using version 4.1.1, were considered, using identical large-scale boundary forcing, more specifically the global reanalysis dataset from National Centers for Environmental Prediction. Model version 3.7.1 uses a simple Manabe-based (*Manabe et al.*, 1965) land surface scheme and version 4.1.1 is coupled with CLASS version 2.7 (*Verseghy*, 2000). The length of simulation in the experiment 'abf' is 1960 to 1990 and in the 'ade' is 1960 to 2005. Five years of data 1986 to 1990 have been selected for the comparison. Outputs from the regional models driven by the reanalysis (assimilated) data set are expected to be a real representation of the present climate where the model will add further detail to the driving data to produce finer resolution output.

Two variables, precipitation and temperature, have been extracted and spatially averaged

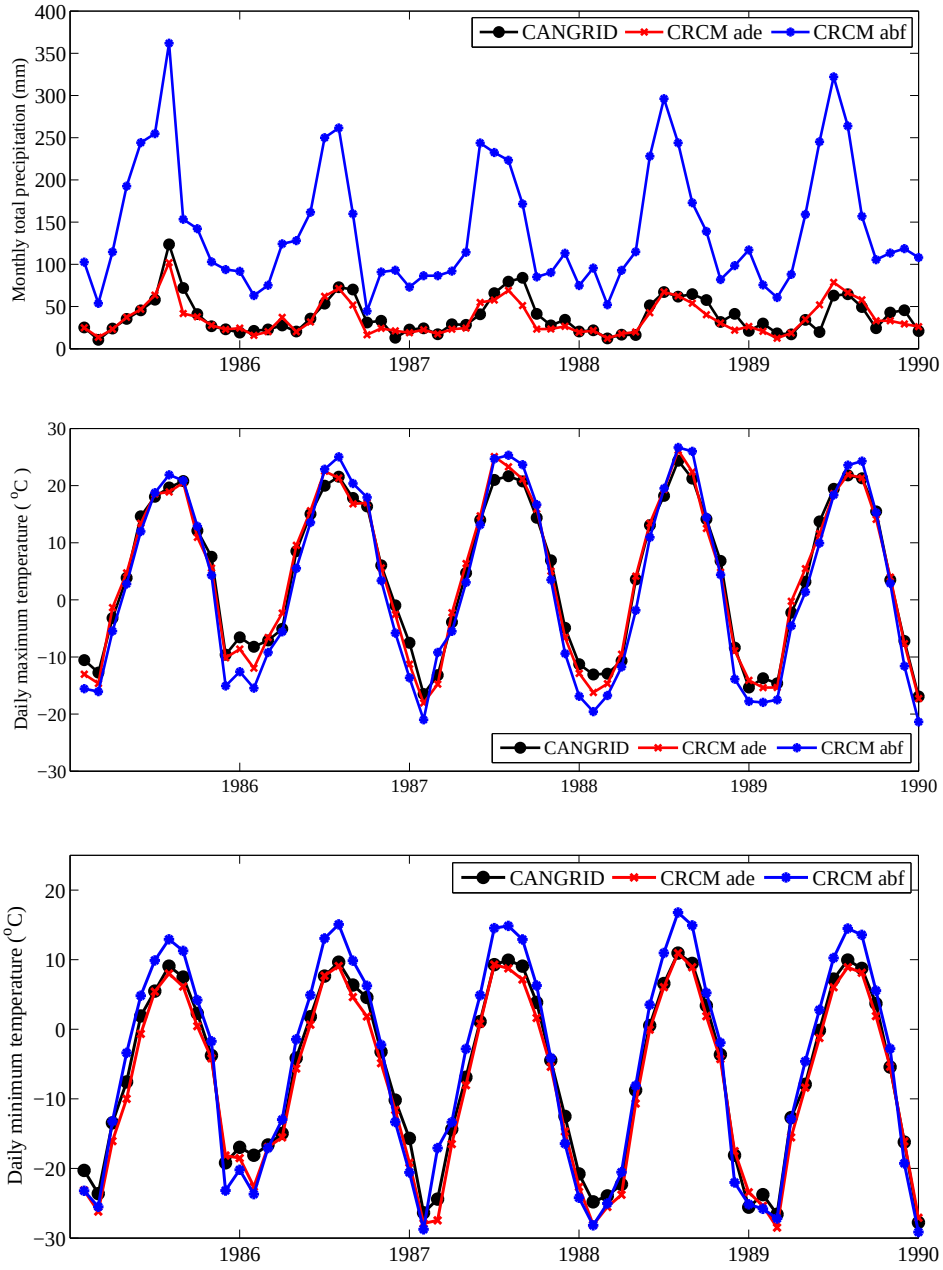

Figure 5.2: Two CRCM simulations compared with observed CANGRID. The simulation 'abf' uses model version 3.7.1 with simple land surface scheme and the simulation 'ade' uses version 4.1.1, which is coupled with CLASS. The top figure shows monthly precipitation averaged over the CRB; the middle figure shows maximum temperature °C and the bottom figure shows minimum temperature °C averaged over the CRB.

over the CRB domain to compare monthly time series. Observed precipitation and temperature data from CANGRID over the same domain for the same period have been extracted for comparison. Figure 5.2 shows a plot of two CRCM time series with observed CANGRID over the same domain. The precipitation time series (Figure 5.2 in top) shows a noticeable overestimation in experiment 'abf' compared to CANGRID, whereas the precipitation from experiment 'ade' is in close agreement with CANGRID with some minor overestimation in late summer (July-August). A similar tendency of precipitation overestimation in the CRCM 3.7 was also found by *Music and Caya* (2007). The researchers concluded that improvement of the boundary layer mixing in the land surface scheme enhanced the CRCM results, a fact that is noticeable in the precipitation of the experiment 'ade'. One can conclude from Figure 5.2 that the inclusion of a sophisticated land surface scheme in the CRCM 4.1 does produce a significant improvement in precipitation. The time series of temperature (maximum and minimum) shown in Figure 5.2 (in the middle and in the bottom) also show improvement with the use of CLASS. Based on the comparison, it can be concluded that CRCM 4.1 with CLASS performs better in simulating precipitation, and hence was selected for this study.

A further comparison of CRCM simulation 'ade' with observed CANGRID for 1999 - 2004 is shown in Figure 5.3. The monthly time series again show a good agreement with the CANGRID precipitation. Table 5.1 shows monthly precipitation and the difference between CRCM 'ade' and CANGRID. The monthly time series shows an acceptable agreement with CANGRID precipitation (mean annual precipitation is overestimated by 1.8 %). The correlation coefficient and RMSE found between the two series are 0.91 and 8.49 mm, respectively. The highest difference of CRCM minus CANGRID precipitation of 10.6 mm exhibits during early summer for the month of June. This deviation could be a limitation of the model's surface processes where convection is poorly handled. Many researchers have concluded that simulations for summer are more locally controlled than for other seasons (*Caya and Biner*, 2004). *Fowler and Kilsby* (2007) also suggested a seasonal bias correction in the RCM. Even with the improvements in CRCM 4.1.1, a seasonal bias correction should

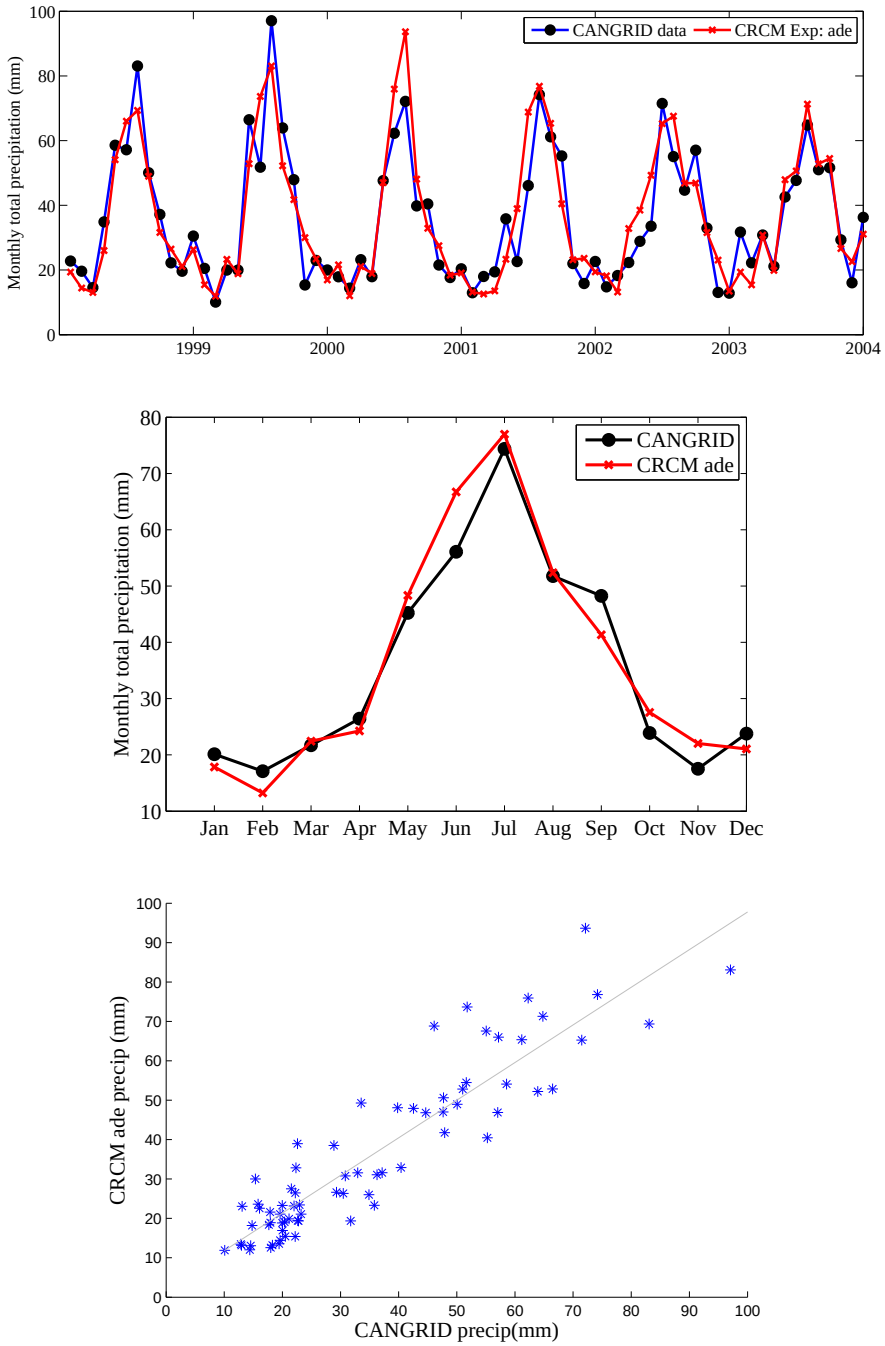

Figure 5.3: Monthly precipitation time series of the CRCM 4.1.1 from the simulation 'ade' compared with the observed CANGRID precipitation over the CRB shown in the top. The correlation coefficient and RMSE found between two series are 0.91 and 8.49 mm respectively. Annual cycle of the CRCM precipitation compared with the observed CANGRID shown in the middle. A scatter plot of CRCM monthly precipitation vs observed CANGRID is presented in the bottom.

Table 5.1: Comparison of CRCM 4.1.1 and CANGRID precipitation time series (1999-2004) averaged over the CRB.

Months	CRCM Precip (mm)	CANGRID Precip (mm)	CRCM - CANGRID (mm)
January	17.8	20.1	-2.2
February	13.2	17.0	-3.8
March	22.4	21.7	0.7
April	24.2	26.4	-2.2
May	48.3	45.2	3.1
June	66.7	56.0	10.6
July	76.9	74.3	2.5
August	52.3	51.7	0.6
September	41.3	48.2	-6.9
October	27.5	23.9	3.6
November	22.0	17.5	4.4
December	21.0	23.7	-2.7
Annual	434.1	426.2	7.8

be applied to precipitation before using the CRCM data in hydrological models. Bias correction will be discussed in Chapter 6.

5.4.1 NARR water budget components

The North American Regional Reanalysis (NARR) dataset has been used to validate the CRCM model data. *Choi et al.* (2009) used the NARR for hydrological modelling in the data sparse Northern Manitoba. The study provides a detailed comparison of NARR precipitation and temperature with NCEP-NCAR[1] Global Reanalysis - 1 (NNGR) and station data, as the researchers used these two variables as input to the hydrological model. A couple of other studies (*Nigam and Ruiz-Barradas*, 2006; *Woo and Thorne*, 2006) also evaluated NARR data from a similar perspective. In this section, we consider the atmospheric datasets from NARR rather than surface variables. The aim is to validate the vertical integrated moisture convergence and precipitable water calculated from the atmospheric variables of NARR.

Components of the atmospheric water budget (Equation 5.2) can be derived from NARR's atmospheric datasets. Specifically, $\{\overline{\nabla_H \cdot \mathbf{Q}} + \overline{\partial W/\partial t}\}_{NARR}$ should be equal to

[1]The National Center for Environmental Prediction (NCEP) - National Center for Atmospheric Research (NCAR)

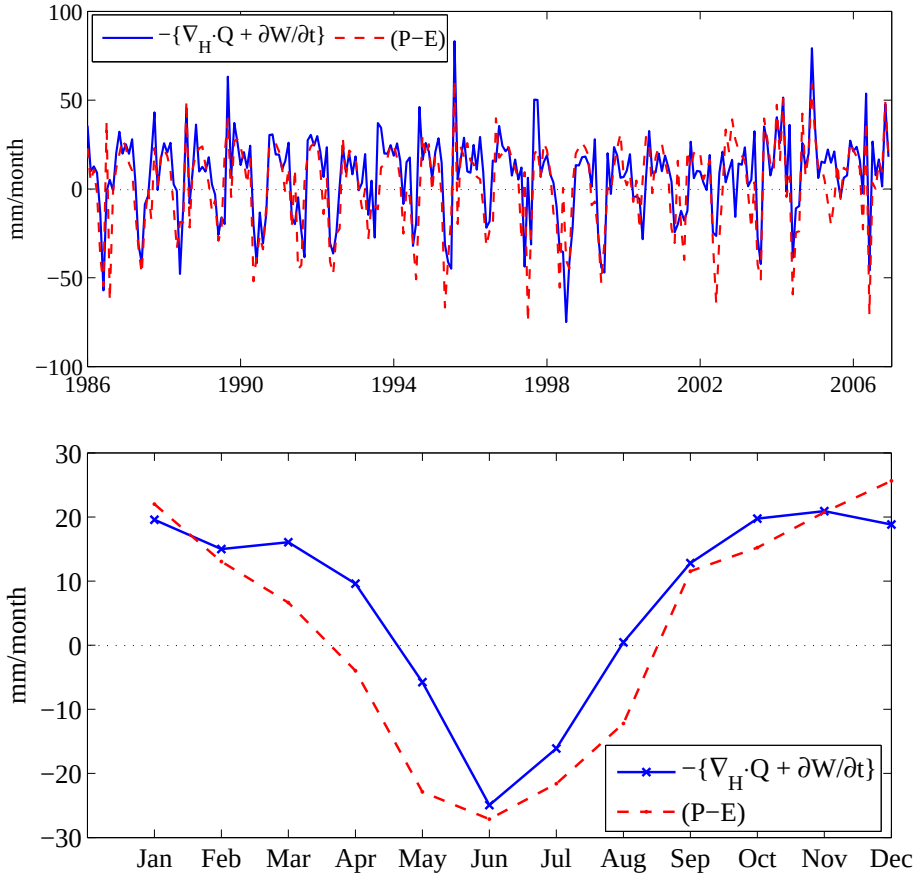

Figure 5.4: Monthly time series of NARR $\{\overline{\nabla_H \cdot \mathbf{Q}} + \overline{\partial W/\partial t}\}$ compared with precipitation minus evaporation over the CRB shown in the top. The correlation coefficient and RMSE found between the two series are 0.74 and 18.45 mm/month respectively. Annual cycle of the same two series is presented in bottom.

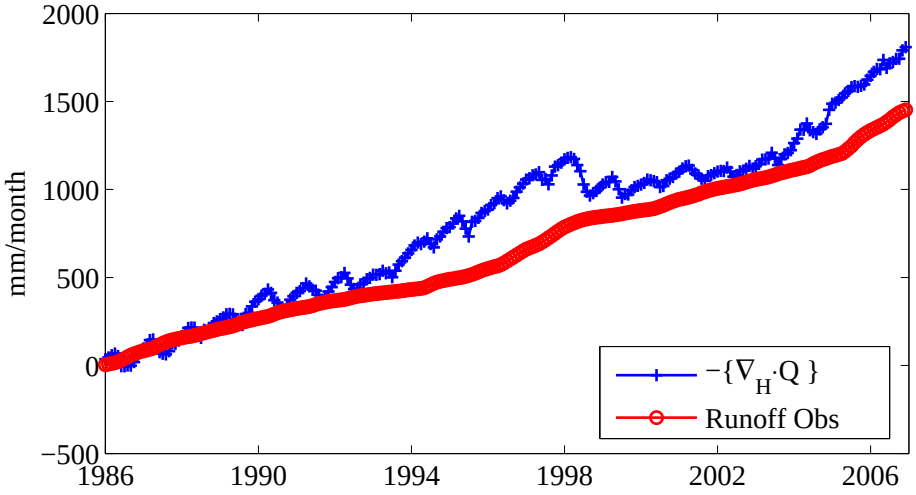

Figure 5.5: Cumulative $\{\overline{\nabla_H \cdot \mathbf{Q}}\}$ of NARR is compared with observed outflow of the CRB at the Otter Rapids (Station # 06CD002). The difference shows from the cumulative plot is 17.83 mm/year

evaporation minus precipitation calculated from NARR over the CRB. Figure 5.4 (top) shows components of the atmospheric water budget equation. It can be seen that the two time series agree fairly well except for some years. The correlation coefficient and RMSE between the two series are 0.74 and 18.45 mm/month, respectively. Figure 5.4 (bottom) shows the annual cycle of $\{\overline{\nabla_H \cdot \mathbf{Q}} + \overline{\partial W/\partial t}\}$ along with the $E - P$; $E - P$ exceeds $\{\overline{\nabla_H \cdot \mathbf{Q}} + \overline{\partial W/\partial t}\}$ in almost all months of the year except November, December and January. It is apparent here that there is a budget closure error in the model. This shortcoming could be related to the surface scheme's partitioning of moisture. In order to further explain the atmospheric water budget closure, calculated moisture divergence $\{\overline{\nabla_H \cdot \mathbf{Q}}\}$ is compared with observed outflow of the basin for a long-term basis.

From the combined atmospheric and terrestrial water budget in Equation 5.5, we can conclude that the moisture divergence term $\{\overline{\nabla_H \cdot \mathbf{Q}}\}_{NARR}$ should be equal to the outflow (R_{obs}) of the basin considering that the two terms $\{\overline{\partial W/\partial t}\}$ and $\{\overline{\partial S/\partial t}\}$ are negligible over a long period. Figure 5.5 shows the cumulative plot of moisture divergence calculated over the CRB and the observed outflow of the basin. Both cumulative plots show the overall trend. The CRB basin is a Prairie wetland and works as a flow-through system

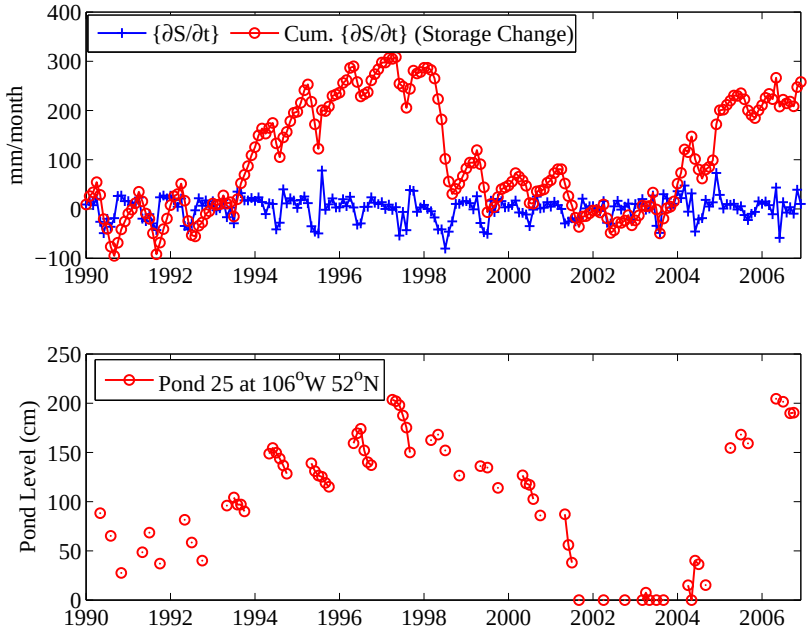

Figure 5.6: Cumulative storage (sub-surface and surface) change $\{\overline{\partial S/\partial t}\}$ of NARR is compared with observed pond level 25 at St. Denis wildlife area. The Pond 25 is located at 106°W 52°N) and the center of the watershed is at 107°W 54°N.

(*LaBaugh et al.*, 1998). The cumulative outflow plot in Figure 5.5 shows a fairly smooth line. The mean annual difference from the cumulative plot is 17.8 mm/year. The effects of dryness and wetness within the basin is dampened in the cumulative outflow plot which can be seen during 1995 to 1999. The cumulative atmospheric moisture divergence plot is providing episodes of dryness and wetness of the basin. It is known that this area suffered severe drought during 2001/2002 (*Bonsal and Regier*, 2007; *Hanesiak et al.*, 2011). The atmospheric moisture divergence indicates a drought signal for these years.

The NARR atmospheric data has been used to calculate components of Equation 5.10. The cumulative $\{\overline{\partial S/\partial t}\}$ is the storage change which is compared with the pond level data[2] shown in Figure 5.6 (bottom) published in *Conly and van-der Kamp* (2001) and *Spence* (2007). The Pond 25 is located (106°W 52°N) at the St Denis National Wildlife (SDNW) area and the center of the CRB watershed is 107°W 54°N.

[2]Pond level data used with permission by Dr. Chris Spence, Environment Canada, Saskatoon, Saskatchewan, Canada

Figure 5.6 (top) shows the sub-surface and surface storage change calculated from NARR atmospheric data in conjunction with the observed outflow of the watershed. The storage change derived from the NARR atmospheric data shows variations of storage levels that follow the observed pond level data in Figure 5.6 (bottom). The pond level data shows a record low (near zero) starting from 2002 due to severe drought during 2001-2002 and starts rising in 2004, corresponding to the cumulative storage change derived from the NARR. The peak of the pond level data recorded in the SDNW is in the spring of 1997 (*van-der Kamp et al.*, 1999) that can also be seen from the storage change derived from the NARR.

5.4.2 CRCM water budget components

The CRCM simulated hydrological cycle components are analysed in this sub-section. Long-term annual means and the annual cycle (monthly means) of observed and quasi-observed datasets are discussed. The analysis is limited to the 1986-2004 period where the most reliable observed datasets are available. The CRCM (version 4.1.1) simulation 'adj' coupled with CLASS version 2.7 (*Verseghy*, 2000) is used in this section of study.

Annual means of the CRCM water budget components

Table 5.2 summarizes annual means (1986-2004) of the atmospheric and terrestrial water budget components over the CRB. The Canadian Prairies receives an average annual precipitation of 1.25 mm/day (450 mm/year) (*McGinn and Shepherd*, 2003). The mean annual precipitation over the basin simulated by the CRCM is compared with observations obtained from three other independent datasets (CANGRID, NARR, and weather station) shown in Table 5.2. The mean annual CRCM precipitation obtained is 1.20 mm/day which is 2.5 % lower than the precipitation recorded at weather stations and 2.6 % higher than the homogenized CANGRID precipitation. The NARR mean annual precipitation is 1.32 mm/day. The CANGRID mean annual precipitation in 1.17 mm/day. The CANGRID precipitation data are corrected to remove systematic biases and account for site specific

Table 5.2: Annual means (1986 - 2004) of atmospheric/ terrestrial water budget components over the CRB in mm/day

Models/Reanalysis/Obs	$\{\overline{\nabla_H \cdot \mathbf{Q}}\}$ (mm/day)	Precipitation (mm/day)	Evaporation (mm/day)
CRCM	0.22	1.20	1.10
NARR	0.24	1.32	1.34
CANGRID	-	1.17	-
Weather/Gauge Stn.	-	1.23	-
Quasi-observed	-	-	1.02

errors caused by observation system change and station re-location, and is perhaps the most reliable precipitation data for climate studies (*Mekis and Hogg*, 1999; *Vincent and Mekis*, 2006).

The water budget of the Prairies is governed by the cold, semi-arid climate that makes evaporation difficult to estimate (*van-der Kamp et al.*, 2003). A quasi-observed evaporation is calculated from multi-year observed CANGRID precipitation and observed basin runoff following Equation 5.8. The quasi-observed evaporation is 1.02 mm/day. Since the quasi-observed evaporation is calculated from multi-year observed dataset, it should be reasonably accurate. The estimated CRCM mean annual evaporation is 1.10 mm/day which is 8% higher then the quasi-observed. The estimated NARR evaporation is even higher at 1.34 mm/day.

By combining Equations 5.7 and 5.8 over a long period the moisture flux convergence $\{\overline{\nabla_H \cdot \mathbf{Q}}\}$ should balance with precipitation minus evaporation $\{\overline{P} - \overline{E}\}$ and should show an acceptable agreement with observed basin outflow $\{\overline{R}_{obs}\}$. The observed outflow from the gauge station data over the basin $\{\overline{R}_{obs}\}$ is 0.2 mm/day. The CRCM precipitation minus evaporation (1.20 - 1.10 = 0.10 mm/day) does not correspond to the observed basin outflow. The hydrological closure error is 0.10 mm/day. A fair part of the error may be caused by the evaporation bias related to the land surface scheme due to lack of vegetation resistance (*Music and Caya*, 2007).

The moisture flux convergence $\{\overline{\nabla_H \cdot \mathbf{Q}}\}$ calculated from the CRCM is 0.22 mm/day, which should be equal to the observed basin outflow on a long-term basis. An error of

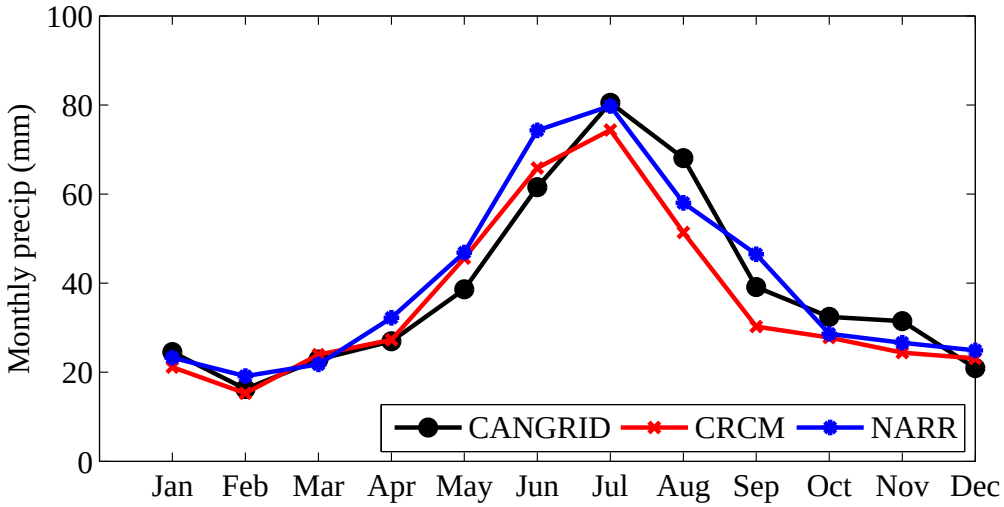

Figure 5.7: Annual cycle of precipitation comparison from CANGRID, CRCM, and NARR, averaged over the CRB for the periods of 1986-2004.

'closure' of CRCM moisture flux convergence with observed basin outflow is 0.02 mm/day. The NARR moisture flux convergence is 0.24 mm/day. Similarly, the error of 'closure' of NARR moisture flux convergence with observed basin outflow is 0.04 mm/day. The CRCM moisture flux convergence shows better 'closure' than the NARR moisture flux convergence with observed basin outflow. The error of 'closure' may be related to inaccuracies in : (a) the model's horizontal and vertical resolution and the time sampling of the moisture flux calculation, or (b) the model physics that can introduce bias in layers of atmospheric moisture and wind profiles (*Music and Caya*, 2009).

Annual cycle of the CRCM water budget components

Figure 5.7 shows a comparison of mean monthly precipitation derived from CANGRID, CRCM, and NARR over the CRB. The CANGRID dataset is gridded from observed station data that uses *Mekis and Hogg* (1999) procedure for precipitation gridding and adjustment. Since the gridded CANGRID precipitation data has been corrected and homogenized, it can be used as observed reference. The CRCM precipitation slightly overestimates during May-June and underestimates precipitation during July - November compared to CANGRID. The

Table 5.3: Comparison of monthly CANGRID, CRCM, and NARR precipitation (1986-2004) averaged over the CRB.

	Precipitation (mm)			Bias (%)[a]	
Months	CANGRID	CRCM	NARR	CRCM	NARR
January	24.5	21.1	23.3	-14	-5
February	16.2	15.2	19.1	-6	18
March	22.8	23.9	21.8	5	-4
April	26.9	27.3	32.2	1	20
May	38.6	45.6	46.8	18	21
June	61.5	65.8	74.3	7	21
July	80.4	74.4	79.8	-7	-1
August	68.1	51.3	58.1	-25	-15
September	39.1	30.2	46.5	-23	19
October	32.4	27.8	28.6	-14	-12
November	31.5	24.4	26.6	-23	-16
December	20.9	23.1	24.9	11	19
Annual	462.9	430.1	482.0	-7	4

[a]Bias (%) is calculated as $(P_{CRCM} - P_{CANGRID})/P_{CANGRID} \times 100$

correlation coefficient and RMSE between CANGRID and CRCM monthly time series are calculated as 0.94 and 6.7 mm, respectively. NARR over-estimates spring and summer precipitation during April - June compared to gridded CANGRID precipitation. The correlation coefficient and RMSE between CANGRID and NARR monthly time series are calculated as 0.95 and 6.3 mm, respectively. Annual total precipitation of CRCM under-estimates by 8% compared to CANGRID and annual total precipitation of NARR overestimates by 4% compared to CANGRID, as it can be seen from the Table 5.3. Overall, the CRCM annual cycle of precipitation shows a slightly better agreement with the CANGRID compared to the NARR precipitation. *Mishra et al.* (2012) examined NARCCAP[3] RCMs across US and found the ensemble mean percentage precipitation bias of $\pm$10% compared to observations.

The annual cycle of evaporation is presented in Figure 5.8. Along with CRCM and NARR evaporation, a quasi-observed evaporation is also presented. The quasi-observed evaporation is calculated using Equation 5.9, where $\{\overline{\nabla_H \cdot \mathbf{Q}}\}$ and $\{\overline{\partial W/\partial t}\}$ are calculated from the NARR atmospheric datasets (i.e., relative humidity, wind) and precipitation from

[3]North American Regional Climate Change Assessment Program (NARCCAP)

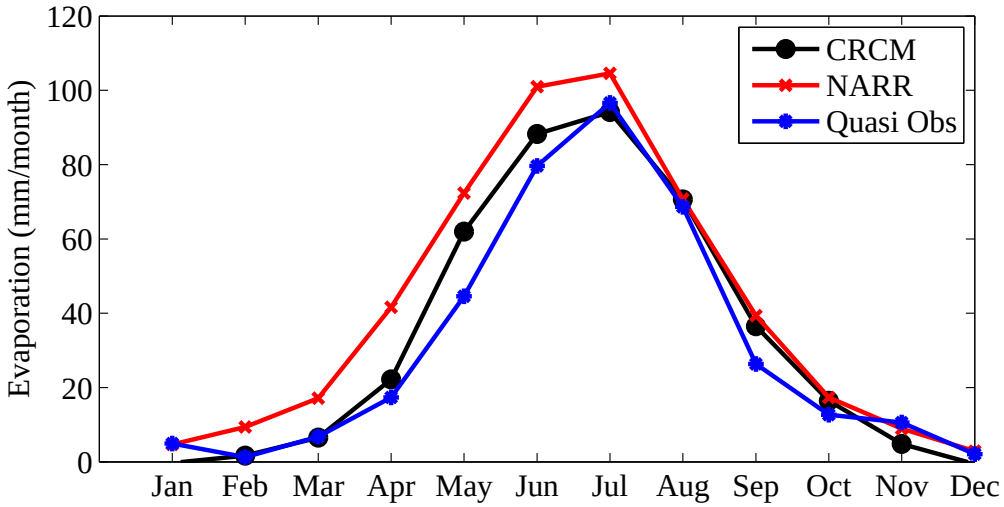

Figure 5.8: Annual cycle of evaporation presented. The quasi-observed evaporation is calculated from $E_{quasi-obs} \approx -\{\overline{\nabla_H \cdot \mathbf{Q}} + \overline{\partial W/\partial t}\}_{NARR} + P_{CANGRID}$. The CRCM and NARR evaporation is calculated over the CRB.

the observed CANGRID dataset. The CRCM simulated evaporation agrees well with quasi-observed evaporation except during spring. NARR over-estimates the quasi-observed evaporation during spring and summer months. The positive evaporation bias reaches its maximum (0.7 mm/day) in May which could possibly be related to Prairie wind and warm air temperature and soil moisture available for evaporation during this period of the year, variables which are not well captured by the NARR assimilation procedure. Overall, the implementation of CLASS in the CRCM (Version 4.1) has improved the boundary layer mixing, resulting in improvement in evaporation over the basin. Similar findings have been reported by *Brochu and Laprise* (2007). The CRCM evaporation is in good agreement with calculated quasi-observed evaporation.

Table 5.4 shows the monthly evaporation derived over the CRB. All three datasets (i.e.,CRCM and NARR, and quasi-observed) show maximum evaporation in July. Evaporation estimates are evidently more uncertain and very limited observations can be found. Inter-comparison of evaporation estimates in the context of the atmospheric water balance is an important component of this study. A comparison of Figures 5.7 and 5.8 shows that for both CRCM and NARR, precipitation are generally larger that evaporation (precipitation $\geq$

Table 5.4: Comparison of monthly CRCM, NARR, Quasi-obs evaporation (1986-2004) averaged over the CRB.

	Evaporation (mm)		
Months	CRCM	NARR	Quasi-obs[a]
January	0.00	4.67	4.94
February	1.69	9.38	1.26
March	6.53	17.16	6.79
April	22.17	41.62	17.35
May	61.97	72.32	44.58
June	88.22	100.94	79.62
July	94.13	104.55	96.6
August	70.61	70.73	68.64
September	36.49	39.37	26.34
October	16.44	17.33	12.70
November	4.81	8.91	10.58
December	0.00	2.86	2.09
Annual	403.07	489.84	371.49

[a]Quasi-obs evaporation is calculated as $E_{quasi-obs} \approx -\{\overline{\nabla_H \cdot \mathbf{Q}} + \overline{\partial W/\partial t}\}_{NARR} + P_{CANGRID}$

evaporation) during October - April, while the opposite (precipitation $\leq$ evaporation) is true in other months. This observation supports the wetland Prairies evaporation trend (*Winter and Rosenberry*, 1995; *van-der Kamp et al.*, 2003; *Szeto*, 2007; *Brimelow et al.*, 2010). The mean annual evaporation for NARR is 1.34 mm/day (490 mm/year) and CRCM is 1.10 mm/day (403 mm/year) and the quasi-observed is 1.02 mm/day (371 mm/year). *Szeto* (2007) reported CRCM evaporation of 1.05 mm/day over the Saskatchewan River Basin.

The water budget equations were presented in Section 5.3.1, where assumptions and evaluations of individual components were discussed. For annual cycle analysis (changes of monthly means), water budget equations should take into account the storage terms ($\{\overline{\partial S/\partial t}\}$ and $\{\overline{\partial W/\partial t}\}$) which are neglected for multi-year means. These terms can be significant during spring and summer (*Rasmusson*, 1968; *Music and Caya*, 2009).

The annual cycle of vertically integrated area averaged moisture flux divergence (convergence) over the CRB is shown in the top panel of Figure 5.9, and the annual cycle of precipitable water over the basin is shown in bottom panel. The CRCM moisture flux over the CRB shows convergence during October - April as can be seen from Figure 5.9 (top).

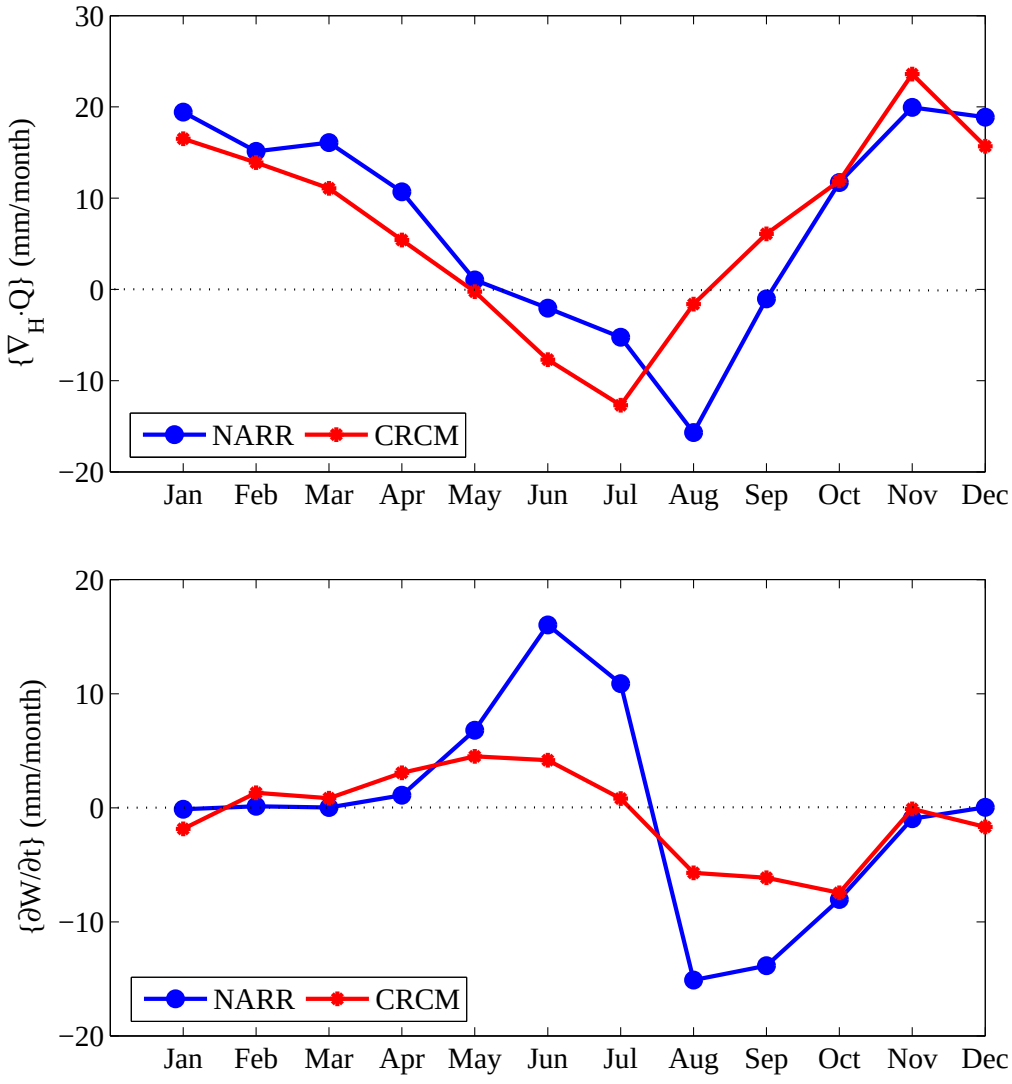

Figure 5.9: Annual cycle of $\{\overline{\nabla_H \cdot \mathbf{Q}}\}$ (in top) and $\{\overline{\partial W/\partial t}\}$ (in bottom) for NARR and CRCM over the CRB.

Table 5.5: Comparison of monthly $\{\overline{\nabla_H \cdot \mathbf{Q}}\}$ and $\{\overline{\partial W/\partial t}\}$ calculated from CRCM, and NARR atmospheric dataset averaged over the CRB.

	$\{\overline{\nabla_H \cdot \mathbf{Q}}\}$ (mm)		$\{\overline{\partial W/\partial t}\}$ (mm)	
Months	NARR	CRCM	NARR	CRCM
January	-19.44	-16.52	-0.13	-1.85
February	-15.12	-13.90	0.13	1.31
March	-16.08	-11.08	0.03	0.84
April	-10.70	-5.42	1.10	3.07
May	-1.03	0.26	6.97	4.51
June	2.05	7.71	16.03	4.16
July	5.24	12.69	10.88	0.81
August	15.68	1.62	-15.11	-5.07
September	1.05	-6.08	-13.85	-6.13
October	-11.70	-11.91	-8.04	-7.46
November	-19.95	-23.60	-0.96	-0.09
December	-18.87	-15.68	0.04	-1.68
Annual	-88.88	-81.91	-2.91	-7.58

Szeto (2007) reported similar atmospheric moisture flux tendencies for the CRCM over a Prairie basin. Prairie evaporation picks up and moisture flux becomes divergent from May and evaporation keeps contributing moisture to the atmosphere until September. During the summer months, Prairie moisture fluxes are generally divergent as evaporation exceeds precipitation (*Winter and Rosenberry*, 1995). Similar moisture flux tendencies appear in the CRCM and NARR. Table 5.5 shows the peak of moisture flux divergence (12.69 mm/month) appears for the CRCM in July, while NARR shows its peak divergence (15.68 mm/month) in August. The correlation coefficient and RMSE found between CRCM and NARR moisture flux tendencies are 0.85 and 5.94 mm.

Figure 5.9 (bottom) shows the annual cycle (mean monthly change) in atmospheric moisture storage $\{\overline{\partial W/\partial t}\}$. Typically, this storage term should be small. The amplitude of derived moisture storage $\{\overline{\partial W/\partial t}\}$ from the CRCM is much smaller compared to that of the NARR. The CRCM moisture storage term changes its sign between July and August. Despite the large variations of NARR precipitable water $\{\overline{\partial W/\partial t}\}$ during the months of May to September (Figure 5.9, bottom), the sign of NARR moisture storage also change between July and August.

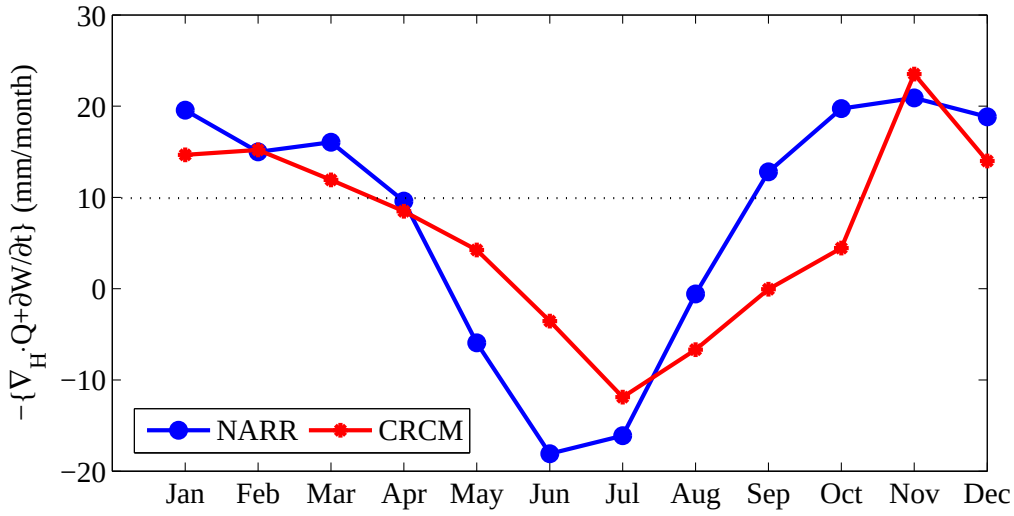

Figure 5.10: Annual cycle of $-\{\overline{\nabla_H \cdot \mathbf{Q}} + \overline{\partial W/\partial t}\}$ for NARR and CRCM over the CRB.

The noticeable variations in NARR precipitable water during May to September is likely a shortcoming of the assimilation, since the evaporation is not directly nudged or adjusted during NARR assimilation. During assimilation, when model precipitation needs to be reduced over a certain grid box, the storage term $\{\overline{\partial W/\partial t}\}$ bears the entire burden of precipitation reduction (*Nigam and Ruiz-Barradas*, 2006).

Figure 5.10 shows a comparison of moisture flux divergence with atmospheric storage $-\{\overline{\nabla_H \cdot \mathbf{Q}} + \overline{\partial W/\partial t}\}$ from the CRCM and NARR. This quantity evolves similarly in both CRCM and NARR, showing positive amplitude in the early part of the year, negative during summer months, and again becomes positive during autumn/winter months. Month-to-month amplitude differences in the two curves are noticeable. The NARR peak appears in June. The contribution of the atmospheric storage $\{\overline{\partial W/\partial t}\}$ in NARR is the cause of the moisture peak in June, as discussed earlier and presented in Figure 5.9 (bottom).

The amplitude of simulated moisture is lower in the CRCM than NARR during the summer months. Since precipitation removes moisture from the atmosphere and evaporation adds moisture to the atmosphere, the NARR evaporation greatly exceeds the CRCM during May to July. Figure 5.8 shows the evaporation bias in NARR, specifically that NARR evaporation greatly exceeds the quasi-observed evaporation during spring and summer.

The implementation of CLASS in version 4.1 of the CRCM has resulted in significant improvement in the mixing of boundary water vapour and consequently adjustment of summer moisture flux divergence (*Music and Caya*, 2007), which means summer convection is more controlled and evaporation more closely follows the quasi-observed evaporation that can be seen from the comparison of evaporation in Figure 5.8.

Figure 5.11 shows the time series of mean monthly (solid line) as well as mean annual (dots) moisture flux divergence over the basin from 1986 to 1999. The top panel of the figure shows NARR moisture and the bottom panel shows the CRCM moisture. The monthly means vary noticeably from month to month. The seasonal variation of moisture flux can be seen from the monthly time series plot. The monthly time series (Figure 5.11) indicates that usually moisture flux is divergent during summer months and moisture flux is convergent during winter months. Similar findings of atmospheric moisture flux over the Saskatchewan River Basin using NCEP-NCAR reanalysis are presented by *Liu and Stewart* (2003). The magnitude of monthly maximum and minimum shows that in a year monthly gain or loss of moisture could be as high as 65 mm/month while net moisture flux in a year is divergent in almost all years in the series both for CRCM and NARR. The long-term average annual moisture flux is 5.97 mm/month for CRCM, and 6.06 mm/month for NARR.

The ten-year average of estimated annual moisture flux is divergent as seen in Figure 5.11. The ten-year average of moisture flux result is somewhat inconsistent with the general hydrology of the basin. The atmospheric transport of moisture into and through the basin should show a balance. This implies that there may be a bias in the moisture flux calculation. Theoretically, the long-term average of moisture flux divergence should be equal to the long-term outflow of the basin. The long-term measured average outflow of the basin is about 0.2 mm/day at the Otter Rapids station (06CD002). The moisture flux convergence of the basin is calculated as 0.24 mm/day from NARR reanalysis and 0.22 mm/day from the CRCM. Therefore, there is a bias of 0.04 mm/day, and 0.02 mm/day from NARR and CRCM, respectively, in estimation of the moisture flux divergence overt the basin. This bias

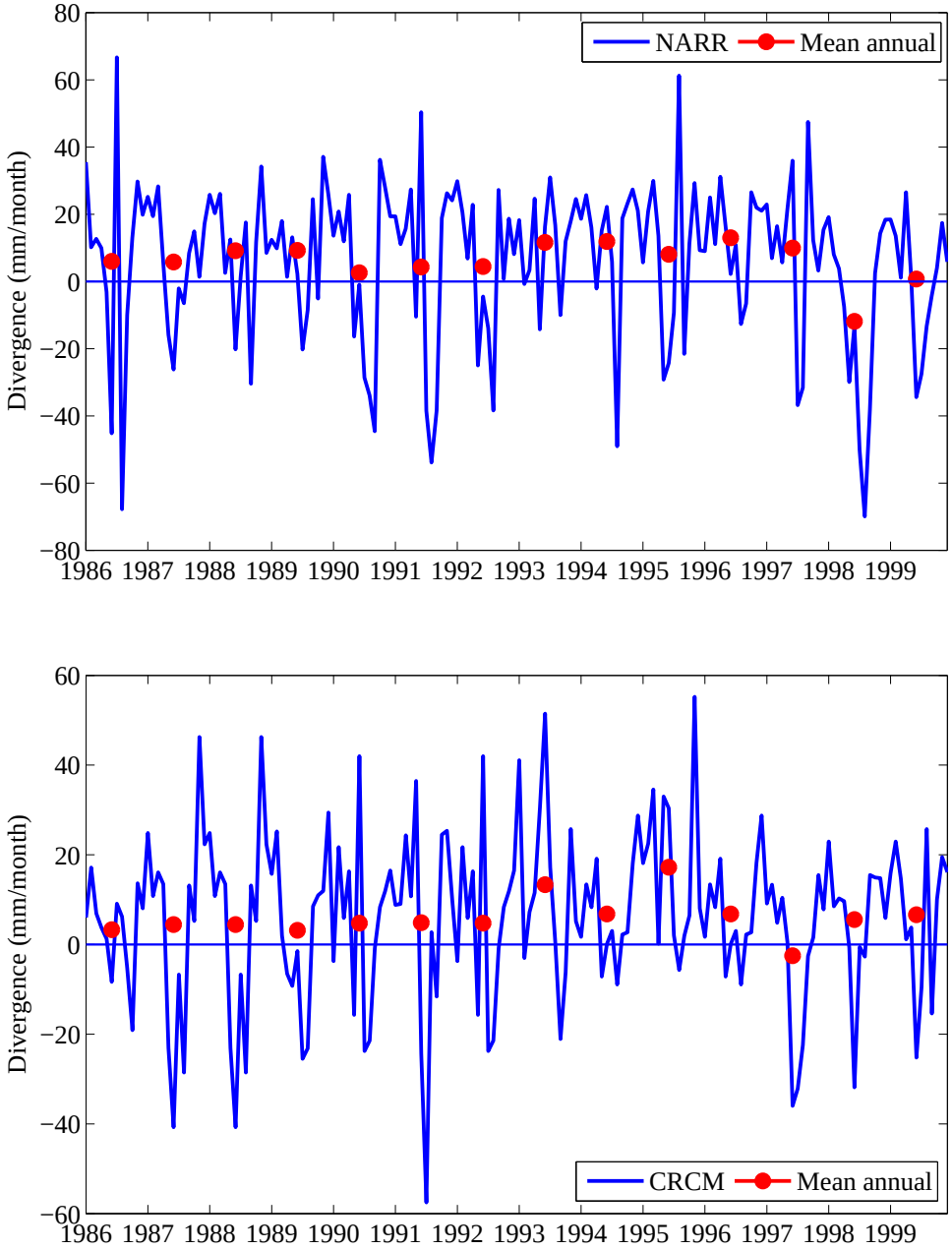

Figure 5.11: Mean monthly time series (solid line) of moisture divergence/ convergence (mm/month), and mean annual moisture divergence (dots) over the CRB from 1986 to 1999. NARR in top, and CRCM in bottom.

is probably related to the size of the domain and pressure level data used in the calculation. Despite the bias in the moisture flux calculation, the estimates provide insight into the basin's moisture flux and transport and complements our understanding of atmospheric processes relevant to hydrological modeling.

5.5 Conclusions

This study presents an attempt at developing state-of-the-art water budget estimates for the CRB and demonstrates the capability of the recent CRCM model to capture the water cycle of this northern and data-sparse region. The motivation for this undertaking is to demonstrate that a CRCM realistically represents many complex sub-grid scale processes involved in the hydrological cycle, and hence can be used in basin scale hydrological process studies. A comprehensive validation of the CRCM water budget components over the Churchill River Basin (CRB) has been performed to demonstrate the consistency of CRCM with observational data. In this regard, *Knutti* (2008) states that the most we can hope for from a model is to demonstrate that the model does not violate our theoretical understanding of the climate system and that it is consistent with the available data within the observational uncertainty.

The North American Regional Reanalysis is used as quasi-observed data where direct observational data are not available. Therefore, NARR's components of atmospheric water budget has been evaluated. Moisture divergence derived over the CRB from NARR is compared with long-term outflow of the basin, showing reasonable agreement. Also, storage change derived from the NARR atmospheric water budget equation shows reasonable agreement with pond level data from a neighbouring pond. Therefore, the NARR assimilated dataset is found to be convincing although NARR evaporation remain suspect, as discussed in Section 5.4.1.

The annual means of CRCM water budget components were first analysed. The annual

means were computed by integrating spatial averages over the basin and averaging over time (multi-year). Mean annual precipitation shows agreement with CANGRID and station precipitation. The CRCM evaporation shows reasonable agreement with quasi-observed data, whereas NARR evaporation shows an over-estimation. Implementation of CLASS in CRCM 4.1 has resulted in improvements in simulated annual mean evaporation over the basin. The CRCM simulated mean annual moisture flux convergence does not exactly correspond with the long-term observed basin outflow. However, the CRCM moisture flux convergence shows reasonable closure with the observed basin outflow compared to NARR moisture.

The annual cycle analysis shows an overestimation of precipitation during summer in both CRCM and NARR compared to the observed CANGRID. Such positive bias is related to summer convection process and inadequate boundary layer distribution in the region. Such limitations of boundary layer mixing also affect the moisture flux divergence calculation over the CRB from May to July. During summer, Prairie evaporation exceeds precipitation and thus moisture flux remains divergent. The long-term annual moisture flux over the CRB is generally divergent in both CRCM and NARR. The annual mean (multi-year) moisture flux is reasonably close in CRCM and NARR. The CRCM atmospheric moisture fluxes and storage tendencies are consistently represented, and therefore show reasonable agreement with the NARR. Atmosphere-land surface interactions are better represented by inclusion of CLASS in the CRCM.

The hydrology of the CRB is governed by complex interactions between atmosphere and surface processes. Representation of these process are related to cold region hydrology while some of them are specific for the CRB. Some of these processes are represented in very simplified form or not at all represented in the model. These simplifications will certainly affect the water budget of the region. Despite these limitations and considerable differences between the model physics that are employed in the NARR, and CRCM, the water budgets derived from these datasets for the CRB are reasonable, and in general compare well to

available observations.

Chapter 6

Bias correction of the CRCM Precipitation and Temperature

6.1 Introduction

Modelling regional hydrology using the Canadian Regional Climate Model (CRCM) data is one the main interests of this study. A distributed hydrology model has been selected in order to make the best use of gridded CRCM data with different climate scenarios as input. It is expected that the CRCM will produce more reliable data compared to global climate models as the model better resolves physical processes and the local terrain. The physical processes controlling precipitation are, in particular, expected to improve with the CRCM's higher resolution because precipitation depends heavily on topography which is more realistic at higher resolution. The expectation of improved precipitation simulation at higher resolution is well documented in the literatures (*Leung and Ghan*, 1995; *Brankovic and Gregory*, 2001; *Rauscher et al.*, 2010). The reliability of a hydrological model output is strongly dependent on the quality of the forcing data. Therefore, these forcing data must be carefully examined. In this chapter, the CRCM precipitation and temperature bias are investigated and a bias correction is devised to adjust present and future climate data. The

present study assumes that the model's ability to simulate present climate conditions will be carried over to the future climate conditions. All bias-correction methods follow the underlying assumption considering the fact that a bias correction considerably improves hydrological simulations (*Teutschbein and Seibert*, 2012).

6.2 Literature Review

The use of hydrological models with input from RCMs in climate change studies has been carried out by many researchers (*Fowler and Kilsby*, 2007; *Leander and Buishand*, 2007; *Piani et al.*, 2010). No straightforward guidelines are available regarding the most effective use of the RCM output in hydrological modelling (*Teutschbein and Seibert*, 2010). RCM simulations of temperature and precipitation are subject to uncertainties and biases which restricts their direct application for hydrological impact studies.

Christensen et al. (2008) suggest the need for bias correction when using RCMs for projections of hydrological change. This study highlights that the sources of bias derives from a model's inability to accurately simulate present-day climate conditions, which essentially means that models have varying levels of systematic biases (*van Pelt et al.*, 2009; *van Roosmalen et al.*, 2010). For example, typical biases include the occurrence of too many wet days with low intensity rain or incorrect estimation of extreme temperature and precipitation (*Ines and Hansen*, 2006).

Graham et al. (2007b) use 11 different RCMs to assess hydrological change. Their study concludes that hydrological results from different RCMs vary considerably from model to model, although all RCMs include representations of hydrology. Several other studies (*Fowler and Kilsby*, 2007; *Leander and Buishand*, 2007; *Piani et al.*, 2010) demonstrate that high-resolution RCMs suffer from varying levels of systematic biases. The researchers attribute this issue to poor partitioning of atmospheric moisture in the model's surface schemes.

In order to utilize these high resolution data, different studies (*van Pelt et al.*, 2009; *Piani et al.*, 2010) suggest that prior bias correction is required to achieve realistic output. *van Pelt et al.* (2009) apply two different correction approaches to RCM output before using the data into a hydrological model. Although the results indicate a difference between the two correction methods, bias-corrected data always improved over the uncorrected result, which confirms the importance of an appropriate bias correction.

The bias correction requires a process of scaling the climate model output in order to account for systematic errors in the climate models. The scaling of model output is performed by identifying differences between simulated series of current climate and observations. Biases can then be removed from climate control runs as well as scenario runs. Different techniques are available in order to translate RCM output into variables that can be used in hydrology models. RCMs simulations are biased by the occurrence of too many wet days with low intensity rain (*Ines and Hansen*, 2006). Therefore, the number of rainfall events with very low intensity rainfall (e.g. ≤ 0.1 mm) are sometimes adjusted (e.g., redefine as dry day; $P = 0$ mm) by applying a 'precipitation threshold'. The simple 'delta' method consists of the addition of the climatological difference between a climate scenario and a control simulation to an observed base time series. A 'linear transformation' of RCM variables can be used to adjust the mean and variance (*Shabalova et al.*, 2003; *Horton et al.*, 2006). Some researchers (*Leander and Buishand*, 2007; *Leander et al.*, 2008; *Choi et al.*, 2009) use 'power transformation' by applying a non-linear equation $P' = aP^b$ for correction. P' is the corrected precipitation. The parameters a and b can be determined iteratively by matching the mean and the coefficient of variation (CV) of the corrected precipitation with the mean and the CV of observed precipitation. *Piani et al.* (2010) use a 'transfer function' derived from historical observed and simulated cumulative distribution functions (CDFs). Different CDFs can be used depending on the data series to be corrected.

A 'precipitation model' can also be used, wherein precipitation is modelled with a stochastic weather generator (*Hansen and Mavromatis*, 2001). Observations are used

in order to derive relationships to estimate the climate parameters of the temporal and spatial precipitation model. Use of an advanced stochastic model will provide realistic data that preserve day-to-day and seasonal variability; however, they are computationally more demanding. A comprehensive review of bias correction techniques can be found in *Teutschbein and Seibert* (2010). The review indicates that although RCMs have been used in recent years to provide the hydrologist with fine-scale climate parameters for hydrological predictions, no clear rules exist as to how RCMs can be best applied in impact studies. Therefore, a bias correction procedure is outlined and discussed in the following Section.

6.3 Methodology

The main objective of the bias correction is to obtain corrected daily time series of temperature, precipitation and possibly other variables that can then be applied for hydrological simulation in order to assess long term changes in hydrology.

Different bias correction techniques were discussed in Section 6.2. The most common correction technique used to date is the delta approach (*Fowler and Kilsby*, 2007; *Graham et al.*, 2007a), often referred as 'delta change'. The 'delta change' method is a straightforward approach in which the differences in the mean values of the relevant climate variables, typically precipitation and temperature, are extracted from the control and the scenario simulations, and then superimposed on an observed data series. The method implicitly assumes that the observed variability of a climate variable will also prevail in a future climate - apart from a scaling factor. The method does not adjust the number of wet days (*Graham et al.*, 2007a) which may lead to undesirable results in the hydrological simulations of this study. Seasonality is dealt with by using monthly delta values.

In order to select a suitable technique for bias correction, the precipitation and temperature time series from the CRCM were first compared with observed station data. Two stations, Winnipeg and Churchill, which both have more then thirty years of daily data

series were selected. A comparison of biases in the seasonal and annual cycles and their corrections in these two data series are proposed later in this chapter. Two techniques for correcting precipitation and temperature bias are discussed below.

A distributed hydrological model (VIC) is used for hydrological simulation in this study. The VIC hydrological model performs simulations for each grid cell independently; thus the model requires a set of input data (i.e. temperature and precipitation) for each model grid. Therefore, each individual input grid from the CRCM data series must be corrected for bias. In order to perform the bias correction on the individual input grid, observed station data and CRCM data for both present and future have been re-gridded according to the VIC model grid. The synergraphic mapping system (SYMAP) interpolation algorithm of *Shepard* (1984), previously implemented in similar studies (*Maurer et al.*, 2002; *Paulat et al.*, 2008; *Yong et al.*, 2009), is used for the re-gridding. A detailed description of the SYMAP mapping is discussed by *McHaffie* (2000). The correction techniques that are found suitable are applied for bias correction of re-gridded CRCM dataset.

Precipitation Correction: A quantile-quantile mapping technique is used in this study to transform the cumulative distribution function (CDF) of CRCM data. The CDF is based on the two-parameter gamma distribution. Shape and scale parameters are estimated from the CRCM and observed data using the maximum likelihood estimation method. The gamma distribution is a common choice for representing daily precipitation (e.g., *Aksoy* (2000); *Piani et al.* (2010); *You et al.* (2007)).

Before fitting the gamma distribution to precipitation amounts, the dry-day probabilities of observed and simulated data are determined. A threshold value is defined and simulated precipitation amount below the threshold is set to zero. The threshold is chosen in such a way that the simulated dry-day equals the observed dry day probability.

The two-parameter gamma distribution function is given by

$$F(x;\alpha,\beta) = \frac{1}{\beta^{\alpha}\Gamma(\alpha)} x^{\alpha-1} e^{-x/\beta}; \quad x \geq 0 \tag{6.1}$$

where α is the shape and β is the scale parameter. The gamma distribution is applied to observed and CRCM simulated precipitation for current climate. Let F_{Obs} and F_{Sim} be the fitted gamma cumulative distribution functions. The corrected CRCM data can then be obtained by following quantile-quantile mapping:

$$x_{Corr-Sim} = F_{Obs}^{-1}(F_{Sim}(x_{Sim})) \tag{6.2}$$

where F_{Obs}^{-1} is the inverse of the observed CDF and $x_{Corr-Sim}$ is the corrected CRCM data. F_{Obs} and F_{Sim} are obtained for each re-gridded observed and simulated time series. The correction described by Equation 6.2 is applied to each grid cell. The correction is applied on a ninety days window block of precipitation time series over thirty years of data. *Terink et al.* (2009) use sixty five days of window block for bias correction of RCM precipitation data as input to the VIC hydrology model. At each grid cell, a bias of Δx is calculated as shown below:

$$\Delta x = x_{Corr-Sim} - x_{Sim} \tag{6.3}$$

This Δx can be obtained for each grid cell in the watershed and can be used for bias correction of future CRCM simulations. The transformed time series $x_{Corr-Scen}$ values of each grid cell can be calculated as:

$$x_{Corr-Scen} = x_{Scen} + \Delta x(F_{Sim}(x_{Scen})) \tag{6.4}$$

where $x_{Corr-Scen}$ is the transformed time series of future scenarios of each grid cell. The subscript $Scen$ in the equation denotes a future climate scenario. The transformation

technique shown in Equation 6.4 is applied to the CRCM future climate with an assumption that the bias correction Δx for each grid cell is the same for the corresponding grid for both in present and future climate.

Temperature Correction: A different bias correction technique is used for daily temperature. This method involves shifting and scaling to adjust the mean and variance and follows the work of *Shabalova et al.* (2003), *Leander and Buishand* (2007), and *Terink et al.* (2009). The bias correction is applied to each gridded maximum and minimum daily temperature. The corrected daily temperature $T_{Sim-Corr}$ is obtained as:

$$T_{Sim-Corr} = \overline{T}_{Obs} + \frac{\sigma(T_{Obs})}{\sigma(T_{Sim-Area})}(T_{Sim} - \overline{T}_{Obs}) + (\overline{T}_{Obs} - \overline{T}_{Sim-Area}) \tag{6.5}$$

where $T_{Sim-Corr}$ is the corrected daily CRCM temperature; T_{Sim} is the uncorrected daily CRCM temperature; T_{Obs} is the observed temperature; $T_{Sim-Area}$ is the uncorrected daily CRCM temperature areal average over the basin; and an over bar denotes the thirty year average; and σ is the standard deviation. Both mean and standard deviation are calculated on a fifteen days window of the thirty year time series of data. *Shabalova et al.* (2003) used a ten days window block for bias correction of RCM temperature. Corrected daily temperature $T_{Scen-Corr}$ of CRCM future climate is also obtained using Equation 6.5.

6.4 Results

In order to assess temperature and precipitation biases in the CRCM, the annual cycle, the seasonal mean, and the annual mean of these two variables are compared with observed weather station data. Two Environment Canada (EC) stations, Winnipeg and Churchill, are used. Findings from these two stations are used to determine suitable adjustment methods for bias correction. The correction techniques that are found suitable are applied to build bias corrected gridded dataset. In order to take into account multi-annual natural climate

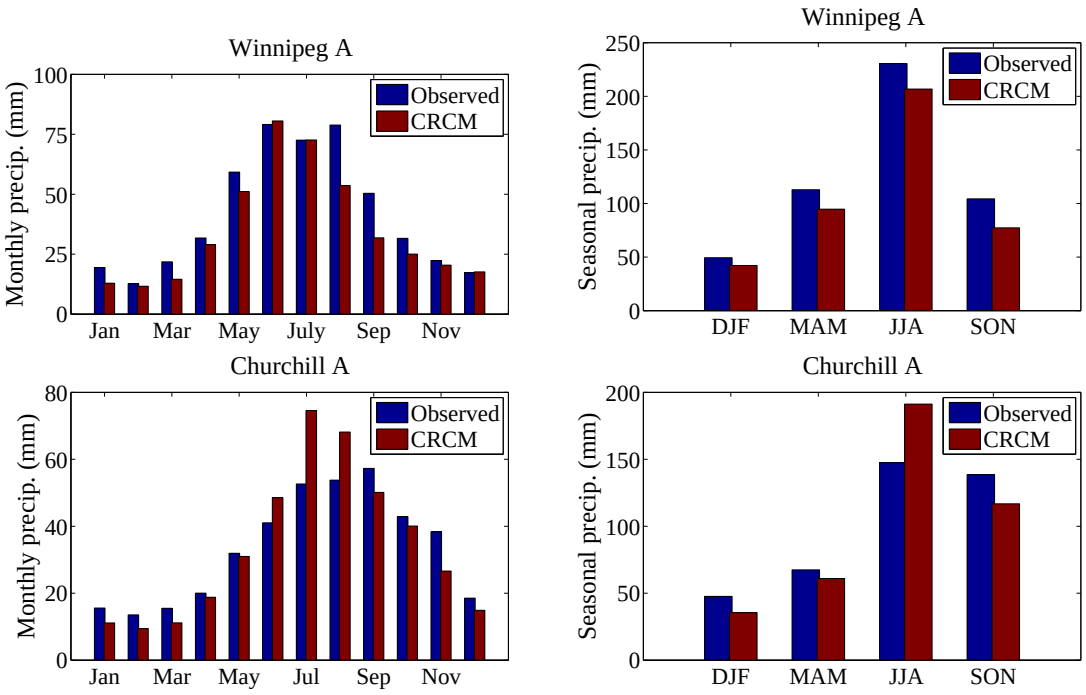

Figure 6.1: Mean monthly (left) and seasonal (right) precipitation (mm) at Winnipeg A (top), and Churchill A (bottom) stations for the CRCM simulation and observations for the period of 1961-1990.

variability, a thirty year period (1961-1990) is used to construct correction functions, and the same corrections are applied to correct the bias of the time series (1976-2005) used for hydrological modelling.

6.4.1 Precipitation

Figure 6.1 provides a comparison of mean monthly and seasonal cycles of precipitation at the Winnipeg and Churchill weather stations based on CRCM and observations for the period of 1961-1990. The CRCM successfully reproduced the basic precipitation pattern as can be seen from the monthly plots (Figure 6.1 right panels) for both stations. During the months of June and July, the CRCM overestimates precipitation at both stations; However, the CRCM precipitation for August underestimates at Winnipeg and overestimates at Churchill. The largest bias was found in July at Churchill. The precipitation bias varies over the region which was also found in *Jiao and Caya* (2006)'s study of six subregions over the CRCM North American domain.

Table 6.1: Bias corrected CRCM seasonal precipitation compared with observed station precipitation and percent bias for the period 1961-1990.

Station Name	Season[a]	CRCM Precip (mm)		Observed Precip(mm)	Bias[b] (%)	
		Raw	Corr.		Raw	Corr.
Winnipeg A	Winter	42	47	49	-15	-3
	Spring	94	108	112	-16	-3
	Summer	206	217	230	-10	-5
	Fall	77	99	104	-26	-5
	Annual	420	473	497	-15	-5
Churchill A	Winter	35	48	47	-26	2
	Spring	60	65	67	-10	-3
	Summer	191	142	147	30	-4
	Fall	116	136	138	-16	-2
	Annual	404	392	401	1	-2

[a]Winter: December-January-February, Spring: March-April-May, Summer: June-July-August, Fall: September-October-November

[b]Bias (%) from seasonal precipitation (raw/corrected) is calculated as $P_{bias} = (P_{CRCM} - P_{obs})/P_{obs} \times 100$

Even though the CRCM replicates the annual cycle, Figure 6.1 (right panels) shows an underestimation of seasonal precipitation during winter (December-January-February) and fall (September-October-November) for both stations; overestimation shows during the summer at Churchill with slightly underestimation at Winnipeg. A similar bias is also recognized in the *Jiao and Caya* (2006) study, which finds that, in central Canada, the CRCM underestimates winter and fall precipitation and overestimates during the summer. Table 6.1 shows CRCM bias (%) statistics comparing those observed at Winnipeg and Churchill. The largest seasonal positive bias of 30% is found during the summer at Churchill. The mean annual precipitation is underestimated by 15% at Winnipeg and overestimates by 1% at Churchill.

Figure 6.2 shows a Q-Q mapping of daily observed and CRCM simulated precipitation for Winnipeg and Churchill. A 45-degree solid line is also plotted to provide a reference. The Q-Q plot should approximately follow the $y = x$ line, if simulated precipitations fit well with observed precipitations. The Q-Q plot in Figure 6.2 shows that simulated precipitation is underestimated (negatively biased) at both Winnipeg and Churchill stations. It can also be seen from the Q-Q plots that the higher quantiles experiences higher bias. *Leander and*

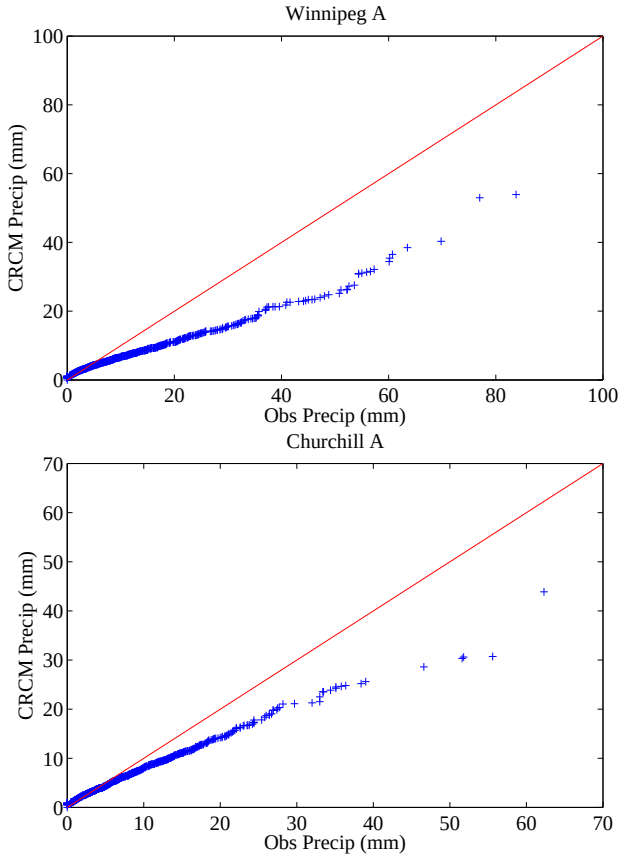

Figure 6.2: Q-Q plot of daily precipitation at Winnipeg A (top), and Churchill A (bottom) stations for the CRCM simulation and observed for the period of 1961-1990

Buishand (2007) and *Kjellstrom et al.* (2010) report a similar level of underestimation of model precipitation in higher quantiles. Unless proper treatment is provided for precipitation of higher quantiles, results may show an underestimation of climate extremes related to floods. In order to provide appropriate adjustments of these biases, higher quantiles of the CRCM precipitation are adjusted based on the corresponding ranked observed precipitation using the Q-Q mapping.

Additional checks have been performed on precipitation occurrences (i.e., wet/dry days) as they are important for hydrological modelling. A dry day is defined as a day with precipitation amount less than a threshold precipitation. Table 6.2 shows a comparison of mean annual dry day statistics at the Winnipeg and Churchill stations. At both stations, the CRCM underestimates the dry day frequency by 28%. The findings of *Sushama et al.* (2010)

Table 6.2: Dry day statistics (per year) of Observed, Raw CRCM, and Corrected CRCM, using precipitation time series for the period 1961-1990.

	Number of dry days per year		
Stations	Observed	Raw CRCM	Bias Corr. CRCM
Winnipeg A	279	217	263
Churchill A	263	204	259

also suggest that the CRCM underestimates the mean number of dry days over Canada.

Leander and Buishand (2007) and *Piani et al.* (2010) report a persistent over estimation of wet days in RCMs due to too many days of weak precipitation. In order to adjust the weak precipitation days in the CRCM, the method of 'precipitation threshold' has been applied in this study. *Sushama et al.* (2010) apply four different thresholds to CRCM simulated precipitation in order to compare dry day statistics with observations. Their results suggest that at a low precipitation threshold, the mean number of dry days is significantly underestimated. A careful selection of a suitable threshold is essential in order to adjust dry/wet day statistics. After multiple trials, a cut-off precipitation of 0.5 mm is selected and applied in this study. Table 6.2 shows mean annual dry day statistics of observed, raw CRCM, and corrected CRCM, using a precipitation time series for the period of 1961-1990. The adjusted mean annual dry days of corrected CRCM indicates a clear improvement compared, with underestimation of 5% for Winnipeg, and 1% for Churchill.

Figure 6.3 presents a comparison of mean seasonal precipitation of raw CRCM, corrected CRCM, and observations. Bias corrections are applied to daily precipitation following Equation 6.2 on the ninety-day seasonal window for the time series of 1961-1990. Significant adjustments of precipitation are required in most seasons and generally result in a reasonable agreement with observed seasonal precipitation. Table 6.1 presents the statistics of seasonal precipitation adjustments. The bias column in Table 6.1 shows the improvement after correction is applied. After adjustment, the CRCM seasonal precipitation demonstrates a close agreement with observed station data for both Winnipeg and Churchill with bias reduced to the order of 5% or less. This improvement can be considered reasonable for

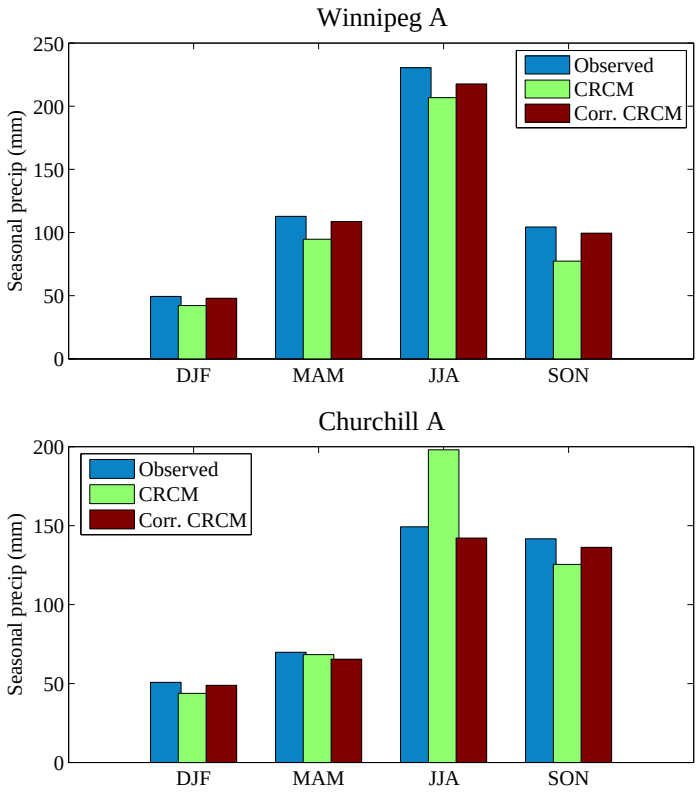

Figure 6.3: Mean seasonal precipitation (mm) at Winnipeg A (top), and Churchill A (bottom) stations for the CRCM simulation and observed for the period of 1961-1990

application of the corrected time series in hydrological modelling.

Summer precipitation simulations are more locally controlled than those of the other seasons (*Caya and Biner*, 2004; *Plummer et al.*, 2006). Therefore, improvements in bias during summer months are examined separately. Table 6.3 presents monthly statistics of bias during summer. The bias correction indicates noticeable improvement during summer months at both stations except for the month of August at Winnipeg.

The hydrological modelling performed in this study employs a distributed hydrology model (VIC) that requires bias corrected gridded data. Time series data for every grid must therefore be corrected for bias. Previous studies address this issue in a number of ways: i) Several of these studies (*Christensen et al.*, 2008; *Ashfaq et al.*, 2011) use available gridded observed data to adjust climate data of the corresponding grid. ii) Some studies (*Ines and Hansen*, 2006; *Sennikovs and Bethers*, 2009) construct a bias correction function

Table 6.3: Bias corrected mean monthly CRCM precipitations (Summer: June-July-August) compared with observed station precipitation and percent bias for the period 1961-1990.

Station Name	Month	CRCM Precip (mm)		Observed Precip(mm)	Bias (%)	
		Raw	Corr.		Raw	Corr.
Winnipeg A	June	89.54	80.54	79.10	13	2
	July	72.62	73.86	72.56	0	1
	August	53.62	64.42	78.82	-32	-18
Churchill A	June	50.88	36.91	41.69	22	-11
	July	76.74	56.66	53.17	44	6
	August	70.39	49.95	54.42	29	-8

from observed station data and corresponding control simulation. The correction functions are than spatially interpolated and applied to all model grids.

In this research, observed station data within the basin or in the neighbourhood of the basin are used to build a gridded dataset of 1/8° resolution according to VIC model grid. The gridding is performed by using the SYMAP interpolation algorithm of *Shepard* (1984), which is inverse square of the distances to the target grid cell, previously implemented in similar studies (*Maurer et al.*, 2002; *Paulat et al.*, 2008; *Yong et al.*, 2009). For a target grid cell, values are calculated from the surrounding data points within a search radius. The radius is chosen in such a way that at least four stations contribute to the interpolation. A detailed description of the SYMAP mapping is discussed by *McHaffie* (2000). Similar gridding is applied to CRCM present and future climate data. The gridded observed and the CRCM dataset is then used to derive a bias adjustment for each grid using Equation 6.3. The same bias adjustment of the grid is used in future CRCM simulations following Equation 6.4, with an assumption that the same bias correction is applicable for both present and future climates.

Figure 6.4 presents the mean monthly precipitation plot along with error bars for raw CRCM (top panel) and bias-corrected CRCM (bottom panel), along with observations for the period of 1976-2005. The error bars show the standard deviation of the monthly data series. Figure 6.4 suggests that most adjustment appears during May to August.

Table 6.4 presents the overall statistics of raw and corrected CRCM and observed

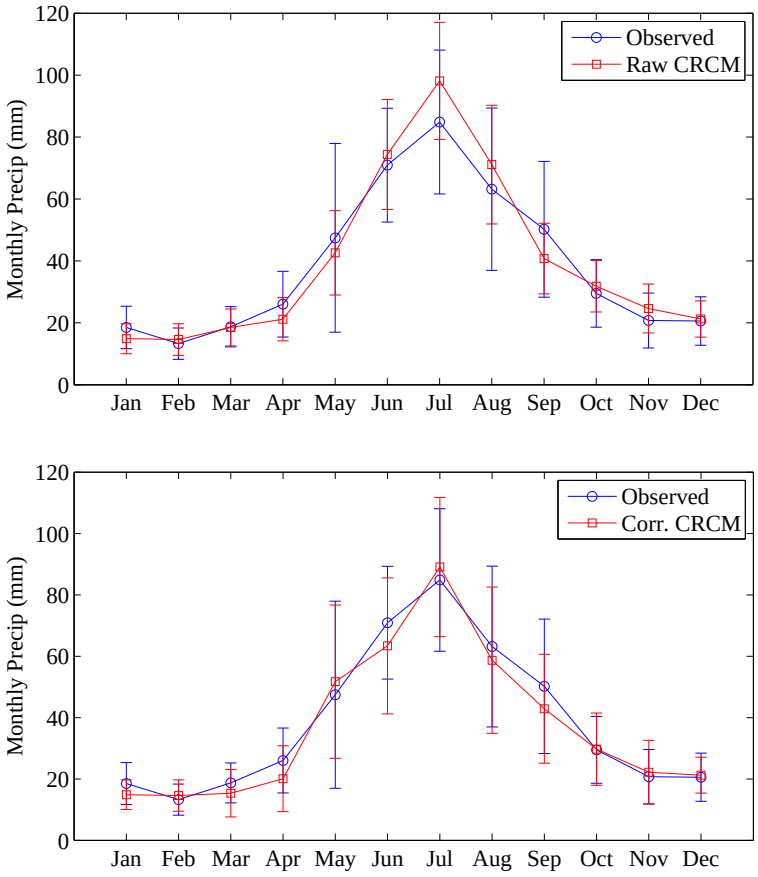

Figure 6.4: Mean monthly precipitation for raw CRCM (top) and bias corrected CRCM (bottom) simulations with observations for the period of 1976-2005 over the Churchill River basin.

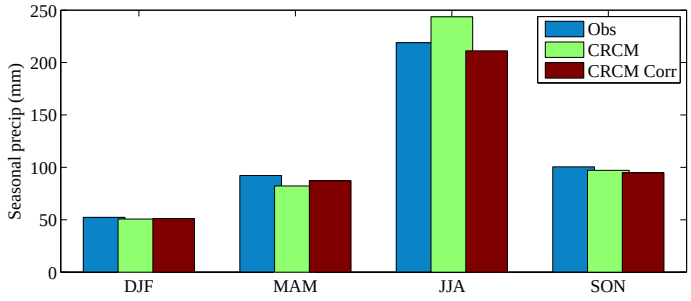

Figure 6.5: Mean seasonal precipitation for raw CRCM, bias-corrected CRCM, and observations for the period of 1976-2005 over the Churchill River basin.

Table 6.4: Summary statistics of precipitations for Raw CRCM, Corr CRCM, and Observed for the period 1976-2005 averaged over the Churchill River basin.

Statistics	CRCM Precip (mm)		Observed
	Raw	Corrected	Precip (mm)
Annual:			
Minimum	14.60	14.60	13.27
Maximum	98.16	89.07	84.85
Mean	39.48	37.00	38.66
Std	27.45	24.12	23.98
Seasonal:			
Average winter (DJF)	50.69	51.08	52.34
Average Spring (MAM)	82.26	87.16	92.17
Average Summer (JJA)	243.64	211.16	218.93
Average Fall (SON)	97.17	94.77	100.45

precipitation. Annual statistics show improvements after bias correction. The bias-corrected results for maximum precipitation statistics show a slight overestimation (Table 6.4 annual). Figure 6.5 presents mean seasonal precipitation for raw CRCM, bias-corrected CRCM, and observations for the period of 1976-2005. The seasonal precipitation exhibits improvement after bias correction. The difference in CRCM seasonal average precipitation from Table 6.4 is approximately $\pm 5\%$ of the observed precipitation.

Figure 6.6 shows the Q-Q plot of daily precipitation averaged over the basin for raw CRCM (top panel) and bias corrected CRCM (bottom panel) simulations with observed, for the period of 1976-2005. After bias correction, the Q-Q plot shows an overall improvement in the daily precipitation series except for several extreme outliers. The gamma distribution is employed in this research to represent the distribution of precipitation in order to provide an overall good fit to precipitation. *Rasmussen et al.* (2012) considered that extreme values cannot be represented with a single gamma distribution and hence should be treated separately.

6.4.2 Temperature

The bias correction of temperature is simpler and more straightforward than that of precipitation, as the CRCM simulated temperature shows (Figure 6.7) better resemblance to the

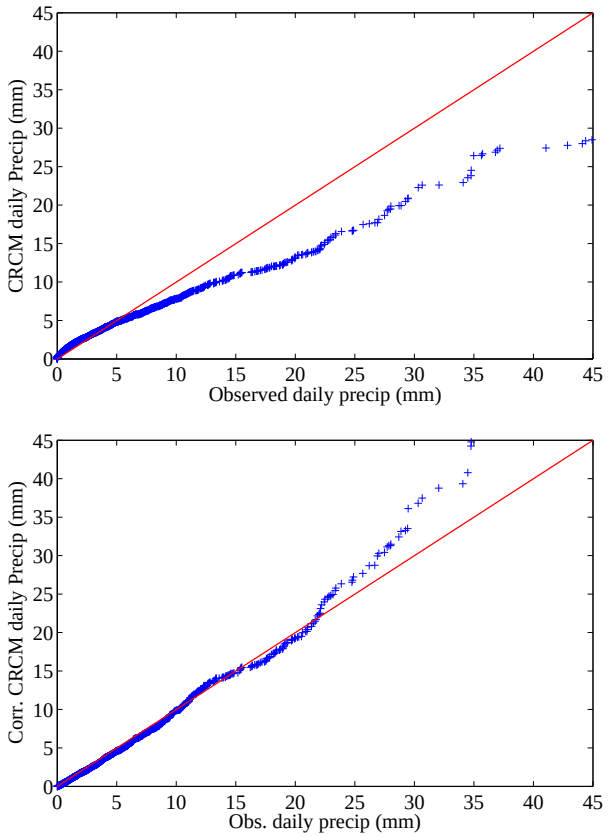

Figure 6.6: Q-Q plot of daily precipitation for raw CRCM and bias corrected CRCM simulations with observations for the period of 1976-2005 over the Churchill River basin.

observed. The temperature bias correction involves shifting and scaling in order to adjust the mean and variance, respectively. The CRCM daily temperature at 2m is used in this study. The temperature bias at the Winnipeg station for 1961-1990 is examined in order to understand the characteristic of bias. Figure 6.7 provides a plot of daily (top) and mean monthly (bottom) temperatures. Although the CRCM simulations reasonably reproduces the annual cycle, the CRCM systematically underestimates the temperature. The largest underestimation of CRCM mean monthly temperature compared to observed is around 5.5°C and is found during the summer months, Figure 6.7, bottom panel. These findings are in agreement with *Plummer et al.* (2006) who report that the CRCM simulated surface air temperatures are colder than the observations.

Bias correction is applied to the CRCM daily temperature series following Equation 6.5

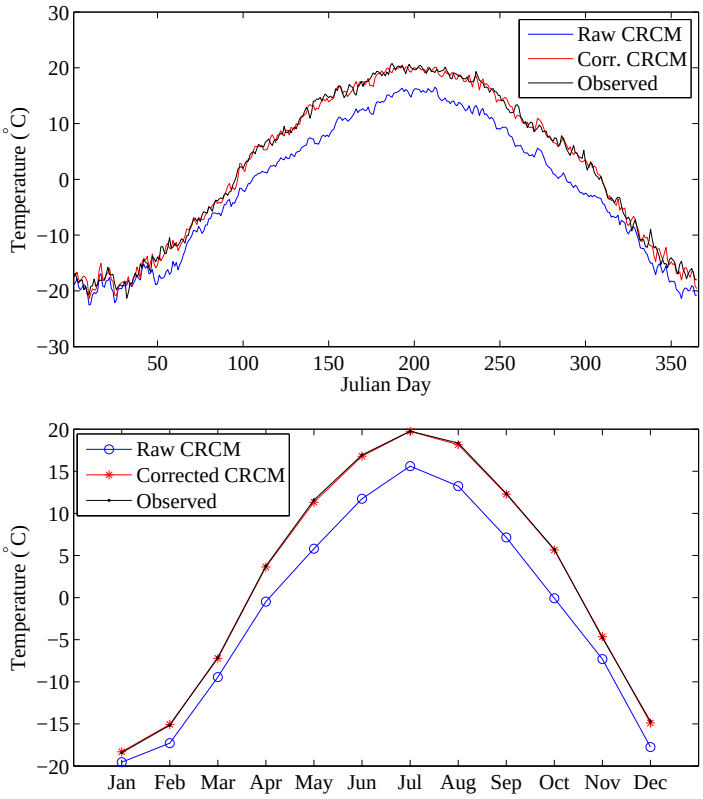

Figure 6.7: Daily temperature for raw/corrected CRCM and mean monthly raw/corrected CRCM with observations for the period of 1961-1990 at Winnipeg A.

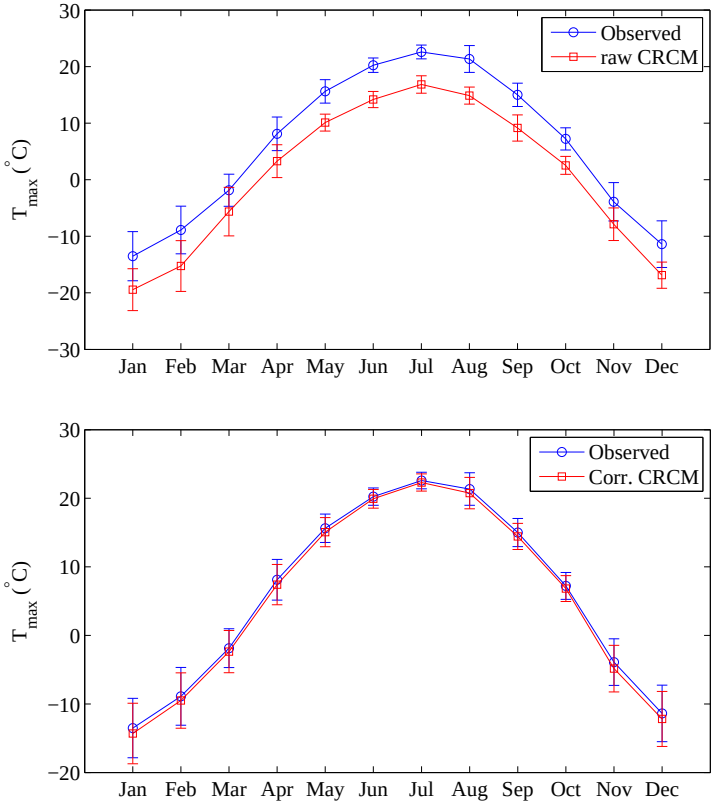

Figure 6.8: Daily T_{max} for CRCM (raw/corrected) compared with observations for the period of 1976-2005 averaged over the Churchill River basin.

Table 6.5: Summary statistics of annual temperature (T_{max}/T_{min}) for Raw CRCM, Corr CRCM, and Observed for the period 1976-2005 averaged over the Churchill River basin.

Variables	Annual statistics	CRCM temp. (°C)		Observed temp. (°C)
		Raw	Corr.	
T_{max}	Mean	0.49	5.30	5.88
	Std	13.12	13.48	13.34
T_{min}	Mean	-8.06	-6.50	-5.95
	Std	12.58	13.01	12.85

in the methodology section. The bias-corrected CRCM temperature demonstrates excellent improvement throughout the year and compare well with observed temperatures (Figure 6.7) at Winnipeg. For all 12 months, the differences between CRCM and observed temperatures do not exceed 0.5°C.

The hydrological modelling performed in this study requires time series of maximum and minimum temperature. The CRCM and observed temperature data are therefore interpolated onto the VIC model grid. Bias correction is applied on time series of the interpolated CRCM daily temperature. The hourly temperature data are used to build time series of daily maximum temperature (T_{max}) and daily minimum temperature (T_{min}). Figure 6.8 shows mean monthly T_{max} plots along with errorbars for raw CRCM (top panel) and bias corrected CRCM (bottom panel), along with observations for the period of 1976-2005. The error bars indicate the standard deviation of the monthly data series. Daily CRCM T_{max} shows systematic underestimation compared to the observed mean for all 12 months over the basin, with biases ranging from 3°C to 6°C. After performing the bias correction, the CRCM T_{max} shows considerable improvement for all 12 months of the year, with maximum differences between CRCM and observed ranging from 0.3°C to 0.8°C.

Figure 6.9 shows mean monthly T_{min} raw (top) and bias corrected (bottom) CRCM along with observed mean monthly temperature. T_{min} shows a similar systematic underestimation as T_{max} throughout the year with a magnitude of underestimation of 3°C. After bias correction, the CRCM T_{min} suggests an excellent improvement for all 12 months of the year, with maximum differences between CRCM and observed ranging between 0.3°C and 0.5°C.

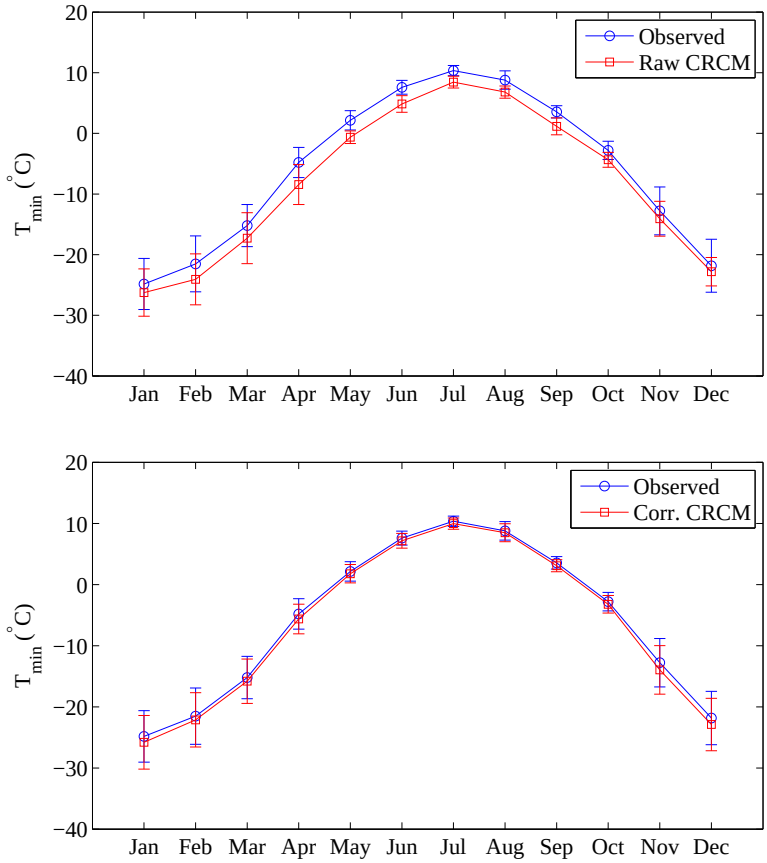

Figure 6.9: Daily T_{min} for CRCM (raw/corrected) compared with observed for the period of 1976-2005 averaged over the Churchill River basin.

Table 6.5 presents summary statistics of the annual temperature (T_{max}/T_{min}) for raw CRCM, corrected CRCM, and Observed for the period 1976-2005 averaged over the basin. Table 6.5 suggests that the bias correction mainly affects the mean and only imparts relatively small changes to the standard deviation. This finding signifies that the CRCM performs more effectively in simulating the variability of the daily temperatures than it does in simulating the mean level. Results shows that bias correction method employed for temperature correction performs well in removing bias in temperatures (T_{max}/T_{min}) and observed annual statistics are fully preserved.

6.5 Conclusions

In this chapter, bias correction for precipitation and temperature is discussed. The bias is defined as the difference between simulated model data and observed data. Bias correction is a post processing step of CRCM data before applying them as input to a hydrological simulation. The bias treatment does not add skill to the CRCM simulations but fixes problems with systematic errors. The bias correction adjusts the CRCM time series so that they have the same statistics as the observed station data. Bias correction is applied to the daily time series. In order to build a set of observed gridded data, selected station data within the basin and in neighbourhood of the basin are interpolated using the SYMAP algorithm of *Shepard* (1984). No correction is applied to the observed station data during interpolation. The interpolation of station data to a grid does not introduce a significant error.

As mentioned in the methodology section, bias correction is much more complicated in the case of precipitation than in the case of temperature. No single bias correction procedure has been generally argued upon and in practice and the correction method must be chosen as a function of the modelling objectives (*Teutschbein and Seibert*, 2010). In this research, a combination of techniques are applied for precipitation adjustment.

The results from the precipitation bias correction shows that techniques employed here

performed successfully, not only for mean quantities but also for improvement in the number of wet/dry days statistics which are quantities that may have a significant influence on hydrological modelling. Also, the results from the temperature bias correction shows substantial improvements during all months of the year, although a simple technique of shifting and scaling of mean and variance is used. The bias-corrected CRCM climate presented in this chapter will prove to be useful for the hydrological change assessments over the CRB presented in the next chapter.

Despite the considerable improvement of precipitation and temperature time series after applying bias corrections, some shortcomings remain (e.g. precipitation extreme outliers). This observation could be related to limitations of the bias correction techniques employed in this research, limitations of RCMs itself, or inconsistencies of the observed station data used as a basis for bias adjustment. One of the known RCM limitations is related to its land surface process and its ability to capture summer convection as well as other surface processes (*Music and Caya*, 2007).

Chapter 7

Assessing Changes in Hydrological Processes using the VIC model

7.1 Introduction

Greater knowledge of climate variability is required in order to understand the potential impacts of changes in hydrological processes (*Xu et al.*, 2005). As discussed in the literature review (Section 2.2), a regional climate model (RCM) is a useful tool to investigate regional climate variability. Climate data from the Canadian Regional Climate Model (CRCM) are used in this chapter in order to investigate changes in hydrological processes. In Chapter 5, an attempt was made to evaluate regional hydrology from the atmospheric dataset of the CRCM, using the combined atmospheric and terrestrial water balance technique. In this chapter, changes in hydrological processes will be examined by using the distributed hydrological model VIC, with inputs from the CRCM. The Churchill River Basin (CRB) above the Otter Rapids (station # 06CD002) is modelled using the VIC model. Modelling of the CRB hydrological processes is not an easy task due to the complexity of the terrain and scarcity of data which make hydrological model calibration and validation difficult.

The goal of this effort is to capture adequately the physics of the watershed, especially

the winter processes. Calibration of the model is achieved through the comparison of the model simulated streamflow with the available measured streamflow record. Assessing the performance of a hydrological model from its observed and simulated flow only may not be sufficient. The climate variable inputs from the CRCM are propagated through the modelled hydrological systems and produce the hydrological variables of interest. If the internal variables from the model can be demonstrated to compare favourably with measured values, then the confidence in the model simulated streamflow will increase. Additionally, the study will provide more conclusive estimates of water budget components by comparing the hydrological model output with the output obtained from the atmospheric-based water budget estimates from Chapter 5.

7.2 Literature Review

The impacts of the changing climate on the regional hydrology is already evident (*IPCC*, 2007a, Chapter 11). Methods used for assessing changes in regional hydrology have evolved over time. The use of a RCM in the study of regional hydrological process changes have been pursued by several researchers (*Leander and Buishand*, 2007; *van Roosmalen et al.*, 2010; *Piani et al.*, 2010). These studies used RCMs as input to hydrological models in order to provide flow estimations as well as to study regional/basin scale processes.

The use of future climate projections from RCMs is an obvious choice for assessing the impacts of regional-scale climate change on hydrological processes, as discussed in Section 2.2. These RCM simulations are depending on the GCM data used at the boundaries and the chosen emission scenarios. *Graham et al.* (2011) demonstrated the potential use of RCM projections in assessing hydrological responses to climate change. *Olsson et al.* (2011)'s study suggests that the RCM simulations providing the best representations of the recent past may provide dependable projections of the near future that can be used for climate change assessments. In Chapter 5, it was demonstrated that the CRCM's present climate is

in agreement with available observations and with re-analysis data.

Canadian regional climate projections from the CRCM are used in this study. The CRCM projections of future climates are driven by CGCM3 for the emission scenario SRES-A2. The CRCM simulations used in the present study were realized by the Ouranous Consortium and provided by the Ouranous climate simulation team. A list of the CRCM simulations used in this research are provided in Table 4.1.

Selection of an appropriate hydrological model is important (*Leavesley*, 1994). Different hydrological models were discussed earlier in Section 2.3.3. The distributed hydrological model VIC has been selected for the present study in order to account for the spatial variability in sub-basin scale processes as well as to make best use of gridded spatially-distributed RCM data. The CRCM data used as input to the VIC model has been corrected for biases. Bias correction of CRCM data was discussed in Chapter 6.

The VIC model has been applied to major North American basins such as the Colorado River basin (*Christensen and Lettenmaier*, 2007; *Cayan et al.*, 2010; *Gao et al.*, 2011), the Columbia River basin (*Hamlet et al.*, 2010), and the conterminous United States (*Maurer et al.*, 2002). *Hurkmans et al.* (2010) investigated streamflow dynamics using the VIC model under three scenarios of the regional climate model. *Liang and Xie* (2003) discuss the surface runoff generation process and interactions between surface and groundwater using the VIC. Their results show that the VIC model properly simulates the total runoff and groundwater table of the Little Pine Creek watershed in Pennsylvania for multiple years. *Gao et al.* (2011) used RCMs from the North American Regional Climate Change Assessment Program (NARCCAP) to evaluate implications of climate change for the discharge of the Colorado River basin. Another study, by *Liu et al.* (2009), used the VIC model to assess the impact of climate change on streamflow with input data from PRECIS (*Jones et al.*, 2004) used to drive the model. Both studies suggest that RCM data may be used effectively with the VIC model for hydrological change assessment.

7.3 Methodology

This chapter will present the approach to modelling regional hydrology under different climate conditions using the VIC hydrology model. The bias-corrected CRCM climate data are used as input to the hydrology model. The Churchill River basin (CRB) above Otter Rapids has been selected for this research. Use of area specific information such as digital elevation maps (DEMs), land use, and soil data, climatological data, as well as hydrometric data plays a key role in the modelling process. The following subsection will present a site description and a detailed discussion of data used. Model calibration and validation are also discussed in this chapter. The VIC model calibration is performed using the observed streamflow at Otter Rapids (station # 06CD002 shown in Figure 3.4). Model validation is also performed using streamflow at the basin outlet. Apart from the outflow validation, important hydrological variables such as evaporation, snow, and soil moisture are chosen for a detailed evaluation of VIC's performance and will be presented later in the chapter.

Once the VIC model is calibrated and validated over the watershed with observed data, the validated model can be used with CRCM climate simulations. Streamflow is the aggregation of many different hydrological processes in the watershed. Streamflow trends are evaluated and presented using a non-parametric Mann-Kendall (*Mann*, 1945; *Kendall*, 1975) test. Assessment of trends for changes in streamflow includes tests for mean annual, maximum and minimum streamflow along with different percentiles of streamflow. Besides the streamflow comparison, a detailed analysis of snow water equivalent, snow depth, and soil moisture are also presented in order to evaluate hydrological responses in a changed climate.

7.4 Study region and Data

7.4.1 Churchill River Basin

The Churchill River basin has been selected for this study. A detailed discussion of the basin is provided in Chapter 3. The downstream portion of the Churchill River basin is highly regulated because of its diversion for hydro-power development. Therefore, this study will mainly focus on the basin area upstream of the diversion. The basin upstream of the Otter Rapids hydrometric station (# 06CD002) is selected for modelling. The flow regime at Otter Rapids is natural. A map of the delineated basin is shown in Figure 3.5.

7.4.2 Data

A detailed description of the climatological and hydrometric data used in this research is presented in Section 3.1.1 and 3.1.2, respectively. The VIC hydrological model requires input for each model grid. Therefore, in order to perform calibration and validation, observational temperature and precipitation data from selected weather stations are gridded at a spatial resolution of 1/8° using the SYMAP interpolation algorithm of *Shepard* (1984). The interpolation technique is based on an inverse-square-distance rule. A detailed description of the SYMAP mapping is given in *McHaffie* (2000). The minimum and maximum temperatures are derived from the daily time series of station data. In the gridding process, the temperature data were corrected (0.65°C/100m) to the center elevation of grid cells. No correction was applied to the daily precipitation data.

The CRCM climate simulations are used in this study (see Chapter 4). The CRCM climate simulations includes a baseline climate (1976-2005) with observed greenhouse gas and aerosol (GHG+A) evolution and two time slices of future climate (2030s: 2020-2049, and 2050s: 2041-2070) with the SRES A2 scenario. The CRCM baseline and future climate data are also re-gridded at the same spatial resolution of 1/8° of the VIC model grid.

7.5 The VIC model

7.5.1 Description

The Variable Infiltration Capacity (VIC) model is a surface water and energy balance model. The single-layer original version of VIC was developed by *Wood et al.* (1992) as a land-surface hydrology parameterization scheme for general circulation models (GCMs). *Liang et al.* (1994) modified this model to include two soil layers, thereby improving the water and energy balance. Later, *Liang et al.* (1996) determined that an additional thin top layer of 5-15 cm significantly improved the evapotranspiration predictions in arid climates; thus, a third layer was added. The spatial distribution of precipitation, infiltration, and vegetation are considered in the model to simulate the water and energy budget at the surface. *Liang and Xie* (2001) modified the surface runoff parameterization in VIC to express dynamically both the infiltration excess (Horton) and the saturation excess (Dunne) runoff.

The VIC model was upgraded to include a two layer snow model (*Andreadis et al.*, 2009). *Bowling et al.* (2004) added the blowing snow algorithm in the VIC. *Bowling and Lettenmaier* (2009) incorporated a lake and wetland algorithm in the VIC model as storage of runoff in lakes and wetlands influence both the inter-annual and inter-seasonal variability. VIC can also deal explicitly with the dynamics of surface and ground water interactions and calculate the water table (*Liang et al.*, 2003). VIC can be applied under cold climate conditions where snow and frozen soil processes play an important role (*Cherkauer and Lettenmaier*, 1999; *Cherkauer et al.*, 2003). *Mishra and Cherkauer* (2011) investigated cold season climate variability on lakes and wetlands in the Great Lakes region using VIC.

The model used in this study is comprised of two parts : (i) the VIC-3L model (*Liang et al.*, 1994, 1996; *Cherkauer and Lettenmaier*, 1999; *Cherkauer et al.*, 2003; *Andreadis et al.*, 2009); and (ii) a routing model (*Lohmann et al.*, 1996, 1998). The VIC model produces surface runoff and baseflow within each grid cell. The routing model transports grid cell flow to the outlet of that grid cell and then into the river system. The routing model

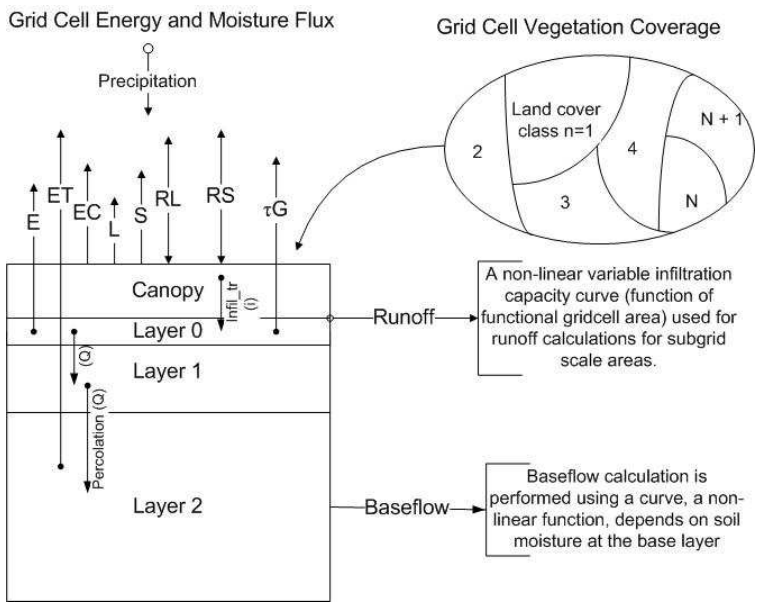

Figure 7.1: The VIC model schematic: a. Grid cell energy and moisture flux - in left; Layer 0 - a thin layer ; Layer 1 - an upper layer; and Layer 2 - a lower layer. b. Grid cell vegetation coverage - in right. 'Runoff' is determined by a nonlinear function of infiltration relationship with fraction of area and 'base flow' is determined by a functional relationship with layer 2 soil moisture.

does not pass any feedback to the VIC, nor does it transport soil water between neighbouring grid cells.

A schematic of the VIC hydrological model appears in Figure 7.1. The VIC-3L model has three soil moisture layers (*Liang et al.*, 1996): (i) a thin layer ; (ii) an upper layer; and (iii) a lower layer. The upper layer is designed to represent the dynamic behaviour of the soil column to rainfall events; the lower layer is used to characterize slowly varying seasonal soil moisture behaviour. The lower layer shows the response to a rainfall event only when the upper layer is wet. Therefore, the subsurface flow is separated from the quick storm response. The top thin layer allows a quick bare soil evaporation following small summer rainfall events. A grid cell area is partitioned into N different types of vegetation including bare soil. Vegetation characteristics such as leaf area index, root distribution, canopy and surface resistance, roughness length, and displacement height are assigned for each vegetation type. Three types of evaporation are considered in the VIC: (i) EC - evaporation from canopy layer; (ii) ET - transpiration from vegetation classes, and (iii) E - evaporation from bare

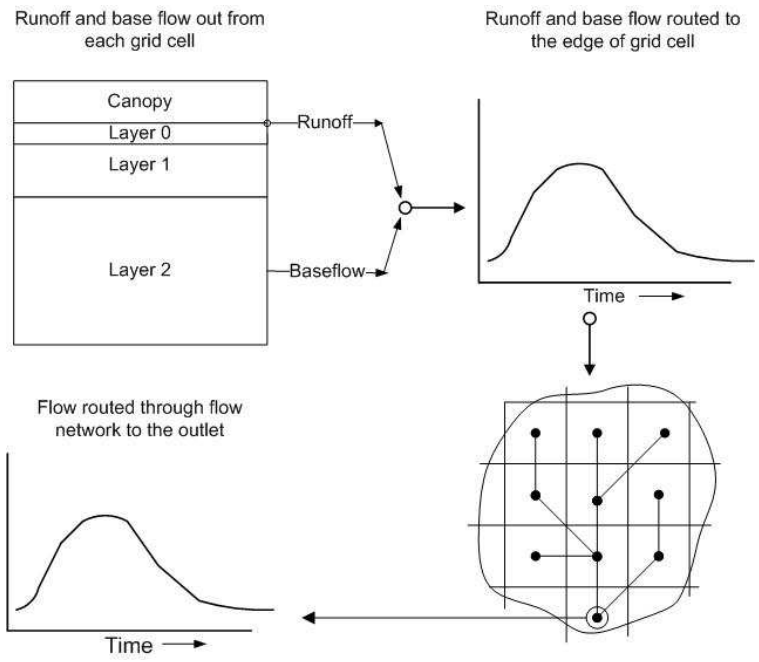

Figure 7.2: The schematic of the routing model used in the VIC; upper right and lower left are two impulse response functions for the internal grid box routing and the river routing, respectively (after *Lohmann et al.* (1996))

soil. Other governing processes in each grid cell within the soil column are infiltration (i), percolation (Q), latent heat flux (L), sensible heat flux (S), ground heat flux (τG), long and shortwave radiation (RL and RS), runoff (R), and baseflow (W). The non-linear variable infiltration capacity curve is used for runoff calculations. Baseflow is also derived using a curve, a non-linear function, that depends on soil moisture at the base-layer. A detailed discussion of the VIC model can be found in *Liang et al.* (1994).

The VIC model produces a time series of runoff values for each grid cell. These time series are not considered as runoff produced at a single point; rather they are distributed non-uniformly over the area of the grid cell in accordance with the soil moisture distribution. To calculate the runoff generated in different parts of the grid cell, VIC is convoluted with a transfer function which simulates routing within the grid cell and transfer the response via deconvolution of the catchment impulse response function with the river network impulse response function belonging to that catchment (*Lohmann et al.*, 1996). Runoff from each cell can only flow into one of its eight neighboring cells and the entire flow must go to the

same neighboring cell. The outflow from each grid cell is then added to a cell in the drainage direction with a time delay based on simple travel distance and velocity assumptions after calculating the outflow using an impulse transfer function described by *Lohmann et al.* (1996). The rive routing model may account for human activities such as extraction or reservoir operation in a specific node, and therefore, need to be implemented separately following the operation rules. A schematic of VIC routing model appears in Figure 7.2.

7.5.2 Model Inputs

The VIC model can be run in two different modes, water balance and energy balance, depending on the availability of meteorological input data. The water balance mode has been selected for use in this study. The forcing data for VIC in the water balance model include daily maximum temperature, daily minimum temperature and daily precipitation. Apart from the climatological data, the model requires input parameters related to soil and vegetation. The energy balance simulation of VIC could not be used as the energy balance simulation requires observations of shortwave radiations which are not available for the basin.

The soil and vegetation parameters are gathered from the University of Maryland 1 km global land cover datasets, and the land data assimilation system (LDAS) vegetation library data and 5-min Food and Agriculture Organization (FAO) global soil datasets. Manitoba Land Initiative (MLI) information is used in this study for a priori estimation of vegetation and soil parameters. The land cover classification map of the Churchill River basin used in this study is shown in Figure 3.6.

A digital elevation model (DEM) of the watershed area from USGS HYDRO1K is used to define the contributing area, which is done by basin delineation using the Arc/Info software. Once the basin boundary is defined, other required data such as flow direction, flow network, elevation mask file, and fraction file for flow routing is also extracted from the DEM. The delineated watershed above Otter Rapids of the CRB is approximately 112,000

km^2 using the HYDRO1K elevation data and is shown in Figure 3.5. The Water Survey of Canada (WSC) estimates a gross drainage area of 119,000 km^2 and an effective drainage area of 112,000 km^2 above Otter Rapids station (# 06CD002).

7.5.3 Parameter Estimation and Calibration

Parameter estimation is a critical aspect of the modelling exercise, because the efficiency of model prediction depends upon the proper estimation of model parameters (*Huang et al.*, 2003). In a hydrological modelling exercise, some parameters are non-changing regionally and can be set at reasonable values from regional datasets based upon the literature.

According to *Nijssen et al.* (1997), the VIC model parameters having the highest effect on streamflow hydrographs are the infiltration capacity shape parameter (b); the maximum velocity of base flow (D_m); non-linear base flow (D_s); the depth of second soil layer (D_2); and the fraction of maximum layer 2 soil moisture at points where non-linear base flow occurs (W_s). *Demaria et al.* (2007) also claims that the infiltration capacity shape parameter (b), and the depth of second soil layer (D_2) are highly sensitive to streamflow and the three other model parameters (e.g., D_m, W_s, and D_3) are only slightly sensitive. A *priori* estimates of seven parameters appear in the Table 7.1. These parameter estimates are chosen based on the calibration of the VIC model in similar Prairie basins (*Wen et al.*, 2009). A parameter estimation scheme for the VIC using MOPEX databases was published by *Xie and Yuan* (2006). A recent study by *Wang et al.* (2012, Table 2) presents maximum and minimum of parameters based on 125 calibrated catchments. Of these parameters, the most sensitive are chosen for systematic manual calibration in this research.

The VIC model calibration is performed manually by systematically adjusting parameters with aim to reduce the differences between observed values and simulated results and the visual match of the shape of the hydrograph. Calibration is performed using the following steps: (i) determine a reasonable value for the thickness of the second soil layer; usually a thicker second layer allows more storage; (ii) adjust values of D_m and D_s in order to fit the

Table 7.1: A priori estimate of parameters values for VIC model.

Parameter	Unit	Value
Infiltration capacity shape parameter (b)	-	0.2
Maximum velocity of base flow (D_m)	mm/day	10
Fraction of D_m where non-linear base flow (D_s)	Fraction	0.02
Fraction of the maximum layer 2 soil moisture where non-linear base flow occurs (W_s)	Fraction	0.8
Thickness of first soil layer (D_1)	m	0.1
Thickness of second soil layer (D_2)	m	0.5
Thickness of third soil layer (D_3)	m	1.5

low flows; (iii) adjust the infiltration capacity shape parameter (b) to match the observed flow peaks. The parameter b dictates the partitioning of rainfall into infiltration and surface runoff. Generally, a higher value increases the peak and a lower value lowers the peak. Then (iv), repeat the above steps to obtain the best simulated result. During the calibration process, the second layer thickness is adjusted and the top layer thickness (0.1 m) is kept constant. The VIC model treats the first and second layers as one entity while calculating the surface runoff (Figure 7.1).

Figure 7.3 presents the calibration (top) and the validation (bottom) of daily flow series as simulated by the VIC model for the CRB above Otter Rapids. The VIC calibration was performed for the period 1985-1991, and validation was performed for 1977-1983. The seven-year calibration and validation periods are assumed to contain sufficient intra-annual and seasonal variability to be representative. Many different test criteria can be used to assess the efficiency of a hydrological model calibration (*Hall*, 2001; *Krause et al.*, 2005). Apart from the visual inspection of plots of streamflow, the Nash-Sutcliff coefficient of model efficiency (NSE) (*Nash and Sutcliffe*, 1970), shown in Equation 7.1, is used to measure the goodness-of-fit between the observed and simulated flow time series. The NSE can be calculated as follows:

$$NSE = 1 - \frac{\sum_{t=1}^{N} \left(Q_{i,o} - Q_{i,m}\right)^2}{\sum_{t=1}^{N} \left(Q_{i,o} - \bar{Q}\right)^2} \tag{7.1}$$

where $Q_{i,o}$ is the observed streamflow, $Q_{i,m}$ is the model-simulated streamflow, and $\bar{Q}$ is the

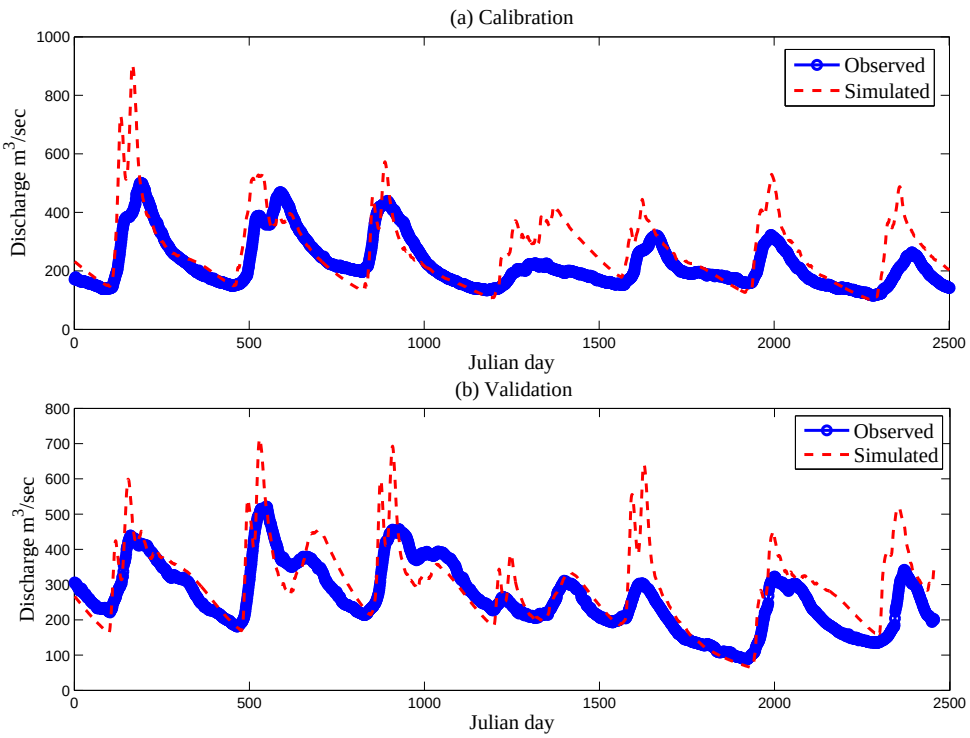

Figure 7.3: Comparison of observed and VIC simulated hydrograph of daily flow series for the upper Churchill River basin. The calibration (top) is performed for 1985-1991 and the validation (bottom) is performed for 1977-1983. The Nash-Sutcliffe coefficient of Efficiency (NSE) is found 0.607 and 0.501 for calibration and validation, respectively. The percent volume bias error (%VB) is found 9% and 12% during calibration and validation, respectively

mean observed streamflow. Higher values of NSE (closer to 1) indicate better agreement. The NSE is 0.607 and 0.501 for calibration and validation periods, respectively. *Henriksen et al.* (2003, Table 4) suggested that values of NSE between 0.5 - 0.65 are considered acceptable.

The volume bias error (%VB), is a second measure of fit used in this research., The %VB can be calculated as follows:

$$\%VB = 100.\frac{\bar{Q_o} - \bar{Q_m}}{\bar{Q_o}} \tag{7.2}$$

where $\bar{Q_o}$ is the mean observed streamflow and $\bar{Q_m}$ is the mean modelled streamflow. The %VB emphasizes volume conservation over the calibration and validation periods and is not sensitive to errors in streamflow timing or seasonality. *Schnorbus et al.* (2011) performed

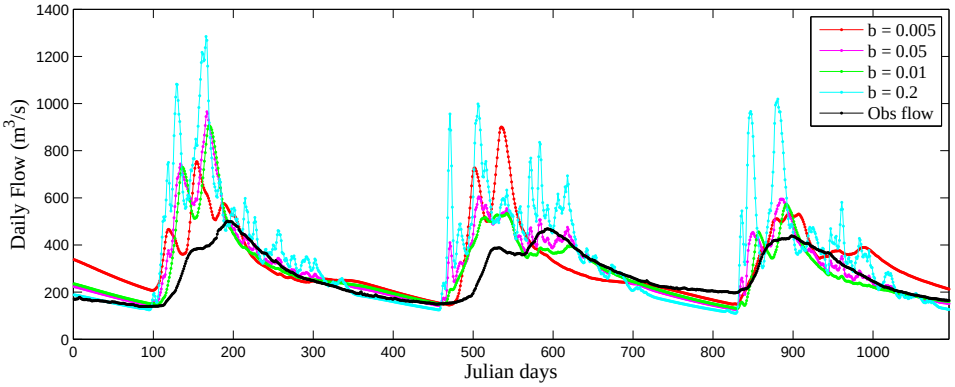

Figure 7.4: The sensitivity of the VIC infiltration capacity shape parameter (b) on the streamflow production.

Table 7.2: The sensitivity of the VIC infiltration capacity shape parameter (b). Calculation of NSE and %VB are shown for different b .

	Inf. capacity shape param (b)			
Statistical test	0.005	0.05	0.01	0.2
Nash-Sutcliff coefficient of model efficiency (NSE)	0.26	0.47	0.56	0.22
Percent volume bias error (%VB)	15.8	11.9	7.5	23.4

successful calibration of VIC while keeping the percent volume bias error within 10%. In this research, the %VB is 9% and 12% for calibration and validation periods, respectively. *Merritt et al.* (2006) also accepted a volume bias error of 13% during validation.

Streamflow is considered highly sensitive to the infiltration capacity shape parameter (b) (*Demaria et al.*, 2007). Therefore, a sensitivity test of the infiltration capacity shape parameter (b) on the streamflow production is carried out in this study. The infiltration capacity curve represents the spatial variability of soil infiltration which is the most distinguishing characteristics of the VIC model. Figure 7.4 presents the streamflow simulated for different shape parameters (b) with all other parameters held constant. Only three consecutive years are shown in Figure 7.4 for better visual interpretation. The b parameter dictates the partitioning of rainfall into infiltration and surface runoff. Figure 7.4 demonstrates that the smaller values of b increase the model infiltration and weaken the surface runoff. Table 7.2 provides values of NSE and %VB for different values of the b parameter. The visual interpretation of flow in Figure 7.4 indicates that b influences both the magnitude and the

timing of the simulated peak flows. The b parameter can play a critical role in partitioning of rainfall into infiltration and surface runoff in a dry, water-stressed basin (*Demaria et al.*, 2007).

Although the statistical performance of the modelled discharge indicates a good model fit, some discrepancies exist between modelled and observed results. Simulated low flow is lower than observations for some years. The simulated snow-melt peaks are not well captured and in most cases are overestimated. The snow-melt issue in VIC was also recognized in the North American Land Data Assimilation System project (*Lohmann et al.*, 2004, Figure 12). The anomaly in the model discharge may be due to the driving observational dataset as there are only a few climate stations located in the Manitoba portion of the delineated basin. Also, this shortcoming could be related to the limitations of the VIC simulations in water balance mode. In this study, VIC simulations are performed in water balance mode. The full energy balance simulation could not be used as the VIC energy balance simulation requires observations of shortwave radiations which are not easily available.

The disagreement in the model discharge may also be due to the modelling limitations of the areas of lakes and wetlands. The lakes and wetlands have influence on the downstream flow regime through attenuation, storage and slow release processes that occur within the lakes. These lakes and wetlands create challenges for hydrological modelling because the input-storage-output relationship between the river system and wetlands/lakes are not fully understood (*Hughes et al.*, 2013). A lake model is not included in the VIC simulation.

The main focus of the study, however, is modelling the hydrological processes not only discharge. Overall, the VIC is able to reproduce the run-off dynamics for the calibration and validation periods. Based on the above validation results, the calibrated VIC hydrological model can be considered suitable for use in the hydrological change assessment of the region.

7.6 Results

One of the main objectives of the study is to increase an understanding of how and to what extent climate change can affect hydrological processes in the CRB. As discussed earlier (literature review section), the CRCM climate data are used to drive a hydrological model over the CRB to assess changes in the hydrological processes. Before applying CRCM data to a hydrological model, bias corrections have been performed (Chapter 6).

The model calibration by adjusting basin outflow is a reasonable approach, but it is possible that internal variables are simulated incorrectly but cancel out and result in accurate outflow of the basin. If the internal variables such as snow and soil moisture simulated from a hydrological model can be validated with alternative data sources, doing so will enhance the reliance of the model's ability to reproduce streamflow over the basin. The following section presents the VIC model evaluation by examining the internal state variables.

The VIC model was used to simulate hydrological regimes of 30-years of baseline climate (1976-2005) and 30-years of future climate of 2030s (2020-2049), and 2050s (2041-2070) with climate forcing from the CRCM. Later in this chapter, hydrological process variables from these climate simulations will be evaluated in order to assess the impact of climate change.

7.6.1 Evaluation of the VIC model

The VIC produces many internal variables as simulation output. The dominant variables are chosen for evaluation. Climatologically, the CRB, a Prairie basin, is classified as semi-arid to sub-humid with cold and relatively long winters (*Pomeroy et al.*, 2007). One-third of Prairie annual precipitation is received as snowfall (*Akinremi et al.*, 1999). Snowpack plays a central role in runoff production. The water stored as snow accounts for a dominant fraction of the spring runoff contributing to streamflow.

Given the importance of snow in the hydrological cycle in the Prairies, the changes

in snowpack are strongly related to the associated changes in evaporation, soil moisture, and runoff dynamics. Therefore variables chosen for model evaluation are the following: (i) evaporation, (ii) snow depth, (iii) snow water equivalent (SWE), and (iv) soil moisture. These variables are rarely observed at the basin scale; therefore, direct comparisons of these variables are performed only at locations where observed data are available. In the following sections, attempts are made to validate these variables with quasi-observed or reanalysis datasets. In some cases, attempts have been made to validate these variables with point measurements, where measurements are available within the basin or the neighbouring area of the basin.

Evaporation

Evaporation is a vital but also the least measured component of the water budget equation. Since evaporation measurements are scarce at a regional scale, validation of hydrological model estimates is difficult. Traditionally, point measurements of evaporation are performed with lysimeters or evaporation pans. The other method of obtaining direct measurements of evaporation is through the flux tower also known as an eddy covariance system. Eddy covariance measurements of evaporation from Great Slave were conducted from GEWEX in the Mackenzie River basin study (MAGS) (*Stewart et al.*, 1998; *Blanken et al.*, 2000).

Using modelled data, a simple method for obtaining regional evaporation is to solve the classic water balance equations. Regional or basin scale evaporation can be obtained from aerological datasets by deriving atmospheric water balance using reanalysis data (*Abdulla et al.*, 1996; *Maurer et al.*, 2002). Evaporation can also be derived as the residual of precipitation and water vapour convergence from an atmospheric water budget calculation (*Rasmusson*, 1968; *Berbery and Rasmusson*, 1999).

In this section, evaporation estimates from different independent calculations are presented. The NARR is used to obtain surface evaporation. A quasi-observed evaporation is calculated from the atmospheric dataset of NARR following the Equation 5.9. Annual

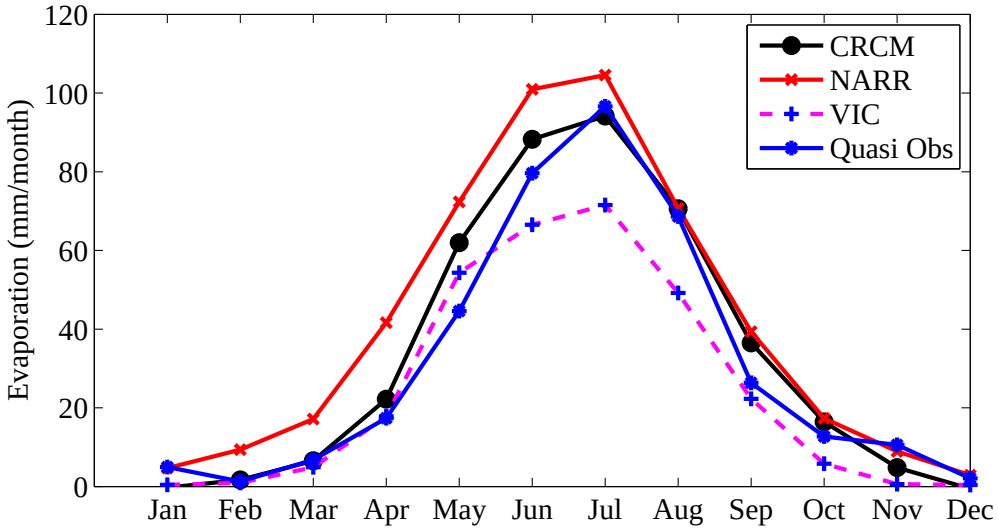

Figure 7.5: Annual cycle of VIC evaporation compared with CRCM, NARR and quasi-observe. The quasi-observe evaporation is calculated as $E_{quasi-obs} \approx -\{\overline{\nabla_H \cdot \mathbf{Q}} + \overline{\partial W/\partial t}\}_{NARR} + P_{CANGRID}$.

cycles of evaporation from these independent calculations are presented in Figure 7.5 along with evaporation derived from VIC simulation.

A seasonal cycle of VIC evaporation, shown in Figure 7.5, clearly demonstrates that the peak evaporation appears in the month of July. The VIC underestimates summer (June-July-August) evaporation. This underestimation may be due to VIC model limitation of defining Prairie lakes and wetlands. A 'surface water' land class is used in the VIC model set-up where small water bodies are included. Evaporation from the water surface is calculated in each time step of the VIC calculation, assuming surface temperature is equal to the air temperature. During summer, surface temperatures are usually higher than air temperatures; therefore, the summer evaporation is underestimated. *Cherkauer et al.* (2003) demonstrates the effect of including surface water from lakes on the average monthly VIC simulated hydrograph. Specifically monthly discharge is reduced due to lakes with little change in the timing of the hydrograph. The authors concluded that the over-prediction of runoff is due to the underestimation of evaporation from the surface water. Seasonal evaporation of these lakes and wetlands are not well known. Evaporation is still a relatively understudied part of the Prairie wetlands hydrological balance (*Waddington et al.*, 2009).

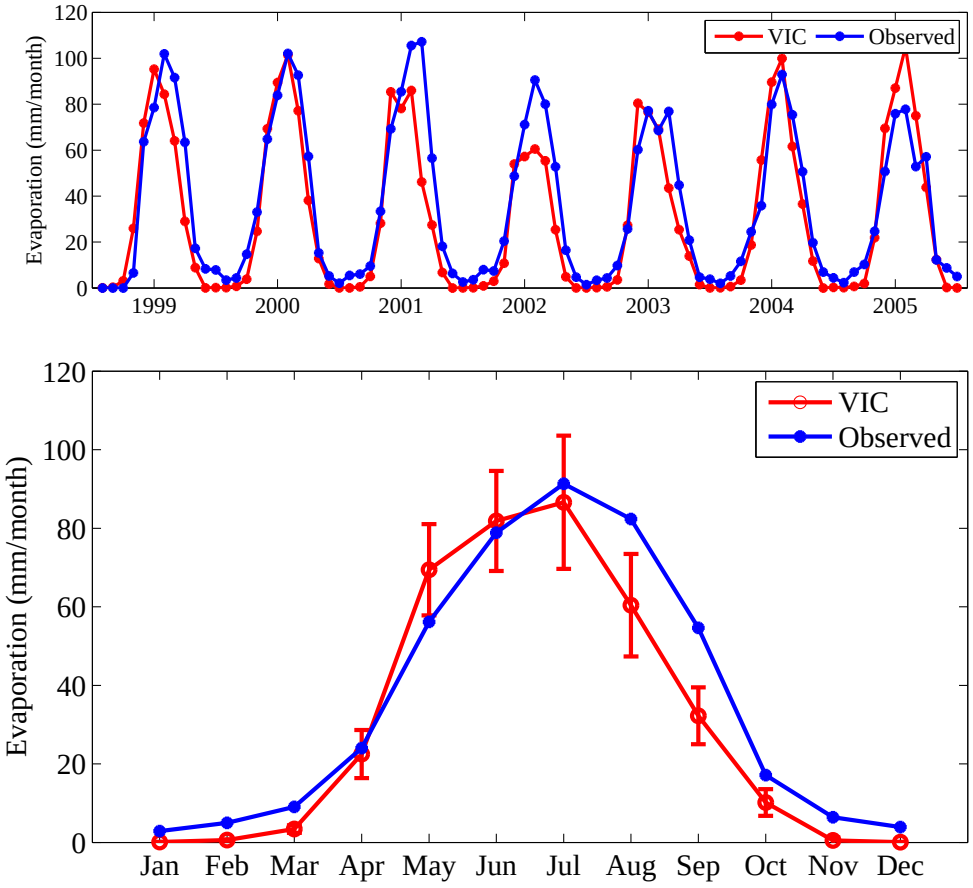

Figure 7.6: Average mean monthly time series for VIC evaporation estimates are compared with measured evaporation at location 53.98°N 105.12°W(in top) for the period 1999-2005. Annual cycle of mean monthly evaporation estimates for VIC is compared with observed (in bottom). The annual cycle of evaporation is calculated from 1999 to 2005 monthly evaporation time series. Observed data are obtained from Fluxnet-Canada at Old Black Spruce, SK. The error bar indicates the standard error (one std.) of the VIC evaporation estimates.

Figure 7.6 shows a comparison of evaporation estimates for the VIC model and measured evaporation for the period 1999-2005. The measured evaporation is obtained from the Fluxnet-Canada[1] at Old Black Spruce, SK. The site is located at 53.98°N 105.12°W and shown in Figure 3.5. The simulated evaporation from the VIC model is extracted from a neighbouring grid at location 53.99°N, 105.44°W. The error bars in the Figure 7.6 (bottom) indicates the standard error (± 1 standard deviation) of the VIC evaporation estimates.

Figure 7.6 (top) shows that in all years, the late fall and winter evaporation estimates from VIC tend to be lower than those of the measured evaporation. Sometimes, during fall and winter, the VIC evaporation tends to have small negative values (not shown). The negative values are most likely due to the model's assumptions and computations. *Yeh et al.* (1998) also found evaporation estimates to be below zero during the late fall and winter months which was explained by the limited accuracy of the model. Another partial explanation may be VIC's snow model, which was not separately calibrated and may contribute to the underestimation of evaporation. The VIC snow model is intended for large-scale applications.

Figure 7.6 exhibits both model and observations has peak evaporation in July of 86.6 mm and 91.3 mm, respectively. The model's peak evaporation is underestimated by 5%. Simulated summer (June-July-August) evaporation of VIC is 228.88 mm and measured summer evaporation is 252.53 mm. VIC underestimates summer evaporation by 9%, which can partially be explained by the assumptions of the VIC model. In water balance mode, VIC assumes a surface temperature equal to the air temperature. Usually the surface temperature during summer is higher than air temperature; therefore, the summer evaporation is underestimated. This limitation can be overcome by using the VIC energy-and-water balance mode where VIC finds the surface temperature through an iterative process of solving the surface energy balance. This mode requires more computational time than the water balance mode and requires a sub-daily simulation time step which was not possible in

[1]Fluxnet-Canada data were accessed on August 04, 2012 with permission through the web portal at ftp://fluxnet.ccrp.ec.gc.ca/PublicMeasuredData/.

this study due to data limitation.

Figure 7.6 (bottom) presents the annual cycle of mean monthly evaporation estimates. Overall, the VIC model underestimates evaporation compared to the measured evaporation at location 53.98°N, 105.12°W, except for the months of May and June. The same tendency can be observed in the spatially averaged evaporation over the basin shown in Figure 7.5. The estimated total annual evaporation for the VIC model is 367.87 mm, whereas the measured total annual evaporation is 431.75 mm. The VIC model's total annual evaporation underestimates the observed by 14%. Although there is an overall underestimation of VIC evaporation, the pattern of the model's annual cycle of evaporation is in close agreement with measured evaporation estimates.

Snow

Snow is a crucial component of the hydrological cycle, especially in high latitude northern basins. Snow processes are integral components of a hydrological model. The VIC model was upgraded to include a snow model in order to represent cold land processes (*Andreadis et al.*, 2009). Validation of the snow process was by no means an easy task due to the limited availability of snow measurements. In this research, observation at the boreal forest sites were taken as a part of the Boreal Ecosystem-Atmosphere Study (BOREAS) (*Sellers et al.*, 1997). In the BOREAS study, manual snow depth and water equivalent measurements were taken at various sites. Two sites (SSA-OBS[2], and SSA-999-NIY01[3]), shown in Figure 3.5, were selected for this study. Apart from the BOREAS data, Western North American domain monthly (Dec-Jan-Feb-March) average snow water equivalent (SWE) data from the Scanning Multichannel Microwave Radiometer (SMMR; 1978-1987) and the Special Sensor Microwave/Imager (SSM/I; 1987 - 2002) were used (*Derksen et al.*, 2002, 2003). There are 10491 grid cells covering the domain. The grid cell close to location 53.98°N, 105.12°W

[2]SSA-OBS: The southern Old Black Spruce snow course is located at 53.98°N, 105.12°W. The site location map of SK-OBS can be seen at http://daac.ornl.gov/BOREAS/bhs/sites/SSA-OBS.html

[3]SSA-999-NIY01: This snow course is located at east of highway #106 about 4.0 km north of the correction facility road. It is about 200m off the highway. The geographic location is 53.85°N and 104.61°W.

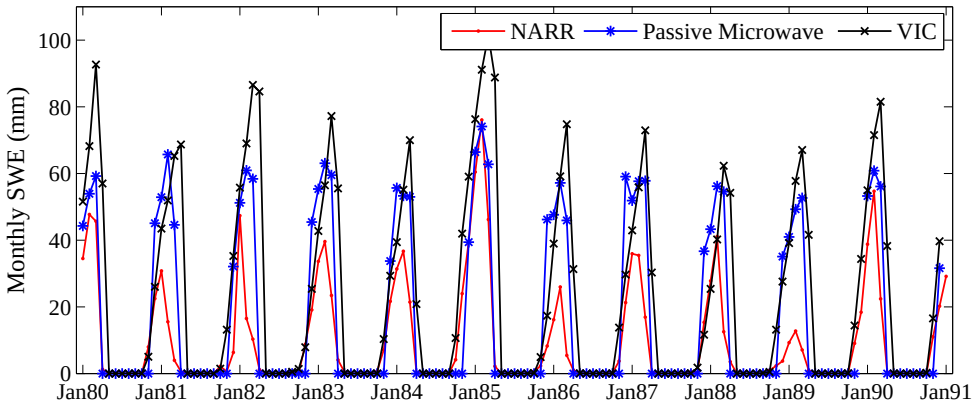

Figure 7.7: The VIC simulated monthly averaged SWE compared with the microwave measured SWE at location 53.98°N, 105.12°W. Passive microwave data are obtained from from the Scanning Multichannel Microwave Radiometer (SMMR; 1978-1987) and the Special Sensor Microwave/Imager (SSM/I; 1987-2002).

was retrieved for comparison. In the following sub-section, snow water equivalent (SWE) followed by snow depth as simulated by VIC hydrological model are validated using these measured datasets.

Figure 7.7 illustrates a comparison of the VIC simulated monthly averaged SWE along with microwave measured SWE. The NARR SWE, representing quasi-observed data, is also included in this figure for comparison. Overall, the monthly VIC SWE overestimates compared to microwave measured SWE. *Andreadis et al.* (2009) examined SWE data at the neighbouring site SSA-OJP[4], where the VIC model overestimates SWE. There are only four months (Dec-Jan-Feb-March) of microwave measured SWE data available; therefore, it is not possible to validate the SWE situation during snow melt from microwave measurements.

Figure 7.7 demonstrates that the VIC SWE follow closely with the NARR SWE during snow accumulation. Overall, the NARR SWE is considerably smaller than microwave measured SWE. Snow information (i.e., depth, SWE, snow cover fraction) are included in the NARR dataset based on the Noah land surface process model. *Brown et al.* (2007) suggested that the Noah model melts snow too quickly in the spring which can be seen in Figure 7.7. *Brown et al.* (2007) present a comparison of snow datasets over Québec

[4]SSA-OJP: The Southern Old Jack Pine site is located at 53.91°N 104.69°W and shown in Figure 3.5

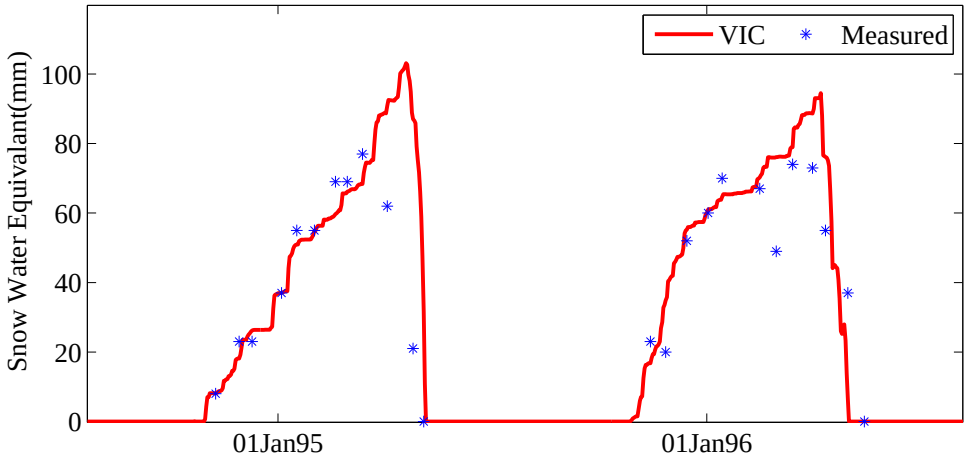

Figure 7.8: The VIC simulated snow water equivalent (SWE) compared with the measured at SSA-999-NIY01 Site. The geographic location of the site is 53.85°N and 104.61°W

and point out that the NARR greatly underestimates SWE over the western Cordillera and Québec. The overall RMSE between NAAR SWE and microwave measured SWE is 16.1 mm, and RMSE between VIC simulated SWE and microwave measured SWE is 9.7 mm.

Figure 7.8 presents the VIC SWE comparison with measured SWE at location 53.85°N and 104.61°W (SSA-999-NIY01). This plot suggests that VIC captures snow accumulations effectively for both 1995 and 1996, but over-predicts the peak SWE. For both years, VIC snowmelt agrees closely with measured values and finally VIC predicts the timing of complete melt of the snowpack fairly accurately. The correlation between the measured and VIC modelled SWE is 0.94, while the RMSE is 20 mm.

Figure 7.9 shows a comparison of snow depth as simulated by VIC along with snow depth measurements at SSA-OBS site. The snow depth measurements were taken in clearings of the site. Figure 7.9 (top) shows that the VIC simulated snow depth is underestimated throughout the winter at this site. Figure 7.9 (top) also demonstrates that the VIC snow model captured an early snowfall event successfully in December 1998. Despite the noticeable underestimation of snow depth, the model appears to follow the accumulation and melt events closely, which suggests a consistent underestimation over the snow period. The underestimation of modelled snow depth may be partly explained by the snow interception.

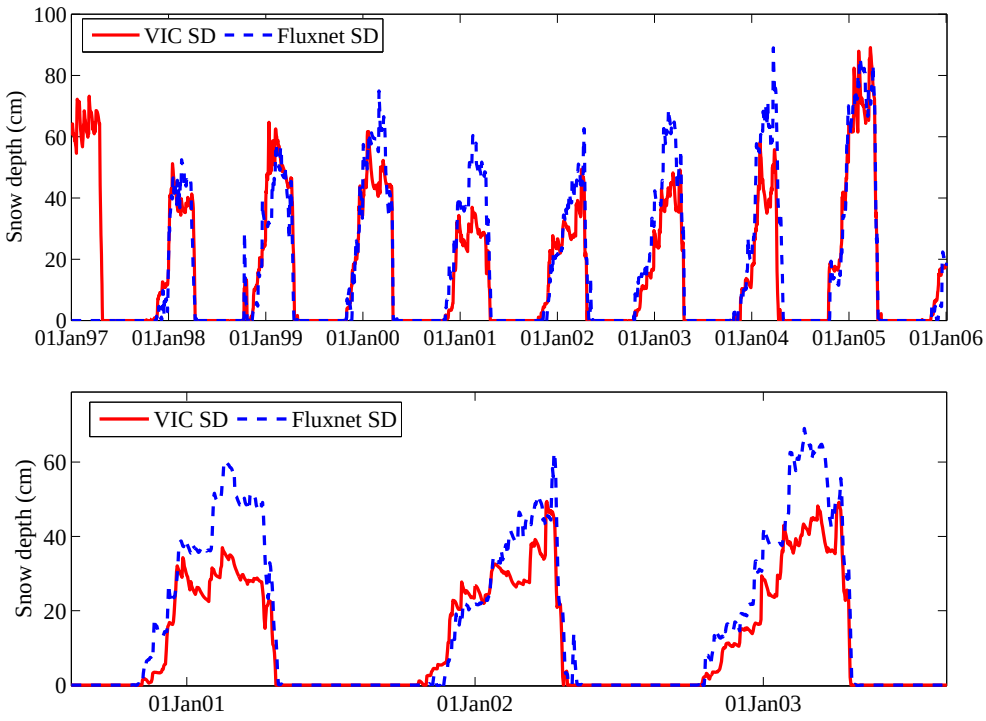

Figure 7.9: The VIC simulated snow depth compared with the observations at SK-Old Blak Spruce site located at 53.98°N, 105.12°W.

The observed snow depth data are collected at the clearings of the site, where there is no canopy interception present. According to *Storck et al.* (2002), the snow interception was observed to reach about 60% of snowfall.

Figure 7.9 (bottom) suggests that model snow accumulations are reasonable in December, but underestimates snow accumulation during February and March, leading to an underestimation of peak snow depth. Overall, the VIC-simulated snow depth follows the observed fairly closely and predicts the timing of complete melt of the snow for all years at this site. The correlation coefficient between VIC-simulated snow depth and measured snow depth is 0.94 with an RMSE of 8.3 cm. The model underestimates snow depth for almost all the years. Despite the model's underestimation, it tends to follow the accumulation and melt events closely.

During calibration of the VIC model , the snow model was not calibrated. A set of default parameters were used for the VIC snow model. The comparison of VIC-simulated

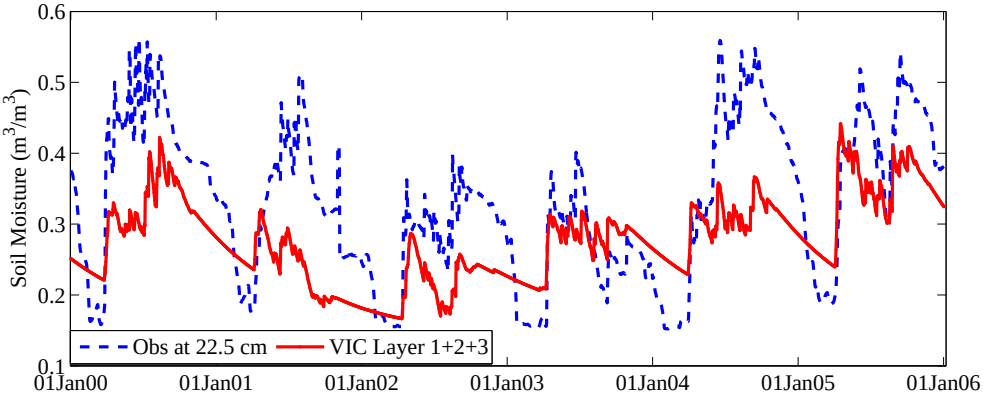

Figure 7.10: The VIC simulated soil moisture from three aggregated layers are compared with the measured soil moisture at SSA-OBS site located at 53.98°N, 105.12°W. A correlation coefficient of 0.7 is found between observed and VIC simulated soil moisture at this location.

snow with measured station data shows that the model is able to predict SWE and snow depth reasonably well. Improved simulations may be obtained by adjusting VIC snow model parameters.

Soil Moisture

The VIC soil moisture has been utilized and evaluated at the basin scale (*Abdulla et al.*, 1996; *Cherkauer and Lettenmaier*, 1999), in the continental US using the North American Land Data Assimilation System (NLDAS) (*Maurer et al.*, 2002), and in the global-scale applications (*Nijssen et al.*, 2001). *Meng and Quiring* (2008) evaluated VIC soil moisture against observations from the Soil Climate Analysis Network (SCAN) over several U.S. sites and found that VIC generally performs well in simulating soil moisture conditions. Field measurement of soil moisture is rarely available at the regional scale. Soil moisture measurements are time consuming as well as expensive. Most research applications that require soil moisture relies on model simulations (*Sheffield et al.*, 2004). Soil moisture validation in this section is limited to observational data obtained from one location of the BOREAS study region.

In this study, soil moisture measurements (six times a day) were obtained from the southern Old Black Spruce (SSA-OBS) site of the BOREAS study region. The SSA-OBS

site is located at 53.98°N 105.12°W. Figure 7.10 compares the soil moisture simulated by the VIC model with measured soil moisture at the SSA-OBS location. Because the VIC model simulations are performed on a daily time step, the measured soil moisture dataset is aggregated to a daily time series. The VIC soil moisture is taken as the addition of the three soil layers, assuming that soil moisture is vertically and homogeneously distributed within each layer of the soil column. The observed soil moisture is measured at 45 cm depth at the site. The VIC model simulation produces a daily variation of soil moisture in the soil column, but the magnitude of daily variations does not agree with the measured daily variations. A correlation coefficient of 0.7 is found between measured observed and VIC simulated soil moisture.

Figure 7.10 indicates that VIC reproduces some aspects of the observed seasonal cycle of soil moisture, although observed soil moisture peaks are clearly underestimated by the VIC. The timing of soil moisture recharge, i.e. the wetting of the soil column, in VIC is consistent with the measured. In comparisons with other soil moisture models, VIC has been shown to simulate the timing of wetting and drying of the soil well (*Meng and Quiring*, 2008). However, the VIC-simulated soil moisture has much less seasonal variation than the measured series.

During snowmelt and rain events, the soil moisture is replenished. The fraction of water contributing to runoff generation decreases when the soil moisture deficit increases. The streamflow is strongly coupled to soil moisture in the wet seasons, and there are time lags between the soil moisture recharge at the onset of snowmelt/rain and the generation of streamflow in the dry season (*Moore et al.*, 2011).

Figure 7.11 (bottom) shows a plot of VIC-simulated soil moisture from the three aggregated soil layers, and a corresponding plot of flow surplus/deficits (top panel) derived from streamflow gauge data. Figure 7.11 demonstrates that the VIC-simulated soil moisture depletion, shown with arrows a,b,c,d, closely follows the streamflow deficits with an average lag of a year. The *Moore et al.* (2011)'s study over a small western Oregon watershed shows

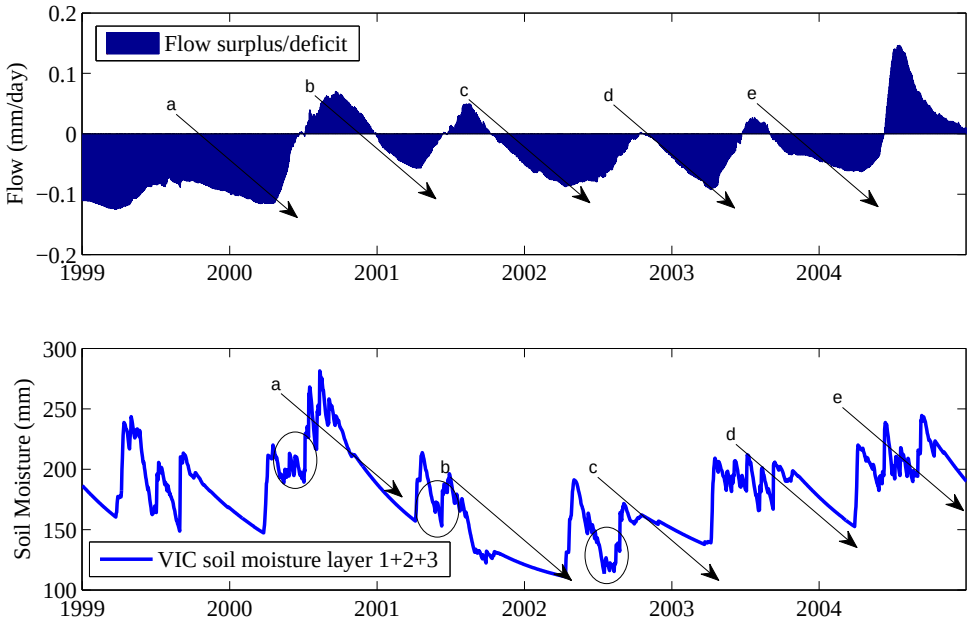

Figure 7.11: The VIC-simulated soil moisture (bottom) corresponding to the flow surplus/deficits (top) calculated from the flow gauge are presented together. VIC simulation is performed using input from the observed climate.

a lag of 48 days to refill the moisture during the wet season. *Andreadis et al.* (2005, Figure 10) showed that the lag could be from 1 to 12 months. The soil moisture depletion shown in circles in Figure 7.11 (bottom) can not be explained by the flow surplus/deficits plot. This soil moisture situation may be explained partly by the local processes occurring during summer months in the lake/wetlands of the Prairies, processes that are not well captured by the VIC model.

Soil moisture data are most pertinent for drought monitoring. A drought index can be calculated as the deficit of soil moisture relative to its seasonal climatology at a location. The soil moisture data can be used in a consistent and meaningful way to identify the occurrence of drought in different locations. *Sheffield et al.* (2004, 2009) used simulated daily soil moisture data and transformed to percentiles in order to derive a drought index. A drought is then defined conceptually as a sequence of spatially contiguous deficits below the 20th percentile. This method has been used in previous applications to the United States and is

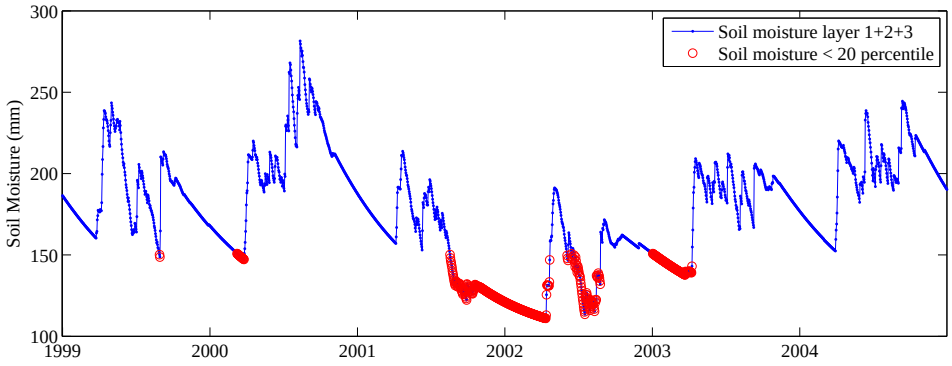

Figure 7.12: Soil moisture drought as simulated by VIC mode. The soil moisture values below 20th percentile are shown in circles. The VIC simulation is performed using input from observed climate.

consistent with drought thresholds used by the U.S. Drought Monitoring network (*Andreadis et al.*, 2005).

Figure 7.12 presents aggregated soil moisture series as simulated by the VIC model. A soil moisture below the 20th percentile is calculated and provided in this figure. The Prairie drought of 2001/2002 is discussed in *Bonsal and Regier* (2007) and *Stewart et al.* (2011). The 2001/2002 drought is reflected in the soil moisture plot presented in Figure 7.12.

The VIC model can simulate the annual cycle of soil moisture fairly closely, as well as the wetting and drying response. Although, the VIC simulations underestimate the soil moisture magnitude and do not capture seasonal variations well, a reasonable correlation coefficient of 0.7 is found between the VIC model simulated and measured soil moisture. The accuracy of the results depends partly on the quality of the observed data used to drive the model and partly on the model's limitations in simulating all aspects of the hydrological cycle in the Prairies.

7.6.2 Hydrological simulation under changing climate

In this research, the evaluation of changes in hydrological processes under a changing climate is the ultimate objective. *Xu et al.* (2005) provided a good review of existing studies, showing the progress made in simulating hydrological consequences of climate change. The

review states that modelling seems to be the well-accepted resort to address and attribute changes in complex hydrological processes under a changing climate. The VIC model simulations in this study utilize climate model scenarios. The scale issue when applying these scenario inputs to a hydrological model must be addressed through downscaling. In order to obtain regional and watershed-scale information, GCM climate scenarios must be downscaled. Dynamically downscaled regional climate model data have been substantially improved and has been given increasing preference by the scientific community. CRCM data are used in this study to evaluate climate change impacts on streamflow, soil moisture, snow, and snow water equivalent. These variables are analysed together with the climatological variables precipitation, maximum and minimum temperature.

Streamflow

Streamflow is the best documented hydrological variable considered here. Streamflow acts as an integrator of the response to all hydrological processes in the basin. Therefore, streamflow offers the opportunity to identify changes due to climate change. Streamflow trend have been examined in a number of studies (e.g. *Zhang et al.* 2001; *Burn et al.* 2008), due to growing need for water usage in irrigation, hydropower, and in the aquatic ecosystems. Also, there has been a growing concern regarding climate change and its impacts on streamflow (*Rood et al.*, 2005; *Masih et al.*, 2011; *Zhang et al.*, 2011).

The detection of past trends and changes in streamflow is useful for the understanding of potential future changes resulting from climate change. The daily streamflow data measured at the gauge station for 1976-2005 are used for trend analysis and presented first in this sub-section. Subsequently, the VIC simulated daily streamflow series for CRCM baseline climate (1976-2005) are used for detecting trends in the present climate. In order to assess trends in the future climate, the VIC simulated daily streamflow using CRCM future climate (2030s and 2050s) are presented in the following sub-section.

To analyse streamflow properties such as volume, peak, and timing of peak appearance,

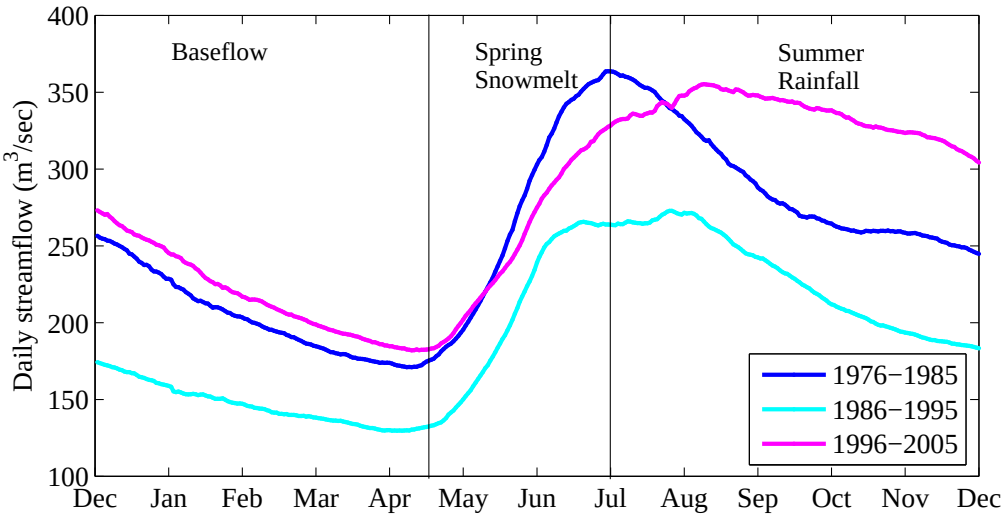

Figure 7.13: Annual hydrograph of the average daily streamflow of three ten year time slices (1976-1985, 1986-1995 and 1996-2005) at Otter Rapids of the Churchill River basin.

it is useful to examine the average hydrograph of the flow regime. Figure 7.13 presents an annual hydrograph of the average daily streamflow of three ten years time slices (i.e., 1976-1985, 1986-1995, and 1996-2005) at the Otter Rapids of the Churchill River Basin (CRB). Streamflow of the CRB varies seasonally. Three distinct flow regimes (the runoff generated due to spring snowmelt, and the runoff that occurs during summer rainfall, the base flow) can be seen from the average hydrograph (Figure 7.13). The snowmelt period begins about mid-April and extends until late June or beginning of July. At the onset of the snowmelt period, streamflow increase substantially and climbs to its peak in late June or beginning of July. The summer follows the snowmelt period. The snowmelt peak is noticeable from the average hydrograph of 1976-1985, where summer rainfall peak is not prominent. The average hydrograph of 1976-1985 indicates that the regime is dominated by snowmelt flow. The average hydrograph of 1986-1995 is bimodal that presents a hybrid response; the first peak is due to spring snowmelt whereas the second peak is due to summer rainfall. The average hydrograph of 1996-2005 did not appear to be bimodal, but a gradual snowmelt, while the hydrograph peak is dominated by summer rainfall. These three ten year time slices show that the flow regime may be in transition in changing from a snowmelt

Table 7.3: List of variables analysed for streamflow trends.

Variables	Descriptions
Annual mean streamflow	Mean discharge (m^3/s) for each year
Seasonal mean streamflow	Seasonal (e.g., spring snowmelt, and summer) mean stream discharge (m^3/s) for months of the season for each year
Annual minimum daily mean streamflow	Minimum daily mean stream discharge (m^3/s) for each year
Annual maximum daily mean streamflow	Maximum daily mean stream discharge (m^3/s) for each year
Percentiles of daily mean streamflow	Stream discharge (m^3/s) exceeding $X\%$ of daily mean streamflow. The X is considered as 10th, 30th, 70th, and 90th percentiles.

dominated regime to a summer rainfall dominated regime.

To examine streamflow trends, the following streamflow statistics were considered: annual maximum and minimum daily streamflow; high daily streamflow percentiles (seventieth, ninetieth); and, low daily streamflow percentiles (tenth, thirtieth). *Zhang et al.* (2001) tested for trends in seven quantiles of daily streamflow, tenth, thirtieth, seventieth, ninetieth percentiles, and annual maximum and minimum values. As the basin shows significant seasonal variations in flow, the streamflow during the spring and summer season are also incorporated for trend analysis. Table 7.3 provides a detailed description of variables analysed for streamflow trends.

The non-parametric Mann-Kendall (MK) test (*Mann*, 1945; *Kendall*, 1975) was used in this study to perform trend analysis. The MK test has been extensively used to assess the significance of trends in hydrological time series (*Zhang et al.*, 2001; *Yue et al.*, 2003; *Yue and Wang*, 2004; *Burn et al.*, 2008). The advantages of the MK test are the following: distribution-free, robust against outliers, and higher power than many other commonly used tests (e.g., *Hess et al.*, 2001). The MK trend detection in a series is affected by the presence of a positive or negative autocorrelation (*Hamed and Rao*, 1998; *Yue et al.*, 2002). Therefore, the modified Mann-Kendall (MK) statistical test (*Rao et al.*, 2003) was used in this study. A detailed description of the Mann-Kendall (MK) statistical test is provided in Appendix

Table 7.4: Trend analysis of measured daily streamflow time series for 1976 - 2005 at Otter Rapids.

Streamflow statistics (observed daily flow series)	Z test statistics	p-value (2-sided)	Trend Slope (m^3/sec/year)	Trend at 95% Sig. Level
Maximum/peak flow (Q_{max})	-0.999	0.318	-2.619	No trend
Minimum/low flow (Q_{min})	-1.427	0.153	-2.000	No trend
Annual mean flow (Q_{mean})	-0.892	0.372	-2.354	No trend
Date of annual peak	2.322	0.020	2.278[a]	Increasing
Percentile flow:				
90th percentile flow (Q_{90})	3.923	0.000	0.134	Increasing
70th percentile flow (Q_{70})	1.296	0.045	0.018	Increasing
30th percentile flow (Q_{30})	-2.738	0.006	-0.005	Decreasing
10th percentile flow (Q_{10})	-2.043	0.041	-0.006	Decreasing
Seasonal flow:				
Spring mean flow (Q_{MAM})	-1.427	0.153	-2.501	No trend
Summer mean flow (Q_{JJA})	-1.320	0.187	-3.052	No trend
Fall mean flow (Q_{SON})	-0.607	0.544	-1.775	No trend
Winter mean flow (Q_{DJF})	-0.563	0.573	-1.020	No trend

[a]Trend slope - days/year

A.1. Here, a significance level of α=0.05 is used. The slope of the time series is estimated by Theil-Sen's (*Theil*, 1950; *Sen*, 1968) method. A detailed description of the Theil-Sen's method is provided in Appendix A.2. This method is a robust linear regression that chooses the median slope among all lines through pairs of two-dimensional sample points.

The MK trend analysis is performed on measured daily streamflow time series for the period 1976-2005. Trend test statistics as well as Sen's slope are presented in Table 7.4. The mean annual flow (Q_{mean}) and annual high (Q_{max}) and low (Q_{min}) did not show any significant trend. The Sen's slopes for Q_{min}, Q_{max}, and Q_{mean} are -2.00, -2.62, and -2.35 m^3/sec/year, respectively.

The trend analysis is also performed on high (Q_{90},Q_{70}) and low (Q_{30},Q_{10}) flow percentiles. Both high flow percentiles (Q_{90},Q_{70}) show statistically significant increasing trends. The estimated annual changes in the Q_{90} and Q_{70} streamflow regimes are small, with a trend slope of 0.13 and 0.02 m^3/s/year, respectively. The low flow percentiles (Q_{30},Q_{10}) show a decreasing trend, the slope of the trend is very small (Table 7.4). Low flow quantiles reflects baseflow which appears to be decreasing. The *Zhang et al.* (2001, Figure 5)'s study of trends

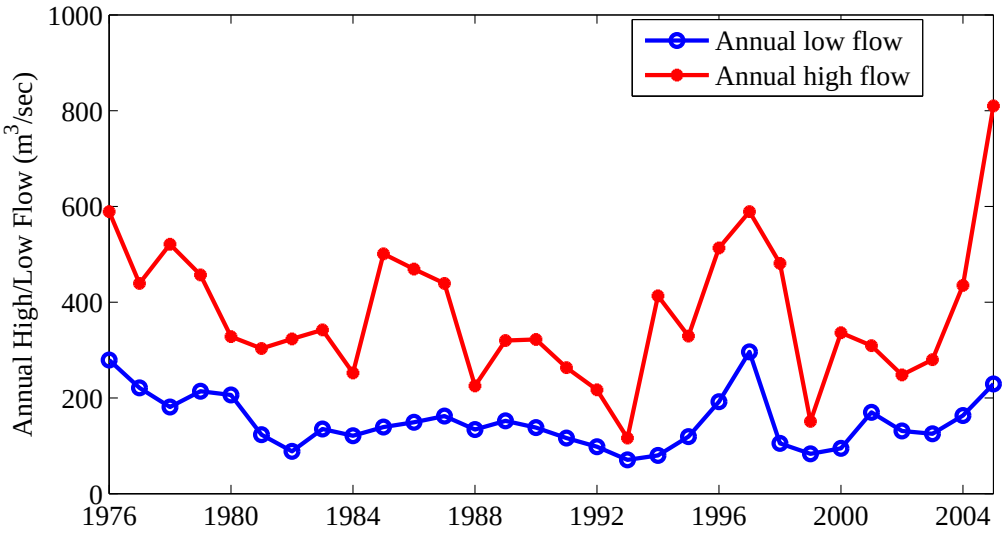

Figure 7.14: Annual high/low flow of the daily streamflow time series (1976-2005) at Otter Rapids of the Churchill River basin.

in Canadian streamflow shows decreasing trends on percentiles of daily mean flow except for the thirtieth percentile.

Figure 7.14 shows one day high and low flow for the daily streamflow time series. The date of peak flow of the daily time series is shown in Figure 7.15. The effect of temperature-driven shifts in the region for streamflow is evident on the date of peak flow. The reason for this shift of the date of annual maximum daily streamflow is that the peak flow events are not all snowmelt related; as well, the secondary peak due to summer rainfall is dominant for some years. *Zhang et al.* (2001)'s study of the date of annual maximum Canadian daily streamflow suggests the fact that earlier dates of peak daily streamflow due to spring snow melt are located in the souther fringe of the country.

In order to analyse the effect of climate on streamflow trends, the climatological variables (daily precipitation, minimum and maximum temperature) are analysed. The basin average daily precipitation, minimum and maximum temperature time series (1976-2005) are used to performed trend tests. Trends in precipitation and temperature for each of the twelve months are tested using the same MK method to explore whether trends for precipitation and temperature coincide with streamflow trends. The trend slope is also calculated using

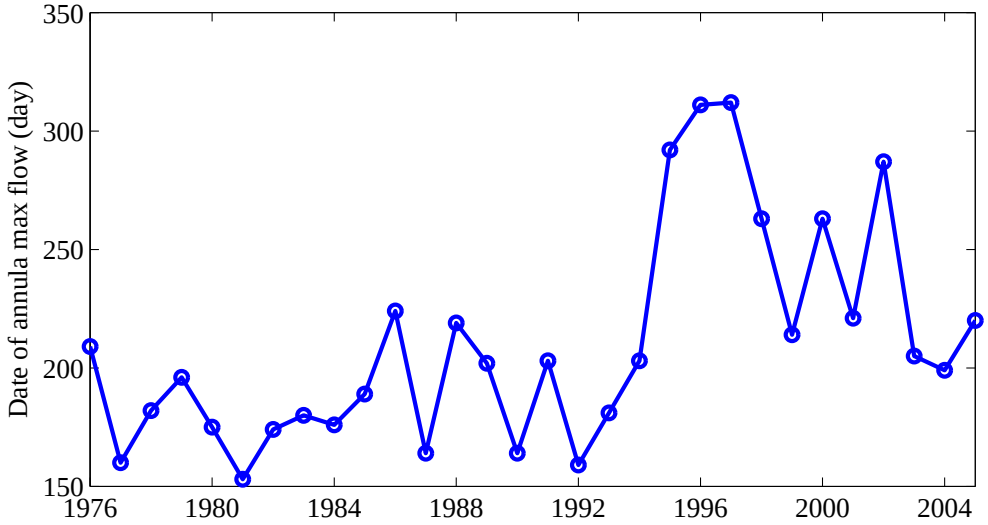

Figure 7.15: Date of annual maximum daily streamflow (1976-2005) at Otter Rapids of the Churchill River Basin.

Theil-Sen's approach for each of the variables analysed. The precipitation variables used to perform the MK test are annual and seasonal total precipitation, 90th percentile of daily precipitation, and the number of dry days in a year. Similarly, the temperature variables tested for trends are the annual and seasonal average temperature, and 90th and 10th percentiles of temperature. Table 7.5 illustrates the trend test results.

Table 7.5 shows trend statistics of daily precipitation. None of the precipitation variables considered for the trend test show statistically significant (2-tailed p-value ≤ 0.05) trend. The reason that no trend in precipitation is observed may be due to the use of a basin spatial average for the trend test. This trend test result agrees with the findings of *Zhang et al.* (2000) in their study of Canadian precipitation trends. Similar findings were reported by *Akinremi et al.* (1999, Figure 3), who found that low-precipitation events show a significant negative trend, while high-precipitation events show a significant positive trend.

Table 7.5 presents trend statistics for daily minimum (T_{min}) and maximum (T_{max}) temperature. The 90th percentile, 10th percentile, and mean annual of both T_{min} and T_{max} did not show any significant trend. Seasonal T_{min} for fall and winter shows an increasing trend with a trend slope of 0.05 and 0.08 °C/year, respectively. As well, seasonal T_{max}

Table 7.5: Trend analysis of observed daily basin average precipitation, minimum and maximum temperature time series for 1976 - 2005.

P and T(max/min) statistics (observed daily time series)	Z test statistics	p-value (2-sided)	Trend Slope[a]	Trend at 95% Sig. Level
Precipitation:				
Annual	-0.646	0.518	-0.888	No trend
Spring (MAM)	-1.666	0.096	-0.644	No trend
Summer (JJA)	0.000	1.000	0.008	No trend
Fall (SON)	1.530	0.126	0.747	No trend
Winter (DJF)	-1.496	0.135	-0.350	No trend
Number of dry day/year	0.561	0.575	0.136[b]	No trend
90th percentile (P_{90})	0.146	0.884	0.000	No trend
Minimum temperature:				
Annual	0.748	0.455	0.019	No trend
Spring (MAM)	-1.836	0.066	-0.060	No trend
Summer (JJA)	-0.238	0.812	-0.004	No trend
Fall (SON)	2.312	0.021	0.055	Increasing
Winter (DJF)	2.401	0.016	0.084	Increasing
90th percentile (T_{min90})	-0.038	0.969	-0.000	No trend
10th percentile (T_{min10})	-1.349	0.177	-0.000	No trend
Maximum temperature:				
Annual	0.000	0.142	0.025	No trend
Spring (MAM)	-2.104	0.035	-0.064	Decreasing
Summer (JJA)	0.986	0.324	0.028	No trend
Fall (SON)	2.413	0.016	0.069	Increasing
Winter (DJF)	1.700	0.089	0.082	No trend
90th percentile (T_{max90})	1.377	0.169	0.000	No trend
10th percentile (T_{max10})	-0.525	0.600	0.000	No trend

[a] Trend slope for precipitation - mm/year and temperature - °C/year
[b] number of days/year

shows an increasing trend for fall with a trend slope of 0.07 °C/year. *Zhang et al.* (2000, Figure 11)'s study reported significant positive trends in annual and summer T_{min} with a slope of 0.04 - .06 °C per year on grids over Prairies. In another figure of *Zhang et al.* (2000, Figure 10)'s study presented a significant positive trends for annual T_{max} with a slope of 0.05 - 0.07 °C per year over the Prairie grid cells.

An increase in temperature during fall and winter is responsible for lower precipitation in the form of snow. An increasing temperature trend of the region found in the fall for T_{min} and for T_{max}, and in winter for T_{min} (see Table 7.5) may partly explain the negative snowfall during fall and winter, which in turn changes the flow regime by causing a lesser snow accumulation during fall and winter.

7.6.3 Baseline and Future Climate

Streamflow

Figure 7.16 presents boxplots of mean monthly streamflows (top panel) and mean annual streamflows (bottom panel) for CRCM future climates as well as the CRCM baseline climate. Each box illustrates the median and inter-quartile (25th and 75th percentiles) ranges at the edges of the box, the whiskers are plotted to the most extreme data points without outliers, and outliers are plotted (+) individually.

Figure 7.16 (bottom panel) shows the CRCM projections of mean annual flow for the Churchill River basin. The median total annual flow for the CRB increased by 19% for the 2030s climate, and increased by 34% for the 2050s climate. The monthly flow statistics (Figure 7.16, top panel) exhibit median flow shifts substantially from the CRCM baseline climate during late spring (May), fall (Sep-Oct-Nov), and early winter (Dec). The timing of peaks does not seem to change.

The minimum temperature of the observed climate for fall and winter indicates a significant increasing trend as presented earlier in the Table 7.5, coinciding with monthly increased flow projections shown in Figure 7.16 (top) for the CRB. The winter warming

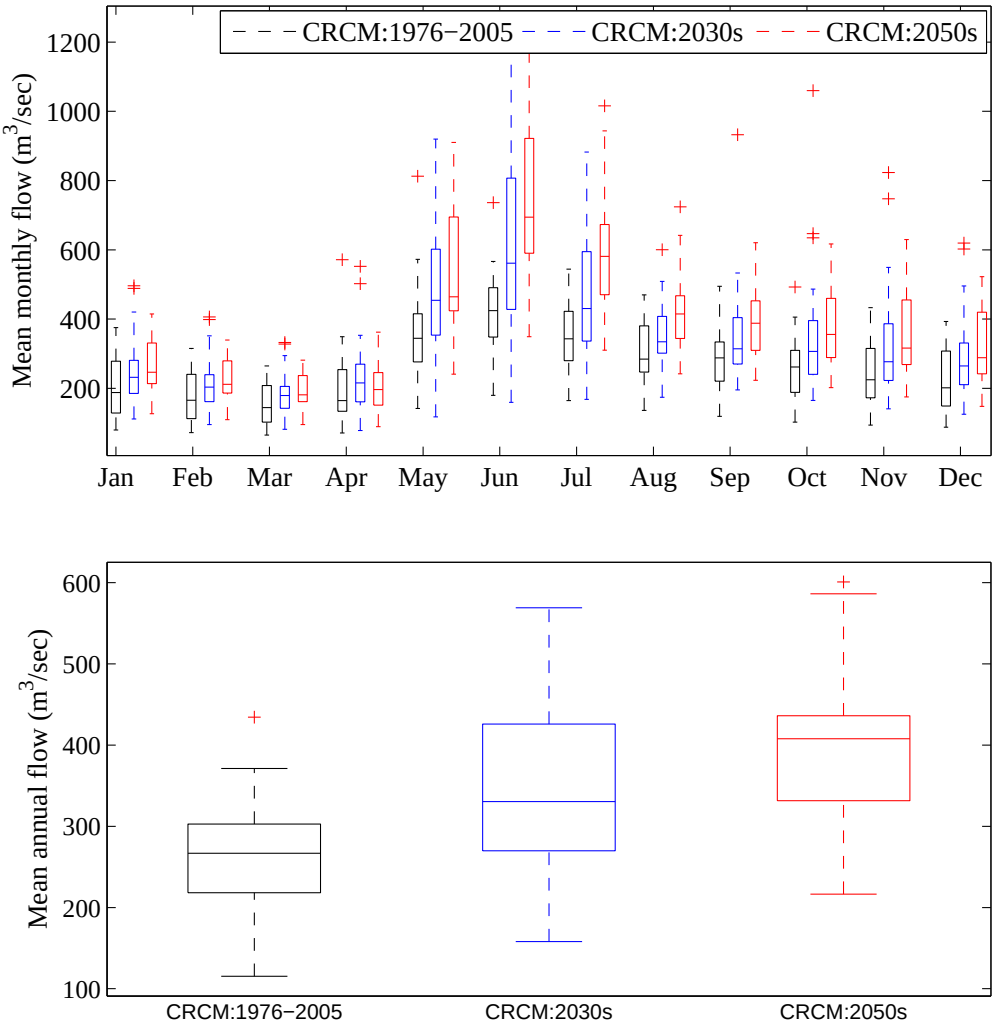

Figure 7.16: Box plots of mean monthly and annual flows for the 2050s and 2030s climates and the baseline climate (1976-2005) at Otter Rapids of the Churchill River basin.

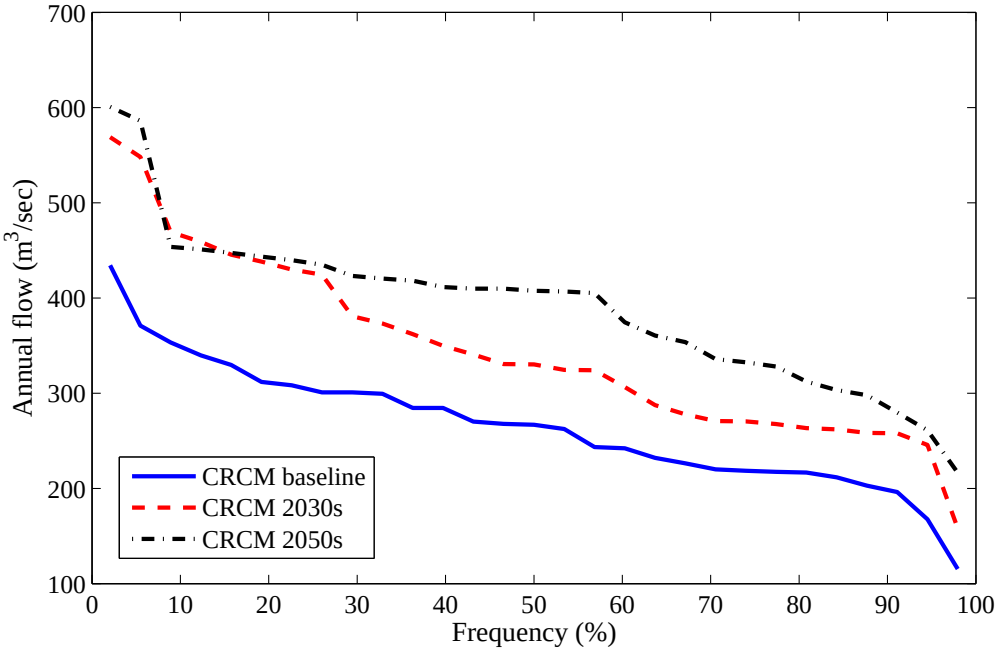

Figure 7.17: Probability of annual streamflow exceedance for the 2050s and 2030s climates compared with the baseline climate at the Otter Rapids of the Churchill River basin.

trend may result in winter precipitation falling as rain-on-snow and rain-on-frozen-ground. The shifting of fall and winter flows based on the SRES A2 scenario, suggest that the basin flow pattern is shifting towards being hybrid or rain-dominated due to climate warming trends.

Flow exceedance plots are cumulative frequency curves that show the percentage of time a specified streamflow is likely to be equalled or exceeded in a given time period. A description of how to construct streamflow exceedance frequency plot is given in Appendix A.3. These flow exceedance plots are particularly useful for planning purposes. Figure 7.17 illustrates the probability of annual streamflow exceedance (constructed from daily streamflow data) for the CRCM baseline and future climates. In both 2030s and 2050s climates, flows are expected to increase in terms of frequency and magnitude, relative to the CRCM baseline climate. The projected increase of flow magnitude that are exceeded 50% of times are greater than that of the projected increase of flow that are exceeded 10% of times of 2050s and 2030s climate relative to the baseline climate.

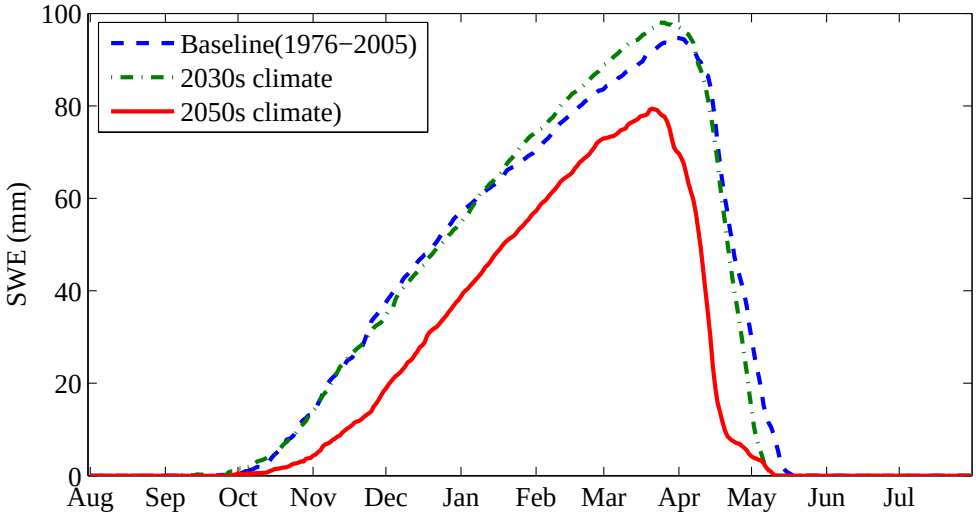

Figure 7.18: Compariosn of VIC simulated snow water equivalent (SWE) for the 2050s and 2030s climates with the baseline climate.

Snow

The volume and extent of snow in the snow-dominated regions are closely linked to climate variability and change (*Stewart*, 2009; *Kapnick and Hall*, 2012). The potential impacts on snow (snow water equivalent, and snow depth) due to climate warming over the Churchill River basin will be evaluated in this section. Three simulations of VIC snow for 2030s, 2050s, and the baseline climate (1976-2005) are analysed and presented in this section. In Section 7.6.1, an evaluation of VIC-simulated snow was performed. The evaluation of snow with measured station data illustrates that the model was able to predict snow water equivalent (SWE), and snow depth reasonably well.

The daily SWE and snow depth data for the grid cell at location 53.98°N, 105.12°W were retrieved from the future climates of 2030s, 2050s as well as from the baseline climate (1976-2005). In order to provide an enhanced understandings of snow change, the snow data from the same grid cell that was used for snow validation is considered here.

Figure 7.18 compares the VIC-simulated SWE for the 2030s and 2050s climates as well as the baseline climate. This plot was prepared using the daily time series of simulated SWE. For both future and baseline climates, the simulated SWE reaches its maximum in

mid-March to early April. The SWE of the 2030s climate does not show a decrease in every month of the snow season; in fact there is a slight increase of SWE during January to March. The average SWE of 2030s climate exhibits a decrease of 6% compared to the baseline climate. An overall decrease of SWE was observed for the 2050s climate with an average decrease of 32%. *Räisänen* (2008, Figure 4a) reported an overall SWE decrease in this region between -30 to -15 mm for a 2050-2099 climate relative to a 1950-1999 climate. The decline in SWE may be associated with increases in temperature (shown in Table 7.5) since there is no significant trend in precipitation. This finding is consistent with trends observed by *Mote* (2003), which were attributed to the increase in air temperature.

The date of maximum SWE is an indicator of when and where the spring snowmelt begins. Figure 7.18 shows the maximum and minimum SWE derived from a daily time series of snow data. There is a shift of peak SWE towards an earlier date relative to the baseline climate. The date of maximum SWE for baseline, 2030s, and 2050s climates is found to be the 90th Julian day (March 31st), 83rd Julian day (March 24th), and 80th Julian day (March 21st), respectively. Similar findings of earlier peaks have been reported by *MacDonald et al.* (2012), while discussing potential impacts of climate change on SWE in the north Saskatchewan River basin.

The days between maximum and minimum SWE is the duration of the snowmelt period. From Figure 7.18, the days between maximum and minimum SWE for the baseline, the 2030s, and the 2050s climates is calculated as 53, 58, and 61 days, respectively. The duration of the snowmelt period increases by 8 days between the VIC-simulated baseline climate and the 2050s climate. *MacDonald et al.* (2012) also found snowmelt duration increases between 2020s to 2080s climate in the north Saskatchewan River basin using the B1 climate scenario.

Table 7.6 presents monthly changes in the VIC-simulated SWE. The monthly change in SWE for the 2050s climate shows an overall decrease for all months of the snow season, with the highest decrease in the month of April. Similar patterns of change can be seen in

Table 7.6: Change in monthly snow water equivalent (SWE) and snow depth as simulated by VIC. The CRCM future climate (2030s, and 2050s) is compared with CRCM baseline climate. Snow depth, and SWE is calculated from daily time series at location 53.98° -105.12°.

	SWE change (mm)		Snow depth change (cm)	
Months	2030s-baseline	2050s-baseline	2030s-baseline	2050s-baseline
September	0.12	-0.07	0.08	-0.05
October	0.08	-4.08	0.25	-2.23
November	-0.74	-15.03	-0.71	-8.11
December	-2.29	-18.44	-1.90	-9.11
January	1.24	-15.01	-1.47	-6.75
February	3.98	-11.85	-1.88	-6.18
March	4.77	-13.54	-0.91	-6.71
April	-4.21	-39.09	-2.12	-12.62
May	-4.67	-5.04	-1.39	-1.63
June	-0.01	-0.01	-0.01	-0.01

Table 7.6 for snow depth change, where the highest decrease is observed in the month of April as well.

Figure 7.19 presents a comparison of VIC-simulated snow depth in future climates and the baseline climate. Although there is a minor increase in snow depth during September-October of the 2030s climate, the snow depth of both future climate projections shows an overall decrease. The average decrease in snow depth for the 2030s climate compared to the baseline climate is -1.00 cm, and for the 2050s climate compared to the baseline climate is -5.35 cm. The maximum decrease in snow depth is observed in April -2.12 cm (2030's) and -12.62 cm (2050's). This decline in snow depth is consistent with *Lawrence and Slater* (2010, Figure 2b), who reported a projected decrease (2080-2099 minus 1950-1969) of annual maximum snow depth between -15 to -5 cm in different grid cells over the region of our interest.

The VIC-simulated snow changes are illustrated in Figures 7.18 and 7.19, where substantial shifts towards earlier maximum and depleted SWE and reduced water storage in the snowpack are clearly seen. The total snow duration period is expected to decrease by 2 days. These findings are consistent with *Scott et al.* (2008), who projected a shorter snow cover season and shallower winter snowpack over most of Canada in response to

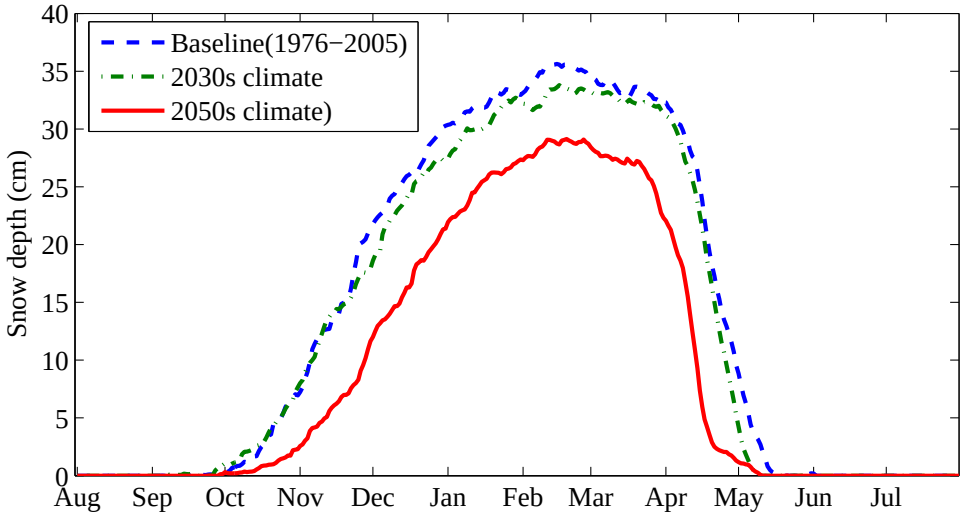

Figure 7.19: Comparison of VIC simulated snow depth for the 2050s and 2030s climates with the baseline climate.

global warming. These assessments based on the SRES A2 scenario suggest that the amount of snow that helps build SWE during the cold season is gradually decreasing, reducing snowmelt-generated flow during spring.

Soil moisture

Soil moisture availability is a key issue in regional hydrology. The impact on hydrological parameters of climate warming has been widely studied, while the impact on soil moisture is less studied. Soil moisture estimates from the VIC model, have been evaluated by a number of authors (*Abdulla et al.*, 1996; *Nijssen et al.*, 2001; *Meng and Quiring*, 2008) and generally compare well with observations. In this section, the potential impacts on soil moisture due to climate warming over the Churchill River basin are evaluated.

The VIC-simulated soil moisture for the 2050s , 2030s, and baseline climates are retrieved at location 53.98°N, 105.12°W for change assessments. Daily soil moisture time series from the model simulations are used for the change analysis. In Section 7.6.1, the VIC-simulated soil moistures were evaluated at the same location and found to be in reasonable agreement with measured soil moisture.

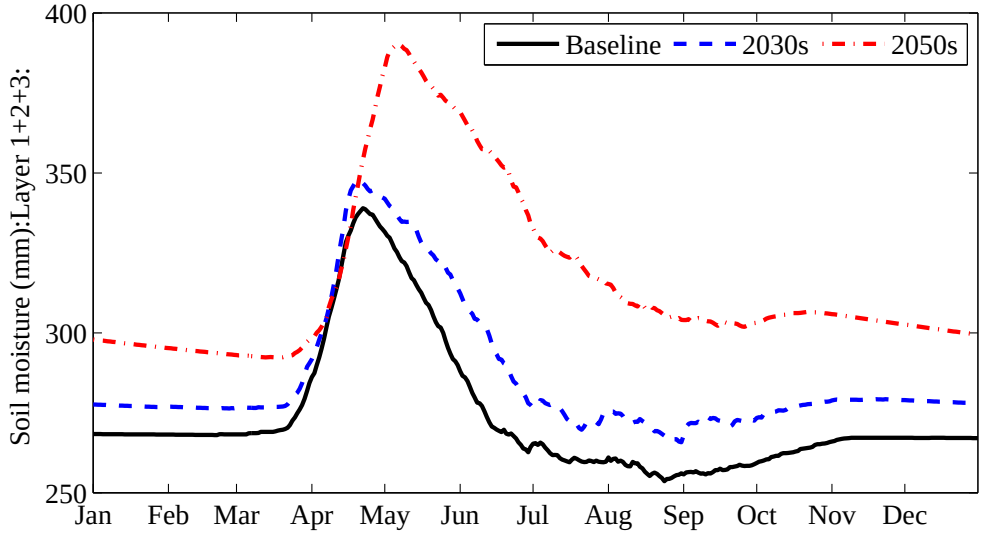

Figure 7.20: Comparison of VIC simulated soil moisture for the 2050s and 2030s climates with the baseline climate.

The graphical representation of the 30-year average soil moisture derived from daily time series of VIC-simulated data for the 2050s, 2030s, and baseline climates are presented in Figure 7.20. The three VIC-simulated soil moisture layers have been added in order to produced these soil moisture plots. Soil moisture projections for the 2050s and 2030s climates exhibit an overall increase compared to the baseline climate throughout the year. Due to climate warming, the near surface soil moisture holding capacity is increasing which is seen in the future projections of Figure 7.20 where an overall increase in soil moisture is observed. The highest increase is between mid-April to late-August. Due to temperature increases during spring and summer, the ground thaws, resulting in an increase in the soil's capacity to hold moisture. In Figure 7.20, soil moisture shows a gradual increase following the spring snowmelt and reaches its peak during mid-spring. There is a gradual shift of peak soil moisture from mid-April to early May between the baseline and 2050s climates.

Table 7.7 illustrates seasonal soil moisture changes, i.e. 2050s minus baseline, and 2030s minus baseline, as simulated by the VIC model. Soil moisture increases in all seasons in both climate projections compared to the baseline climate. The highest projected soil moisture increase compared to the baseline climate is during summer, reaching 19.09 mm

Table 7.7: Changes in seasonal soil moisture as simulated by VIC model. The CRCM future climate of 2030s, and 2050s are compared with baseline climate. Seasonal changes of soil moisture are calculated from daily time series at location 53.9871° -105.1178°. The VIC simulated three soil moisture layers are added together.

	Soil moisture change			
Seasons[a]	2030s-baseline (mm)	% change	2050s-baseline (mm)	% change[b]
Spring	10.70	3.56	34.51	11.46
Summer	19.09	6.10	65.50	24.45
Fall	13.55	5.16	42.00	16.01
Winter	9.54	3.50	29.39	10.97

[a]Spring:March-April-May, Summer:June-July-August, Fall:September-October-November, Winter:December-January-February

[b]% change is calculated as (2050s-baseline)/baseline×100

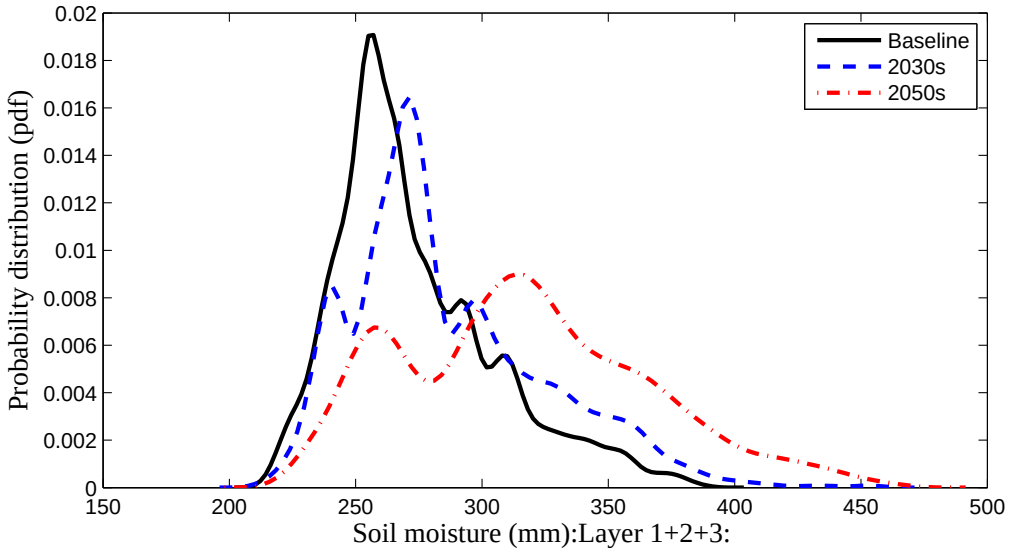

Figure 7.21: PDFs of soil moisture for the 2050s and 2030s climates compared with the baseline climate.

(6.1%) and 65.05 mm (24.5%) for the 2030s, and 2050s climates, respectively. The mean annual soil moisture is projected to increase compared to the baseline climate by 4.5% in the 2030s, and by 15.7% in the 2050s. *Kienzle et al.* (2012)'s study reported a projected increase in the mean annual soil moisture of 0.5% in a 2020s climate, and a 1.4% in a 2050s climate over the north Saskatchewan River basin. *Robock et al.* (2000) used a global soil moisture data bank to analyze soil moisture for 600 stations over the world under grassland and agriculture lands for more than 15 year of data. They concluded that summer soil moisture in the top 1 m has increased while temperatures have risen.

Probability/frequency distributions of soil moisture data for 30 years of daily time series for the 2050s, 2030s, and baseline climates have been derived and are presented in Figure 7.21. These pdfs describe the expected change in soil moisture distribution due to climate change. The pdf of the baseline climate indicates a predominance of soil moisture around 255 mm. In the 2030s climate, the pdf shows a peak around 270 mm. In the 2050s climate, the pdf is shifted to the right and is significant. *Nishat et al.* (2008)'s study using 45 years of climate data over South-Western Ontario demonstrates that there will be an overall increase in growing season soil moisture. These authors also investigated long-term soil moisture conditions and suggested the likelihood of future occurrences of higher soil moistures.

7.7 Conclusions

Dominant hydrological processes over the Churchill River basin have been evaluated in this chapter. The primary goal of this study is to better understand the hydrological processes and their linkage to the climate system and to identify the impacts of climate change on hydrological processes.

The VIC, a distributed hydrological model, has been used to simulate hydrological processes over the Churchill River basin. The calibrated hydrological model showed acceptable results in the validation against measured streamflow. Also, attempts have been made to validate model-simulated evaporation, snow, and soil moisture variables with observed or quasi-observed data. The validation of these internal process variables confirms that the VIC model is capable of simulating these variables adequately.

The validated hydrology model is used to simulate future climate conditions using input from the CRCM model. It is assumed that the hydrology model is able to simulate future climate as the model showed reasonable agreement in simulating present climate. *Knutti* (2008) argued that model's reproducing the current climate should be acceptable for simulating the future as they are based on physical principles include many known processes.

Three 30-year time slices (2050s, 2030s, and a baseline climate of 1976-2005) have been used to simulate the hydrology of the Churchill River basin.

Streamflow outputs have been analysed for trends. The Mann-Kendall (MK) trend test has been used. Besides the MK test, the slope of the time series has been estimated by Theil-Sen's method. Streamflow trends were analysed for mean annual, seasonal, high and low flow, date of annual peak, as well as percentiles of mean daily streamflow. In addition to streamflow trend, precipitation, minimum and maximum temperature trends from the observed data were also analysed in order to derive a linkage with streamflow. Results of the streamflow trend analysis was compared with other published results.

Based on the A2 Scenario, the future projections of streamflow for the 2050s and 2030s climates exhibit an increase compared to the baseline climate . The streamflow trends for the 2050s climate shows a significant increasing trend in high and low flow as well as in the date of annual peak, whereas the streamflow trends for the 2030s climate did not show statistically significant trends. The median of the total annual flow of the basin increased by 19% for the 2030s climate, and by 34% for the 2050s climate relative to the baseline period. The MK test did not find any significant trend in the observed precipitation. An increasing trend is found in fall minimum and maximum temperature, as well as in winter minimum temperature.

Projections of VIC simulated SWE, and snow depth for the 2050s and 2030s climates are compared with the baseline climate at a grid point location. The average SWE of the 2030s, and 2050s climates exhibit a decrease of 6%, and 32% compared to the baseline climate, respectively. The highest decrease of SWE is observed during April for both the 2030s and 2050s climates. The date of maximum SWE is shifted towards an earlier date relative to the baseline climate. The snow depth of both future climates exhibit an overall decrease, with the highest decrease in April. Based on the A2 Scenario, these findings suggest that the amount of snow that builds SWE during the cold season is gradually decreasing, therefore decreasing snowmelt flow.

Soil moisture responses to climate warming in the future have been evaluated using VIC-simulated outputs. Soil moisture at three different layers are added together at a grid point location. Daily time series of soil moisture data are analysed for the 2050s and 2030s climates of the A2 scenario and compared with the baseline climate for change assessment. Soil moisture projections for the 2050s and 2030s climates exhibit an overall increase compared to the baseline climate with the highest increase observed during summer (June-July-August): 6.1% and 24.5% for the 2030s and 2050s climates, respectively. A gradual shift of peak soil moisture is noticed from mid-April to early-May in response to climate warming. Based on the A2 Scenario, the mean annual soil moisture is projected to increase compared to the baseline climate by 4.5% during the 2030s and by 15.7% during the 2050s. The overall increase in soil moisture may partially be explained by the increased holding capacity of soil due to the warming of near surface soil.

Probability distribution functions (PDFs) of 30-year soil moisture data have been analysed to provide insight into soil moisture characteristics and degrees of change. The baseline climate showed a range of moisture between 200 mm to 400 mm, while the 2050s climate exhibits an increase of range between 200 mm to 475 mm. The pdf comparison of 2030s and 2050s climates of the A2 scenario indicates a shift to the right, that is a greater likelihood of occurrences of higher soil moistures conditions. Higher soil moisture indicates higher soil saturation, and may lead to an increase in saturated overland flow (*Bonell*, 1993).

The climate induced changes in hydrological processes discussed above are suggesting a shift in the hydrological regime. Such conclusions generally depend on the climate projections from a particular CRCM. Multiple CRCMs can provide a range of possible future scenarios, but this option was not possible here due to data limitation. Also, there is very limited data available about the long-term effects on land cover due to climate warming (*Innes*, 1994). The hydrological change assessment in this study does not take into consideration of the dynamics of vegetation (e.g., the effect of possible land cover changes) that may occur in future.

Chapter 8

Summary and Discussions

This research has investigated the usefulness of a regional climate model (RCM) in climate change impact studies and has created insight into the hydrological processes dominant in the northern Canadian basins. The evaluation of regional hydrology has been carried out using CRCM data by applying the combined atmospheric-terrestrial water budget techniques. The CRCM simulations were then used as input to the VIC hydrology model in order to assess hydrological process changes due to climate change. In this chapter, a synopsis of the results will be provided, based on conclusions drawn in Chapters 5, 6, and 7. A discussion of shortcomings and recommendations for future research will also be provided.

In Chapter 5, the potential of the CRCM for capturing many sub-grid scale process involved in the hydrological cycle has been demonstrated. The inter-comparison of the NARR and CRCM atmospheric moisture flux divergence (convergence) provided information about seasonal variations of atmospheric moisture over the CRB, where summer moisture fluxes are divergent in both datasets. The long-term CRCM atmospheric moisture fluxes and storage tendencies are consistently represented, and show reasonable agreement with NARR.

This research represents an attempt to uncover a critical aspect of moisture flux over the CRB. The region of CRB is found to be a net source of moisture (Figure 5.11) as the

mean annual moisture flux is divergent. The primary source of moisture is from the active evapotranspiration during summer in the region. As surface evaporation becomes weak during winter, the moisture flux converges into the basin, and the basin becomes a moisture sink. Similar results were found by *Liu and Stewart* (2003) over the Saskatchewan River basin using NCEP-NCAR reanalysis dataset. The findings related to atmospheric moisture over the CRB further contribute to the understanding of Canadian water cycle experiments.

The CRCM atmospheric datasets have been employed in order to evaluate long-term changes in water budget components over the CRB. Overall, the water budget components derived from the CRCM over the CRB were found to be realistic and in general compare well with available observations as well as quasi-observed data. This indicates that the implementation of CLASS in the CRCM has resulted in improvements of boundary layer moisture partitioning. The land surface schemes coupled with atmospheric models are gradually improving as there is a growing need to obtain dependable land surface variables from atmospheric models rather than obtaining land surface variables from an off-line model. The real-time coupling of atmospheric model with land surface hydrology model leaves an area of potential future research.

In Chapter 6, before applying the CRCM data into the VIC model, bias correction of input variables has been performed. The bias correction approach utilized for precipitation and temperature are different as the sources of bias for these two variables are different. The quantile mapping technique applied to the CDFs of CRCM data seemed appropriate for precipitation bias-correction as mean annual precipitation statistics show considerable improvements. After bias-correction, an overall improvement in the daily precipitation is achieved except for several extreme outliers. *Rasmussen et al.* (2012) recommended that extreme outliers should be treated separately, which was not done in this study but could be implemented in future studies.

The bias-correction method employed for temperature performs well, with the differences of CRCM temperature and observations not exceeding 0.5°C. The simulated

temperature also preserved observed annual statistics. There is no standard technique for adjusting RCM biases (*Teutschbein and Seibert*, 2010), but the CRCM bias-correction method employed here is sound and can be applied with confidence in hydrological impact studies. Bias correction techniques should be performed prior to any change analysis.

In Chapter 7, the use of CRCM data in a hydrology model has been explored. The results obtained from the VIC model demonstrated its potential use in simulating hydrological process variables which compare well with measured data.

The soil moisture results obtained from the VIC simulations are validated with measured data. Annual variations of simulated soil moisture, and the timing of the wetting and drying of the soil column showed good agreement with observations. Although a snow model was not calibrated separately, the VIC-simulated snow depth and SWE showed a remarkable agreement with measured BOREAS snow data. The present study demonstrates the value of the VIC-simulated results when the model is properly calibrated. Therefore, the VIC-simulated soil moisture and snow have potential use as an alternative dataset for hydrological studies, especially in areas where measured data are scarce.

The validated VIC model was used to simulate climate scenarios using CRCM data as input over the CRB. The Mann-Kendall (MK) test was used for mean daily streamflow trend analysis. Trend tests on atmospheric variables (i.e., precipitation and temperature) were also conducted in order to explore connections between observed streamflow and atmospheric variables. The slope of the trend has been estimated by Theil-Sen's method. Some conclusions based on the trend tests are:

- Results of trend tests over thirty years (1975-2005) of observed streamflow data have been presented (Table 7.4). The mean annual and seasonal flows did not show any statistically significant trend. Trends appeared on low flow percentiles and high flow percentiles and exhibits decreasing and increasing trends, respectively. The date of the annual peak of the daily flow series show increasing trend. The increasing trend of the date of annual peak appears to be linked with an increasing frequency of annual peaks generated by summer

rainfall for some years. In the averaged hydrograph of ten years observed streamflow for three different time slices (Figure 7.13), there appears to be a gradual shift of hydrograph peaks toward rainfall-dominated peaks which signifies that the flow regime may be in transition from a snowmelt dominated regime to a summer rainfall dominated regime.

- The results of trend tests on observed precipitation and temperature time series have been presented for the same period (1976-2005) as streamflow data (Table 7.5). Trends in daily precipitation were not as significant as those in streamflow for the same period. Fall maximum temperature shows a statistically increasing trend. Also, fall and winter minimum temperatures exhibit an increasing trend. An increase in temperature during fall and winter may lead to a decrease in solid precipitation (*Akinremi et al.*, 1999). The increase in temperature will lead to a change in flow regime by causing lesser snow accumulation during fall and winter. The overall trend analysis suggests that changes in the streamflow regime in the CRB is quite complex. Seasonal trends is a potential area to be further explored.

Climate scenarios were used to perform change analysis. The CRCM future climates of 2030s, and 2050s along with a baseline climate (1976-2005) is used for change analysis. The SRES-A2, a higher end emission scenario, is preferred for this research. The CRCM future simulations were only available for the A2 scenario from the OURANOS consortium. The choice of a single scenario is a limitation of the research, but could be expanded in future research.

The box plots of streamflow scenarios (Figure 7.16) depict a wide range of changes in future projections. For instance, the median of total annual flow for the CRB increased by 19% for the 2030s climate, and increased by 34% for the 2050s climate compared to the baseline climate. A comparison of annual flow exceedance probability shows a relative reduction of larger flow frequency in the 2050s climate compared to the 2030s climate, although the frequency of larger flow increased in both future climates compared to the baseline climate. In the middle to high-latitude basins where larger flows are caused by

snowmelt, a relative reduction of larger flow frequencies indicates a diminished influence of snowmelt flow, as noted by *Arora and Boer* (2001).

The daily snow data (depth, and SWE) data retrieved from VIC simulated future climates of 2030s, 2050s, and a baseline climate are used to develop change scenarios. The average SWE decreased by 6% for the 2030s climate, and by 32% for the 2050s climate compared to the baseline climate. A decrease in SWE in the region of our interest was also reported by *Räisänen* (2008). As precipitation did not show any significant trend (Table 7.5), the SWE decrease must be associated with the temperature increase. Similar findings were obtained by *Mote* (2003). The future projections of snow depth suggest a decline compared to the baseline climates, with the maximum decrease observed during the month of April (Table 7.6). The duration of snow on the ground also exhibits a small decline. *Mote et al.* (2005) reported a decline in April snow in western Canada due to climate warming. It is likely that the loss of snowpack will continue (*Kapnick and Hall*, 2012). The future changes in SWE and snow depth will have profound impact on the flow regime, with consequences for water use in the region.

Soil moisture projections derived from VIC future climate simulations illustrate an overall increase in soil moisture, with the highest increases occurring during summer. A shift of peak soil moisture from mid-April to early-May is observed. In snow dominated basins like the CRB, soil moisture recharge exhibit a close relationship with snowmelt (*Hamlet et al.*, 2007). The time shift of the soil moisture peak corresponds to the findings of the increase in snow duration on the ground presented in Section 7.6.2. An increase of soil moisture is also projected in *Kienzle et al.* (2012)'s study over the north Saskatchewan River basin. Probability distribution functions (pdfs) derived from thirty years time slices of future climate from VIC-simulated soil moisture provided further understanding of the degree of changes in the soil moisture distribution. The pdf of the 2050s climate exhibited bimodality (Figure 7.21). The pdfs of future climate indicate greater likelihood of occurrences of higher soil moistures.

As stated in the objectives, the novelty of the thesis is the following: (a) to validate a CRCM atmospheric dataset from a combined atmospheric and terrestrial approach (Chapter 5), and (b) to assess the use of a CRCM in hydrological change studies over the CRB (Chapter 7). The outfall of these two research components complement each other, and contribute to our understanding of how and to what extent climate change can affect hydrological systems of the CRB. This work appears to be one of the first studies that offers a comprehensive understanding of the dominant hydrological process in the CRB along with an assessment of their sensitivity to climate change.

Despite the efforts to make the research comprehensive, issues still remain for future research. This research did not consider vegetation change while modelling the CRB. Changes in climate forcing, however, may have an effect on land cover type in the permafrost or seasonally permafrost zone, which may eventually alter vegetation types. Presently, very limited data are available about land cover change due to climate warming (*Innes*, 1994). Such information should be included into future hydrology models in order to integrate the land cover change response in hydrology. Northern basins have been examined by scientists from many perspectives. Collectively, these research findings have contributed to our understanding of processes dominant in the northern hydrology. Yet, more research needs to be conducted in order to identify gaps and explore opportunities for collective future research in advancing our knowledge of northern basins and wetlands.

Appendix A

Statistical test

A.1 Mann-Kendall test

The Mann-Kendall (MK) statistics (*Mann*, 1945; *Kendall*, 1975) can be calculated as follows:

$$S = \sum_{i-1}^{n-1} \sum_{j=i+1}^{n} sgn(x_j - x_i) \tag{A.1}$$

The application of the trend test is done to a time series x_i that is ranked from $i = 1, 2, n-1$ and x_j, which is ranked from $j = i+1, 2, .n$. Each data point x_i is taken as a reference point which is compared to the rest of the data points X_j so that

$$sgn(x_j - x_i) = \begin{cases} +1 & \text{if } (x_j - x_i) > 0 \\ 0 & \text{if } (x_j - x_i) = 0 \\ -1 & \text{if } (x_j - x_i) < 0 \end{cases} \tag{A.2}$$

The S statistics is approximately normally distributed when $n \geq 8$, with mean $E(S) = 0$ and the variance statistics is given as

$$V(S) = \frac{(n-1)(2n+5) - \sum_{i=1}^{n} t_i(i)(i-1)(2i+5)}{18} \tag{A.3}$$

where t_i is considered as the number of ties up to sample i. The Z of the MK test and corresponding p-value can be calculated as

$$Z = \begin{cases} \frac{S-1}{\sqrt{Var(S)}} & \text{if } S > 0 \\ 0 & \text{if } S = 0 \\ \frac{S+1}{\sqrt{Var(S)}} & \text{if } S < 0 \end{cases} \tag{A.4}$$

Positive and negative Z values indicate an upward and downward trend, respectively. The p-value of the two-sided Z test is a function of Z alone and can be calculated as

$$p = p(Z) = 2(1 - \Phi(|Z|)) \tag{A.5}$$

In order to compute p-value, apply the standard normal cumulative distribution function (Φ) to both sides. A significance level α is also utilised for which the null hypothesis will be tested. At the significance level of 0.05, if p-value $\leq$ 0.05, then the existing trend is considered to be statistically significant. The Modified MK test has been used for trend detection of an autocorrelated series (*Hamed and Rao*, 1998). Therefore, the corrected variance (after removing serial correlation of de-trended time series) is calculated and replaces the variance of the Equation A.3.

A.2 Slope estimator

The slope estimate (b) is conducted with the nonparametric Theil-Sen method. The well-known robust estimator of the slope was first proposed by *Theil* (1950) and then extended by *Sen* (1968) . This method is suitable for a nearly linear trend in the variable x and is less affected by non-normal data and outliers (e.g., *Helsel and Hirsch*, 1992). The slope is computed between all pairs i of the variable x:

$$\begin{aligned} \beta_i &= \frac{x_j - x_k}{j - k}; \\ with\ j &= 2, \ldots n; \\ and\ k &= 1, \ldots n-1; \\ and\ j &> k \end{aligned} \tag{A.6}$$

(A.7)

where $i = 1 \ldots N$. For n values in the time series of x, the N will result in $N = n(n-1)/2$ values of β. The slope estimate b is the median of β_i,$i = 1, \ldots, N$.

A.3 Frequencies of exceedance

Helsel and Hirsch (2002) provided a description of plot of streamflow exceedance frequencies. To construct a plot of streamflow exceedance frequencies, the data (i.e., peak flow) are ranked from smallest to largest. The rank (i) of smallest is $i = 1$, and largest is $i = n$ where n is sample size. The plotting position of streamflow is a function of the rank i and sample size n. The plotting position can be calculated as

$$p_i = \frac{i}{n+1} \tag{A.8}$$

Appendix B

Acknowledgements

B.1 The Data Access Integration (DAI) Team

The author acknowledges the data access integration (DAI) team for providing the data and technical support. The DAI data download gateway is made possible through collaboration of the Global Environmental and Climate Change Centre (GEC3), the Adaptation and Impacts Research Division (AIRD) of Environment Canada, and the Drought Research Initiative (DRI).

B.2 The NSERC

The author acknowledges the funding support provided by the industrial postgraduate scholarships (IPS) of the Natural Sciences and Engineering Research Council of Canada (NSERC) along with the support from Manitoba Hydro.

B.3 The Drought Research Initiative

This research is partially funded by the the Drought Research Initiative (DRI). The author acknowledges the DRI, its investigators and the data management team for providing the

data through the DRI data legacy. The DRI program details can be accessed through the web link at http://www.drinetwork.ca

B.4 The Manitoba Hydro

The author acknowledges the partial funding support provided by the Manitoba Hydro through its project as well as support provided through the industrial partnership of the Natural Sciences and Engineering Research Council of Canada (NSERC) scholarship.

B.5 The PARC

This research is supported by one time graduate scholarships from the Prairie Adaptation Research Collaborative (PARC). A detailed description of the PARC program can be found by following the web link at http://www.parc.ca

B.6 The Canadian Carbon Program/Fluxnet Canada data

The author acknowledges the Canadian Carbon Program (CCP) - Fluxnet Canada data portal for providing the data support. Permission was granted to the author under the fair-use guidelines for CCP/Fluxnet-Canada data.

B.7 Water level data

The water level data of pond 25 at St Denis National Wildlife Area have been supplied by Dr. Chris Spence[1], Environment Canada. The field measurement methods of pond level data are summarized in *Conly et al.* (2004). A description of the data source can be seen in *van-der Kamp et al.* (2003).

[1]Dr. Chris Spence, Environment Canada, 11 Innovation Boulevard, Saskatoon, SK, Canada S7N 3H5. (e-mail:chris.spence@ec.gc.ca)

References

Abbott, M., J. Bathurst, J. Cunge, P. O'Connel, and J. Rasmussen, An introduction to the European Hydrological System - Systeme Hydrologique Europeen, 'SHE', 1: History and philosophy of a physically-based, distributed modelling system, *J. Hydrol.*, *87*, 45–59, 1986.

Abdulla, F. A., D. P. Lettenmaier, E. F. Wood, and J. A. Smith, Application of a macroscale hydrologic model to estimate the water balance of the Arkansas-Red River basin, *J. Geophys. Res.*, *101*(D3), 7449–7459, 1996.

Akinremi, O. O., S. M. McGinn, and H. W. Cutforth, Precipitation trends on the Canadian Prairies, *J. Clim.*, *12*, 2996–3003, 1999.

Aksoy, H., Use of gamma distribution in hydrological analysis, *Turk. J. Engin. Environ. Sci.*, *24*, 419–428, 2000.

Andreadis, K. M., E. A. Clark, A. W. Wood, A. F. Hamlet, and D. P. Lettenmaier, Twentieth-century drought in the conterminous United States, *J. Hydrometeorol.*, *6*, 985–1001, 2005.

Andreadis, K. M., P. Storck, and D. P. Lettenmaier, Modeling snow accumulation and ablation processes in forested environments, *Water Resour. Res.*, *45*(5), doi:10.1029/2008WR007042, 2009.

Arnell, N. W., Uncertainty in the relationship between climate forcing and hydrological response in UK catchments, *Hydrol. Earth Syst. Sci.*, *15*, 897–912, 2011.

Arora, V. K., Streamflow simulations for continental-scale river basins in a global atmospheric general circulation model, *Adv. Water Resour.*, *24*, 775–791, 2001.

Arora, V. K., and G. J. Boer, Effects of simulated climate change on the hydrology of major river basins, *J. Geophys. Res.*, *106*(D4), 3335–3348, 2001.

Ashfaq, M., C. B. Skinner, and N. S. Diffenbaugh, Influence of SST biases on future climate change projections, *Clim. Dyn.*, *36*, 1303–1319, 2011.

Bell, V. A., A. L. Kay, R. G. Jones, and R. J. Moore, Use of a grid-based hydrological model and regional climate model outputs to assess changing flood risk, *Int. J. Climatol.*, *27*, 1657–1671, 2007.

Berbery, E. H., and E. M. Rasmusson, Mississippi moisture budgets on regional scales, *Mon. Wea. Rev.*, *127*, 2654–2673, 1999.

Beven, K., Changing ideas in hydrology - The case of physically-based models, *J. Hydrol.*, *105*, 157–172, 1989.

Blanken, P. D., et al., Eddy covariance measurements of evaporation from Great Slave Lake, Northwest Territories, Canada, *Water Resour. Res.*, *36*(4), 1069–1077, 2000.

Bonell, M., Progress in the understanding of runoff generation dynamics in forests, *J. Hydrol.*, *150*, 217–275, 1993.

Bonsal, B., and M. Regier, Historical comparison of the 2001/2002 drought in the Canadian Prairies, *Clim. Res.*, *33*, 229–242, 2007.

Bowling, L. C., and D. P. Lettenmaier, Modeling the effects of lakes and wetlands on the water balance of Arctic Environments, *J. Hydrometeorol.*, *11*, 276–295, 2009.

Bowling, L. C., J. W. Pomeroy, and D. P. Lettenmaier, Parameterization of blowing-snow sublimation in a macroscale hydrology model, *J. Hydrometorol.*, *5*(5), 745–762, 2004.

Brankovic, C., and D. Gregory, Impact of horizontal resolution on seasonal integrations, *Clim. Dyn.*, *18*, 123–143, 2001.

Braun, M., D. Caya, A. Frigon, and M. Slivitzky, Internal variability of the Canadian RCMs hydrological variables at the basin scale in Québec and Labrador, *J. Hydrometeorol.*, *13*, 443–462, doi: 10.1175/JHM-D-11-051.1, 2012.

Bresson, R., and R. Laprise, Scale-decomposed atmospheric water budget over North America as simulated by the Canadian Regional Climate Model for current and future climates, *Clim. Dyn.*, *36*(1), 365–384, 2011.

Brigode, P., L. Oudin, and C. Perrin, Hydrological model parameter instability: A source of additional uncertainty in estimating the hydrological impacts of climate change?, *J. Hydrol.*, *476*, 410–425, 2013.

Brimelow, J. C., J. M. Hanesiak, R. L. Raddatz, and M. Hayashi, Validation of ET estimates from the Canadian Prairie agrometeorological model for contrasting vegetation types and growing seasons, *Can. Water Resour. J.*, *35*(2), 209–230, 2010.

Brochu, R., and R. Laprise, Surface water and energy budgets over the Mississippi and Columbia river basins as simulated by two generations of the Canadian Regional Climate Model, *Atmos. - Ocean*, *45*(1), 19–35, 2007.

Brown, R., C. Derksen, L. Wang, D. Tapsoba, and A. Frigon, The snow climate of Québec : A compilation of data sources and information for characterizing the snow cover of Québec, *Tech. rep.*, OURANOS and Environment Canada, 2007.

Burn, D. H., L. Fan, and G. Bell, Identification and quantification of streamflow trends on the Canadian Prairies, *Hydrol. Sci. J.*, *53*(3), 538–549, 2008.

Caya, D., and S. Biner, Internal variability of RCM simulations over an annual cycle, *Clim. Dyn.*, *22*(1), 33–46, 2004.

Caya, D., and R. Laprise, A semi-implicit semi-lagrangian Regional Climate Model: The Canadian RCM, *Mon. Wea. Rev.*, *127*(3), 341–362, 1999.

Cayan, D. R., T. Das, D. W. Pierce, T. P. Barnett, M. Tyree, and A. Gershunov, Future dryness in the southwest US and the hydrology of the early 21st century drought, *pnas*, *107*(50), 21,271–21,276, 2010.

Chen, J., F. P. Brissette, A. Poulin, and R. Leconte, Overall uncertainty study of the hydrological impacts of climate change for a Canadian watershed, *Water Resour. Res.*, *47*, doi:10.1029/2011WR010602, 2011.

Cherkauer, K. A., and D. Lettenmaier, Hydrologic effects of frozen soils in the Upper Mississipi River basin, *J. Geophys. Res.*, *104*(D16), 19,599–19,610, 1999.

Cherkauer, K. A., L. C. Bowling, and D. P. Lettenmaier, Variable infiltration capacity cold land process model updates, *Global Planet. Change*, *38*(1), 151–159, 2003.

Choi, W., S. Kim, P. Rasmussen, and A. Moore, Use of the North American Regional Reanalysis for hydrological modelling in Manitoba, *Can. Water Resour. J.*, *34*(1), 17–36, 2009.

Christensen, J., F. Boberg, O. Christensen, and P. Lucas-Picher, On the need for bias correction of regional climate change projections of temperature and precipitation, *Geophys. Res. Lett.*, *35*(20), 2008.

Christensen, N. S., and D. P. Lettenmaier, A multimodel ensemble approach to assessment of climate change impacts on the hydrology and water resources of the Colorado River Basin, *Hydrol. Earth Syst. Sci.*, *11*, 1417–1434, 2007.

Conly, F. M., and G. van-der Kamp, Monitoring the hydrlogy of Canadian Prairie wetlands to detect the effects of climate change and land use changes, *Env. Monit. Assess.*, *67*, 195–215, 2001.

Conly, F. M., M. Su, G. van der Kamp, and J. B. Millar, A practical approach to monitoring water levels in prairie wetlands, *Wetlands*, *24*(1), 219–226, 2004.

Demaria, E. M., B. Nijssen, and T. Wagener, Monte Carlo sensitivity analysis of land surface parameters using the Variable Infiltration Capacity model, *J. Geophys. Res.*, *112*(D11), doi:10.1029/2006JD007534, 2007.

Derksen, C., R. Brown, A. Walkerr, and B. Breasnett, Comparison of model, snow course, and passive microwave derived snow water equivalent data for Western North America, in *59th Eastern Snow Conference, Stowe, Vermont, USA*, 2002.

Derksen, C., A. Walker, E. LeDrew, and B. Goodison, Combining SMMR and SSM/I data for time series analysis of Central North American snow water equivalent, *J. Hydrometeorol.*, *4*(2), 304–316, 2003.

Dickinson, R. E., R. M. Errico, F. Giorgi, and G. T. Bates, A regional model for the western United States , *Clim. Change*, *Vol. 15*, 383–422, 1989.

Dooge, J. C. I., Hydrological models and climate change, *J. Geophys. Res.*, *97*(D3), 2677–2686, 1992.

Ek, M. B., K. E. Mitchell, Y. Lin, E. Rogers, P. Grunmann, V. Koren, G. Gayno, and J. D. Tarpley, Implementation of NOAH land surface model advances in the National Centers for Environmental Prediction operational mesoscale Eta model, *J. Geophys. Res.*, *108*(D22), doi:10.1029/2002JD003296, 2003.

Elguindi, N., S. Somot, M. Deque, and W. Ludwig, Climate change evolution of the hydrological balance of the Mediterranean, Black and Caspian Seas: impact of climate model resolution, *Clim. Dyn.*, *36*(1), 205–228, 2011.

Eum, H., P. Gachon, R. Laprise, and T. Ouarda, Evaluation of regional climate model simulations versus gridded observed and regional reanalysis products using a combined weighting scheme, *Clim. Dyn.*, *38*, 1433–1457, 2012.

Feser, F., B. Rockel, H. V. Storch, J. Winterfeldt, and M. Zahn, Regional climate models add value to global model data, a review and selected examples, *Bull. Amer. Meteorol. Soc.*, *92*(9), 1181–1192, 2011.

Fowler, H. J., and C. G. Kilsby, Using regional climate model data to simulate historical and future river flows in northwest England, *Clim. Change*, *80*, 337–367, 2007.

Fowler, H. J., C. G. Kilsby, and J. Stunnel, Modelling the impacts of projected future climate change on water resources in Northwest England, *Hydrol. Earth Syst. Sci.*, *11*(3), 1115–1126, 2007.

Frakes, B., and Z. Yu, An evaluation of two hydrologic models for climate change scenarios, *J. Am. Water Resour. Assoc.*, *35*(6), 1351–1363, 1999.

Frigon, A., D. Caya, M. Slivitzky, and D. Tremblay, Investigation of the hydrologic cycle simulated by the Canadian Regional Climate Model over the Québec/ Labrador territory, Advances in Global Change Research, Climatic change: Implications for the hydrological cycle and for water management, 31-55 pp., Kluwer Academic, 2002.

Gao, Y., J. A. Vano, C. Zhu, and D. P. Lettenmaier, Evaluating climate change over the Colorado River basin using regional climate models, *J. Geophys. Res.*, *116*(3), 2011.

Giorgi, F., and L. O. Mearns, Introduction to special section: Regional climate modeling revisited, *J. Geophys. Res.*, *104*(D6), 6335 – 6352, 1999.

Graham, L. P., J. Andreasson, and B. Carlsson, Assessing climate change impacts on hydrology from an ensemble of regional climate models, model scales and linking methods - a case study on the Lule River basin, *Clim. Change*, *81*, 293–307, 2007a.

Graham, L. P., S. Hagemann, and S. Jaun, On interpreting hydrological change from regional climate models, *Clim. Change*, *81*, 97–122, 2007b.

Graham, L. P., L. Andersson, M. Horan, R. Kunz, T. Lumsden, R. Schulze, M. Warburton, J. Wilk, and W. Yang, Using multiple climate projections for assessing hydrological response to climate change in the Thukela River basin, South Africa, *Phys. Chem. Earth.*, *36*, 727–735, 2011.

Grey, D., and C. W. Sadoff, Sink or swim? Water security for growth and development, *Water Policy*, *9*, 545–571, 2007.

Hall, M. J., How well does your model fit the data?, *J. Hydroinf.*, *03*(1), 49–55, 2001.

Hamed, K. H., and A. R. Rao, A modified Mann-Kendall trend test for autocorrelated data, *J. Hydrol.*, *204*, 182–196, 1998.

Hamlet, A., et al., Final report for the Columbia Basin climate change scenarios project, *Tech. rep.*, http://www.hydro.washington.edu/2860/report/, 2010.

Hamlet, A. F., P. W. Mote, M. P. Clark, and D. P. Lettenmaier, Twentieth-century trends in runoff, evapotranspiration, and soil moisture in the Western United States, *J. Clim.*, *20*, 1468–1486, 2007.

Hanesiak, J. M., et al., Characterization and summary of the 19992005 Canadian Prairie drought, *Atmos. - Ocean*, *49*(4), 421–452, 2011.

Hansen, J. W., and T. Mavromatis, Correcting low-frequency variability bias in stochastic weather generators, *Agr. Forest Meteorol.*, *109*(4), 297–310, 2001.

Helsel, D. R., and R. M. Hirsch, *Statistical methods in water resources. Studies in environmental science*, Elsevier: Amsterdam, The Netherlands., 1992.

Helsel, D. R., and R. M. Hirsch, Statistical methods in water resources techniques of water resources investigations, 522 pp., U.S. Geol. Surv., Book 4, chapter A3, 2002.

Henriksen, H. J., L. Troldborg, P. Nyegaard, T. O. Sonnenborg, J. C. Refsgaard, and B. Madsen, Methodology for construction, calibration and validation of a national hydrological model for Denmark, *J. Hydrol.*, *280*, 52–71, 2003.

Hertlein, L., Lake Winnipeg regulation Churchill - Nelson River diversion project in the Crees of Northern Manitoba, Canada, *World Commission of Dams, Thematic Review, Social Issues 1.2, Dams, Indigenous Peoples and Ethnic Minorities,* report can be found at http://www.dams.org/docs/kbase/contrib/soc205.pdf, accessed on July 12, 2008, 1999.

Hess, A., H. Iyer, and W. Malm, Linear trend analysis: a comparison of methods, *Atmos. Environ.*, *35*, 5211–5222, 2001.

Hirschi, M., P. Viterbo, and S. Seneviratne, Basin-scale water-balance estimates of terrestrial water storage variations from ECMWF operational forecast analysis, *Geophys. Res. Lett.*, *33*(21), 2006.

Horton, P., B. Schaefli, B. H. Abdelkader Mezghani and, and A. Musy, Assessment of climate-change impacts on alpine discharge regimes with climate model uncertainty, *Hydrol. Processes*, *20*, 2091–2109, 2006.

Hostetler, S. W., Hydrologic and Atmospheric models: The (continuing) problem of discordant scales, *Clim. Change*, *27*, 345–350, 1994.

Hostetler, S. W., and F. Giorgi, Use of output from high-resolution atmospheric models in landscape-scale hydrologic models: An assessment, *Water Resour. Res.*, *29*(6), 1685–1695, 1993.

Houghton, J. T., and P. Morel, *The Global Climate,* Chapter One: The World Climate Research Programme, ISBN 0 521 25138 9, Cambridge University Press, 1984.

Huang, M., X. Liang, and Y. Liang, A transferability study of model parameters for the variable infiltration capacity land surface scheme, *J. Geophys. Res.*, *108*(D22), doi:10.1029/2003JD003676, 2003.

Hughes, D. A., R. M. Tshimanga, S. Tirivarombo, and J. Tanner, Simulating wetland impacts on stream flow in southern Africa using a monthly hydrological model, *Hydrol. Processes*, dOI: 10.1002/hyp.9725 (online view), 2013.

Hurkmans, R., W. Terink, R. Uijlenhoet, P. Torfs, and D. J. P. A. Troch, Changes in streamflow dynamics in the Rhine Basin under three high-resolution regional climate scenarios, *J. Clim.*, *23*, 679–699, doi: 10.1175/2009JCLI3066.1, 2010.

Ines, A. V. M., and J. W. Hansen, Bias correction of daily GCM rainfall for crop simulation studies, *Agr. Forest Meteorol.*, *138*, 44–53, 2006.

Innes, J. L., Climatic sensitivity of temperature forests, *Environ. Pollut.*, *83*, 237–243, 1994.

IPCC, Climate Change 2007: The physical science basis; summary for policymakers, *Contribution of Working Group I to the Fourth Assessment Report of the Intergovernmental Panel on Climate Change*, 2007a.

IPCC, Climate Change 2007: synthesis report; summary for policymakers, *Working Group contributions to the Fourth Assessment Report of the Intergovernmental Panel on Climate Change*, 2007b.

Jiao, Y., and D. Caya, An investigation of summer precipitation simulated by the Canadian Regional Climate Model, *Mon. Wea. Rev.*, *134*, 919–932, 2006.

Jones, R. G., M. Noguer, D. C. Hassell, D. Hudson, S. S. W. G. J. Jenkins, and J. F. B. Mitchell, Generating high resolution climate change scenarios using PRECIS, *Tech. Rep. 40 pp*, Met Office Hadley Centre, Exeter, UK, 2004.

Jung, W., H. Moradkhani, and H. Chang, Uncertainty assessment of climate change impacts for hydrologically distinct river basins, *J. Hydrol.*, *466-467*, 73–87, 2012.

Kapnick, S., and A. Hall, Causes of recent changes in western North American snowpack, *Clim. Dyn.*, *38*, 1885–1899, doi 10.1007/s00382-011-1089-y, 2012.

Kendall, M. G., *Rank Correlation Methods*, 4th ed., Charles Griffin: London, 1975.

Keshta, N., and A. Elshorbagy, Use of the North American Regional Reanalysis data for hydrological modeling in reconstructed watersheds, *Geophys. Res. Abstracts*, *12*, EGU2010-2255-1, 2010.

Kienzle, S. W., M. W. Nemeth, J. M. Byrne, and R. J. MacDonald, Simulating the hydrological impacts of climate change in the upper North Saskatchewan River basin, Alberta, Canada, *J. Hydrol.*, *412-413*, 76–89, 2012.

Kjellstrom, E., F. Boberg, M. Castro, J. H. Christensen, G. Nikulin, and E. Sanchez, Daily and monthly temperature and precipitation statistics as performance indicators for regional climate models, *Clim. Res.*, *44*, 135–150, 2010.

Knutti, R., Should we believe model predictions of future climate change?, *Phil. Trans. R. Soc. A*, *366*(1885), 4647–4664, 2008.

Krause, P., D. P. Boyle, and F. Base, Comparison of different efficiency criteria for hydrological model assessment, *Adv. Geosci.*, *5*, 89–97, 2005.

LaBaugh, J. W., T. C. Winter, and D. O. Rosenberry, Hydrlogic functions of prairie wetlands, *Great plains Res.*, *8*(1), 17–37, 1998.

Laprise, R., Regional Climate Modelling, *J. Comput. Phys.*, *227*, 3641–3666, 2008.

Lawrence, D. M., and A. G. Slater, The contribution of snow condition trends to future ground climate, *Clim. Dyn.*, *34*, 969–981, doi 10.1007/s00382-009-0537-4, 2010.

Leander, R., and T. Buishand, Resampling of regional climate model output for the simulation of extreme river flows, *J. Hydrol.*, *332*(3-4), 487–496, 2007.

Leander, R., T. A. Buishand, B. J. van den Hurk, and M. J. de Wit, Estimated changes in flood quantiles of the river Meuse from resampling of regional climate model output, *J. Hydrol.*, *351*, 331–343, 2008.

Leavesley, G. H., Modelling the effects of climate change on water resources - a review, *Clim. Change*, *28*, 159–177, 1994.

Lemmen, D. S., F. J. Warren, and J. Lacroix, Synthesis: in from impacts to adaptation: Canada in a changing climate 2007, edited by D. S. Lemmen, F. J. Warren, J. Lacroix and E Bush, pp. 1–20, Government of Canada, Ottawa, ON, 2008.

Leung, L. R., and S. J. Ghan, A subgrid parameterization of orographic precipitation, *Theor. Appl. Climatol.*, *52*, 95–118, 1995.

Liang, X., and Z. Xie, A new surface runoff parameterization with subgrid-scale soil heterogenecity for lanf surface models, *Adv. Water Resour.*, *24*, 1173–1193, 2001.

Liang, X., and Z. Xie, Important factors in landatmosphere interactions: surface runoff generations and interactions between surface and groundwater, *Global Planet. Change*, *38*, 101–114, 2003.

Liang, X., D. P. Lettenmaier, E. F. Wood, and S. Burges, A simple hydrologically based model of land surface water and energy fluxes for general circulation models, *J. Geophys. Res.*, *99*(D7), 14,415–14,428, 1994.

Liang, X., E. F. Wood, and D. P. Lettenmaier, Surface soil moisture parameterization of the VIC-2L model: Evaluation and modification, *Global Planet. Change*, *13*, 195–206, 1996.

Liang, X., Z. Xie, and M. Huang, A new parameterization for surface and groundwater interactions and its impact on water budgets with the variable infiltration capacity (VIC) land surface model, *J. Geophys. Res.*, *108*(D16), doi:10.1029/2002JD003090, 2003.

Liu, J., and R. E. Stewart, Water vapour flux over the Saskatchewan River Basin, *J. Hydrometeorol.*, *4*, 944–959, 2003.

Liu, L., Z. Xu, and J. Huang, Impact of climate change on streamflow in the Xitiaoxi catchment, Taihu Basin, *Wuhan Univ. J. Nat. Sci.*, *14*(6), 525–531, 2009.

Lohmann, D., R. Nolte-Holube, and E. R. Gkss, A large-scale horizontal routing model to be coupled to land surface parametrization schemes, *Tellus*, *48A*, 708–721, 1996.

Lohmann, D., E. Raschke, B. Nijssen, and D. Lettenmaier, Regional scale hydrology: I, Formulation of the VIC-2L model coupled to a routing model, *Hydrol. Sci. J.*, *43*(1), 131–141, 1998.

Lohmann, D., et al., Streamflow and water balance intercomparisons of four land surface models in the North American Land Data Assimilation System project, *J. Geophys. Res.*, *109*(D7), doi:10.1029/2003JD003517, 2004.

MacDonald, R. J., J. M. Byrne, S. Boon, and S. W. Kienzle, Modelling the potential impacts of climate change on snowpack in the North Saskatchewan River watershed, Alberta, *Water Resour. Manage.*, *26*, 3053–3076, doi 10.1007/s11269-012-0016-2, 2012.

Manabe, S., J. Smagorinsky, and R. Strickler, Simulated climatology of general circulation with a hydrologic cycle, *Mon. Wea. Rev.*, *93*, 769–798, 1965.

Mann, H. B., Nonparametric tests against trend, *Econometrica*, *13*, 245–259, 1945.

Masih, I., S. Uhlenbrook, S. Maskey, and V. Smakhtin, Streamflow trends and climate linkages in the Zagros Mountains, Iran, *Clim. Change*, *104*, 317–338, doi 10.1007/s10584-009-9793-x, 2011.

Maslin, M., and P. Austin, Climate models at their limit?, *Nature*, *486*, 183–184, 2012.

Maurer, E. P., Uncertainty in hydrologic impacts of climate change in the Sierra Nevada, California, under two emissions scenarios, *Clim. Change*, *82*(3), 309–325, 2007.

Maurer, E. P., A. W. Wood, J. C. Adam, D. P. Lettenmaier, and B. Nijssen, A long-term hydrologically based dataset of land surface fluxes and states for the conterminous United States, *J. Clim.*, *15*(22), 3237–3251, 2002.

McGinn, S. M., and A. Shepherd, Impact of climate change scenarios on the agroclimate of the Canadian Prairies, *Can. J. Soil Sci.*, *83*(5), 623–630, 2003.

McGuffie, K., and A. Henderson-Sellers, Forty years of numerical climate modeling, *Int. J. Climatol.*, *21*, 1067–1109, doi: 10.1002/joc.632, 2001.

McGuffie, K., and A. Henderson-Sellers, A Climate Modelling Primer, third ed., John Wiley and Sons Ltd., 2005.

McHaffie, P., Surfaces: tacit knowledge, formal language, and metaphor at the Harvard Lab for computer graphics and spatial analysis, *Int. J. Geogr. Inf. Sci.*, *14*(8), 755–773, 2000.

Mekis, E., and W. D. Hogg, Rehabilitation and analysis of Canadian daily precipitation time series, *Atmos. - Ocean*, *37*(1), 53–85, 1999.

Meng, L., and S. M. Quiring, A comparison of soil moisture models using soil climate analysis network observations, *J. Hydrometeorol.*, *9*(4), 641–659, 2008.

Merritt, W. S., Y. Alila, M. Barton, B. Taylor, S. Cohen, and D. Neilsen, Hydrologic response to scenarios of climate change in sub watersheds of the Okanagan basin, British Columbia, *J. Hydrol.*, *326*, 79–108, 2006.

Mesinger, F., et al., North American Regional Reanalysis, *Bull. Amer. Meteorol. Soc.*, *87*(3), 343–360, doi:10.1175/BAMS-87-3-343, 2006.

Metcalfe, J. R., B. Routledge, and K. Devine, Rainfall measurement in Canada: Changing observational methods and archive adjustment procedures, *J. Clim.*, *10*(1), 92–101, 1997.

Mishra, V., and K. A. Cherkauer, Influence of cold season climate variability on lakes and wetlands in the Great Lakes region, *J Geophys. Res.*, *116*(D12), 2011.

Mishra, V., F. Dominguez, , and D. P. Lettenmaier, Urban precipitation extremes: How reliable are regional climate models?, *Geophys. Res. Lett.*, *39*, doi:10.1029/2011GL050658, 2012.

Moore, G. W., J. A. Jones, and B. J. Bond, How soil moisture mediates the influence of transpiration on streamflow at hourly to interannual scales in a forested catchment, *Hydrol. Processes*, *25*, 3701–3710, 2011.

Moss, R. H., et al., The next gebneration of scenarios for climate change research and assessment, *Nature*, *463*, 747–756, 2010.

Mote, P. W., Trends in snow water equivalent in the Pacific Northwest and their climatic causes, *Geophys. Res. Lett.*, *30*(12), doi:10.1029/2003GL017258, 2003.

Mote, P. W., A. F. Hamlet, M. P. Clark, and D. P. Lettenmaier, Declining mountain snowpack in Western North America, *Bull. Amer. Meteorol. Soc.*, *86*, 39–49, doi: 10.1175/BAMS-86-1-39, 2005.

Muleta, M. K., and J. W. Nicklow, Sensitivity and uncertainty analysis coupled with automatic calibration for a distributed watershed model, *J. Hydrol.*, *306*, 127–145, 2005.

Music, B., and D. Caya, Evaluation of the hydrological cycle over the Mississippi River Basin as simulated by the Canadian Regional Climate Model (CRCM), *J. Hydrometeorol.*, *8*(5), 969–988, 2007.

Music, B., and D. Caya, Investigation of the sensitivity of water cycle components simulated by the canadian regional climate model to the land surface parameterization, the lateral boundary data, and the internal variability, *J. Hydrometeorol.*, *10*(1), 3–21, 2009.

Music, B., A. Frigon, M. Slivitzky, A. Musy, D. Caya, and R. Roy, Runoff modelling within the Canadian Regional Climate Model (CRCM): Analysis over the Québec/Labrador watersheds, *IAHS Publ.*, *333*, 183–194, 2009.

Nandakumar, N., and R. Mein, Uncertainty in rainfall-runoff model simulations and the implications for predicting the hydrologic effects of land-use change, *J. Hydrol.*, *192*, 211–232, 1997.

Nash, J. E., and J. V. Sutcliffe, River flow forecasting through conceptual models part I - A discussion of principles, *J. Hydrol.*, *10*(3), 282–290, 1970.

New, M., M. Hulme, and P. D. Jones, Representing twentieth century space-time climate variability. Part II: Development of 1901-96 monthly grids of terrestrial surface climate, *J. Clim.*, *13*(13), 2217–2238, 2000.

Nigam, S., and A. Ruiz-Barradas, Seasonal hydroclimate variability over North America in global and regional reanalyses and AMIP simulations: Varied representation, *J. Clim.*, *19*(5), 815–837, 2006.

Nijssen, B., D. P. Lettenmaier, X. Liang, S. W. Wetzel, and E. F. Wood, Streamflow simulation for continental-scale river basins, *Water Resour. Res.*, *33*(4), 711–724, 1997.

Nijssen, B., R. Schnur, and D. P. Lettenmaier, Global retrospective estimation of soil moisture using the variable infiltration capacity land surface model, 1980-93, *J. Clim.*, *14*(8), 1790–1808, 2001.

Nishat, S., Y. Guo, and B. W. Baetz, Climate change and urban grass land soil moisture conditions in South-Western Ontario, Canada, *J Environ. Informatics*, *12*(2), 105–119, 2008.

Oki, T., K. Musiake, H. Matsuyama, and K. Masuda, Global atmospheric water balance and runoff from large river basins., *Hydrol. Processes*, *9*, 655–678, 1995.

Olsson, J., W. Yang, P. Graham, J. Rosberg, and J. Anderasson, Using an ensemble of climate projections for simulating recent and near-future hydrological change to lake Vanern in Sweden, *Tellus*, *63A*, 126–137, 2011.

Paulat, M., C. Frei, M. Hagen, and H. Wernli, A gridded dataset of hourly precipitation in Germany: Its construction, climatology and application, *Meteorologishe Zeitschrift*, *17*(6), 719–732, 2008.

Peixoto, J., and A. Oort, *Physics of Climate*, 513 pp., American Institute of Physics, New York, NY, 1992.

Piani, C., J. Haerter, and E. Coppola, Statistical bias correction for daily precipitation in regional climate models over Europe, *Theor. Appl. Climatol.*, *99*(1-2), 187–192, 2010.

Plummer, D. A., D. caya, A. Frigon, H. Cote, M. Giguere, D. Paquin, S. Biner, R. Harvey, and R. D. Elia, Climate and climate change over North America as simulated by the Canadian RCM, *J. Clim.*, *19*, 3112–3132, 2006.

Pomeroy, J. W., D. M. Gray, T. Brown, N. R. Hedstrom, W. L. Q. R. J. Granger, and S. K. Carey, The cold regions hydrological model: a platform for basing process representation and model structure on physical evidence, *Hydrol. Processes*, *21*, 2650–2667, 2007.

Räisänen, J., Warmer climate: less or more snow?, *Clim. Dyn.*, *30*(2), 307–319, 2008.

Rao, A., K. Hamed, and H. L. Chen, Nonstationarities in hydrologic and environmental time series, 392 pp., Kluwer Academic Publishers: The Netherlands, 2003.

Rasmussen, J., T. O. Sonnenborg, S. Stisen, L. P. Seaby, B. S. B. Christensen, and K. Hinsby, Climate change effects on irrigation demands and minimum stream discharge: impact of bias-correction method, *Hydrol. Earth Syst. Sci. Discuss.*, *9*, 4989–5037, 2012.

Rasmusson, E. M., Atmospheric water vapor transport and the water balance of North America, II. Large-scale water balance investigation, *Mon. Wea. Rev.*, *96*(10), 720–734, 1968.

Rauscher, S. A., E. Coppola, C. Piani, and F. Giorgi, Resolution effects on regional climate model simulations of seasonal precipitation over Europe, *Clim. Dyn.*, *35*, 685–711, 2010.

Roads, J., and A. Betts, NCEP, NCAR and ECMWF reanalysis surface water and energy budgets for the Mississippi River basin, *J. Hydrometeorol.*, *1*, 88–94, 2000.

Robock, A., K. Y. Vinnikov, G. Srinivasan, J. K. Entin, S. E. Hollinger, N. A. Speranskaya, S. Liu, and A. Namkhai, The global soil moisture data bank, *Global Planet. Change*, *19*, 181–208, 2000.

Rood, S. B., G. Samuelson, J. Weber, and K. Wywrot, Twentieth-century decline in streamflows from the hydrographic apex of North America, *J. Hydrol.*, *306*, 215–233, 2005.

Ruiz-Barradas, A., and S. Nigam, Great plains hydroclimate variability: The view from North American Regional Reanalysis, *J. Clim.*, *19*(12), 3004–3010, 2006.

Rummukainen, M., J. Raisanen, B. Bringfelt, A. Ullerstig, A. Omstedt, U. Willen, U. Hansson, and C. Jones, A regional climate model for northern Europe: Model description and results from the downscaling of two GCM control simulations, *Clim. Dyn.*, *17*(5-6), 339–359, 2001.

Russo, J. M., and J. W. Zack, Downscaling GCM output with a mesoscale model, *J. Environ. Manage.*, *49*, 19–29, 1997.

Sauchyn, D., and S. Kulshreshtha, Prairies; Canada in a Changing Climate 2007, Government of Canada, Ottawa, ON, in *inFrom Impacts to Adaptation*, edited by E. B. D. S. Lemmen, F. J. Warren, pp. 275–328, 2008.

Schnorbus, M. A., K. E. Bennett, A. T. Werner, and A. J. Berland, Hydrologic impacts of climate change in the Peace, Campbell and Columbia watersheds, British Columbia, Canada, *Tech. Rep. 157 pp*, Pacific Climate Impacts Consortium, University of Victoria, Victoria, BC, 2011.

Scott, D., J. Dawson, and B. Jones, Climate change vulnerability of the Northeast U.S. winter tourism sector, *Mitigation and Adaptation Strategies to Global Change*, *13*, 577–596, doi 10.1007/s11027-007-9136-z, 2008.

Sellers, P. J., et al., BOREAS in 1997: Experiment overview, scientific results, and future directions, *J. Geophys. Res.*, *102*(D24), 28,731–28,769, 1997.

Sen, P. K., Estimates of the regression coefficient based on Kendallïs tau, *J. Am. Stat. Assoc.*, *63*, 1379–1389, 1968.

Sennikovs, J., and U. Bethers, Statistical downscaling method of regional climate model results for hydrological modelling, in *18th World IMACS / MODSIM Congress, Cairns, Australia 13-17 July*, 2009.

Shabalova, M. V., W. P. A. van Deursen, and T. A. Buishand, Assessing future discharge of the river Rhine using regional climate model integrations and a hydrological model, *Clim. Res.*, *23*(3), 233–246, 2003.

Sheffield, J., G. Goteti, F. Wen, and E. F. Wood, A simulated soil moisture based drought analysis for the United States, *J. Geophys. Res.*, *109*(D24), doi:10.1029/2004JD005182, 2004.

Sheffield, J., K. M. Andreadis, E. F. wood, and D. P. Lettenmaier, Global and continental drought in the second half of the twentieth century: Severity area duration analysis and temporal variability of large-scale events, *J. Clim.*, *22*(8), 1962–1981, 2009.

Shepard, D. S., Computer mapping: the SYMAP interpolation algorithm, in *Spatial Statistics and Models*, edited by G. L. Gaile and C. J. Willmott, pp. 133–145., D. Reidel Publishing Company, Dordrecht, Netherlands, 1984.

Shepherd, A., and S. M. McGinn, Assessment of climate change on the Canadian Prairies from downscaled GCM data, *Atmos. - Ocean*, *41*(4), 301–316, 2003.

Singh, V. P., Hydrologic Systems: Rainfall - Runoff Modeling, vol. 1, Prentice Hall, ISBN 0-13-448051-1 025, 1988.

Solomon, S., D. Qin, M. Manning, Z. Chen, M. Marquis, K. B. Averyt, M. Tignor, and H. L. Miller, Climate Change 2007: The Physical Science Basis. Contribution of Working Group I to the Fourth Assessment Report of the Intergovernmental Panel on Climate Change, *Tech. rep.*, Cambridge University Press, Cambridge, United Kingdom and New York, NY, USA, 2007.

Spence, C., On the relation between dynamic storage and runoff: A discussion on thresholds, efficiency, and function, *Water Resour. Res.*, *43*(W12), 2007.

Stewart, I. T., Changes in snowpack and snowmelt runoff for key mountain regions, *Hydrol. Processes*, *23*, 78–94, 2009.

Stewart, R., Towards understanding water and energy processes within the Mackenzie River basin, *Atmos. - Ocean*, *40*(2), 91–94, 2002.

Stewart, R., R. Lawford, and A. Boisvert, The 1999-2005 Canadian Prairies drought: Science, impacts, and lessons, ISBN 9780986874901, Drought Research Initiative, 2011.

Stewart, R. E., et al., The Mackenzie GEWEX Study: the water and energy cycles of a major North American river basin., *Bull. Amer. Meteorol. Soc.*, *79*, 2665–2683, 1998.

Storck, P., D. P. Lettenmaier, and S. M. Bolton, Measurement of snow interception and canopy effects on snow accumulation and melt in a mountainous maritime climate, Oregon, United States, *Water Resour. Res.*, *38*(11), doi:10.1029/2002WR001281, 2002.

Strong, G., B. Proctor, M. Wang, E. Soulis, C. Smith, F. Seglenieks, and K. Snelgrove, Closing the Mackenzie Basin Water Budget, Water Years 1994/95 to 1996/97, *Atmosphere - Ocean*, *40 (2)*, 113ï124, 2002.

Sushama, L., N. Khaliq, and R. Laprise, Dry spell characteristics over Canada in a changing climate as simulated by the Canadian RCM, *Global Planet. Change*, *74*, 1–14, 2010.

Szeto, K., Assessing water and energy budgets for the Saskatchewan River Basin, *J. Meteorol. Soc. Japan*, *85 A*, 167–186, 2007.

Szeto, K., H. Tran, M. MacKay, R. Crawford, and R. Stewart, The MAGS water and energy budget study, *J. Hydrometeorol.*, *9*(1), 96–115, 2007.

Terink, W., R. W. L. Hurkmans, P. J. F. Torfs, and R. Uijlenhoet, Bias correction of temperature and precipitation data for regional climate model application to the Rhine basin, *Hydrol. Earth Syst. Sci. Discuss.*, *6*(4), 5377–5413, 2009.

Teutschbein, C., and J. Seibert, Regional climate models for hydrological impact studies at the catchment scale: A review of recent modeling strategies, *Geography Compass*, *4*(7), 834–860, 2010.

Teutschbein, C., and J. Seibert, Is bias correction of Regional Climate Model (RCM) simulations possible for non-stationary conditions?, *Hydrol. Earth Syst. Sci. Discuss.*, *9*, 12,765–12,795, 2012.

Theil, H., A rank-invariant method of linear and polynomial regression analysis, *Nederlandse Akademie Wetenchappen Series A*, *53*, 386–392, 1950.

van-der Kamp, G., W. J. Stolte, and R. G. Clark, Drying out of small prairie wetlands after conversion of their catchments from cultivation to permanent brome grass, *Hydrol. Sci. J.*, *44*(3), 387–397, 1999.

van-der Kamp, G., M. Hayashi, and D. Gallen, Comparing the hydrology of grassed and cultivated catchments in the semi-arid Canadian Prairies, *Hydrol. Processes*, *17*, 559–575, 2003.

van Pelt, S., P. Kabat, H. Ter Maat, B. Van Den Hurk, and A. Weerts, Discharge simulations performed with a hydrological model using bias corrected regional climate model input, *Hydrol. Earth Syst. Sci.*, *13*(12), 2387–2397, 2009.

van Roosmalen, L., J. Christensen, M. Butts, K. Jensen, and J. Refsgaard, An intercomparison of regional climate model data for hydrological impact studies in Denmark, *J. Hydrol.*, *380*(3-4), 406–419, 2010.

Varis, O., T. Kajander, and R. Lemmela, Climate and water: From climate models to water resources management and vice versa, *Clim. Change*, *66*, 321–344, 2004.

Verseghy, D. L., CLASS - A Canadian Land Surface Scheme for GCMs, Part I: Soil model, *Int. J. Climatol.*, *11*(2), 111–133, 1991.

Verseghy, D. L., The Canadian Land Surface Scheme (CLASS): Its history and future, *Atmos. - Ocean*, *38*(1), 1–13, 2000.

Verseghy, D. L., N. A. McFarlane, and M. Lazare, CLASS - A Canadian Land Surface Scheme for GCMs, Part II: Vegetation model and coupled runs, *Int. J. Climatol.*, *13*, 347–370, 1993.

Vincent, L. A., and D. Gullett, Canadian historical and homogeneous temperature datasets for climate change analyses, *Int. J. Climatol.*, *19*(13), 1999.

Vincent, L. A., and E. Mekis, Changes in daily and extreme temperature and precipitation indices for Canada over the twentieth century, *Atmos. - Ocean*, *44*(2), 177– 193, 2006.

Waddington, J. M., W. L. Quinton, J. S. Price, and P. M. Lafleur, Advances in Canadian peatland hydrology, 2003-2007., *Can. Water Resour. J.*, *34(2)*, 139–148, 2009.

Walsh, J. E., X. Zhou, D. Portis, and M. C. Serreze, Atmospheric contribution to hydrologic variations in the Arctic, *Atmos. - Ocean*, *32*(4), 733–755, 1994.

Wang, G. Q., J. Y. Zhang, J. L. Jin, T. C. Pagano, R. Calow, Z. X. Bao, C. S. Liu, Y. L. Liu, and X. L. Yan, Assessing water resources in China using PRECIS projections and a VIC model, *Hydrol. Earth Syst. Sci.*, *16*, 231–240, 2012.

Warren, F. J., Climate change impacts and adaptation : A Canadian perspective, *Tech. rep.*, Natural Resources Canada, ISBN: 0-662-33123-0, 2004.

Wen, L., C. A. Lin, Z. Wu, G. Lu, J. Pomeroy, and Y. Zhu, Real time drought monitoring and forecasting over the Canadian Prairies using the Variable Infiltration Capacity model, http://www.meteo.mcgill.ca/dri/09precip/lei.pdf, 2009.

Wilby, R. L., and I. Harris, A framework for assessing uncertainties in climate change impacts: Low-flow scenarios for the River Thames, UK, *Water Resour. Res.*, *42*(W02419), doi:10.1029/2005WR004065, 2006.

Winter, T. C., and D. O. Rosenberry, The interaction of ground water with prairie pothole wetlands in the cottonwood lake area, east-central North Dakota, 1979-1990, *Wetlands*, *15*(3), 193–211, 1995.

Wolock, D. M., and G. J. McCabe, Estimates of runoff using water-balance and atmospheric general circulation models, *J. Am. Water Resour. Assoc.*, *35*(6), 1341–1350, 1999.

Woo, M. K., and R. Thorne, Snowmelt contribution to discharge from a large mountainous catchment in subarctic Canada, *Hydrol. Processes*, *20*(10), 2129–2139, 2006.

Wood, A., L. Leung, V. Sridhar, and D. Lettenmaier, Hydrological implications of dynamical and statistical approaches to downscaling climate model outputs, *Clim. Change*, *62*, 189–216, 2004.

Wood, E. F., D. P. Lettenmaier, and V. G. Zartarian, A land-surface hydrology parameterization with subgrid variability of general circulation model, *J. Geophys. Res.*, *97*(D3), 2717 – 2728, 1992.

Xie, Z., and F. Yuan, A parameter estimation scheme of the land surface model VIC using the MOPEX databases, *IAHS Publ.*, *307*, 2006.

Xu, C., E. Widén, and S. Halldin, Modelling hydrological consequences of climate change - progress and challenges, *Adv. Atmos. Sci.*, *22*(6), 789–797, 2005.

Yeh, P. J., M. Irizarry, and E. A. B. Eltahir, Hydroclimatology of Illinois: A comparison of monthly evaporation estimates based on atmospheric water balance and soil water balance., *J. Geophys. Res.*, *103*(D16), 19,823–19,837, 1998.

Yong, B., L. Ren, L. Xiong, X. Yangi, W. Zhange, X. Chen, and S. Jiang, A study coupling a large-scale hydrological model with a regional climate model, *IAHS Publ.*, *333*, 203–210, 2009.

You, J., K. G. Hubbard, S. Nadarajah, and K. E. Kunkel, Performance of quality assurance procedures on daily precipitation, *J. Atmos. Oceanic Technol.*, *24*, 821–834, 2007.

Yue, S., and C. Wang, The Mann-Kendall test modified by effective sample size to detect trend in serially correlated hydrological series., *Water Resour. Manage.*, *18*, 201–218, 2004.

Yue, S., P. Pilon, and G. Cavadias, Power of the Mann-Kendall and Spearmanïs rho tests for detecting monotonic trends in hydrological series, *J. Hydrol.*, *259*, 254–271., 2002.

Yue, S., P. Pilon, and B. Phinney, Canadian streamflow trend detection: impacts of serial and cross-correlation, *Hydrol. Sci. J.*, *48*(1), 51–63, 2003.

Zhang, X., L. Vincent, W. D. Hogg, and A. Niitsoo, Temperature and precipitation trends in Canada during the 20^{th} century, *Atmos. - Ocean*, *38*(3), 395–429, 2000.

Zhang, X., K. D. Harvey, W. D. Hogg, and T. R. Yuzyk, Trends in Canadian stream flow, *Water Resour. Res.*, *37*(4), 987–998, 2001.

Zhang, X., R. Brown, L. Vincent, W. Skinner, Y. Feng, and E. Mekis, Canadian climate trends, 1950-2007. Canadian biodiversity: Ecosystem status and trends 2010, *Technical thematic report no. 5*, Canadian Councils of Resource Ministers. Ottawa, ON, 2011.